Marleen Ophorst

Purifying IJssellake water

Operation and performance analysis of direct hollow fiber nanofiltration on raw IJssellake water

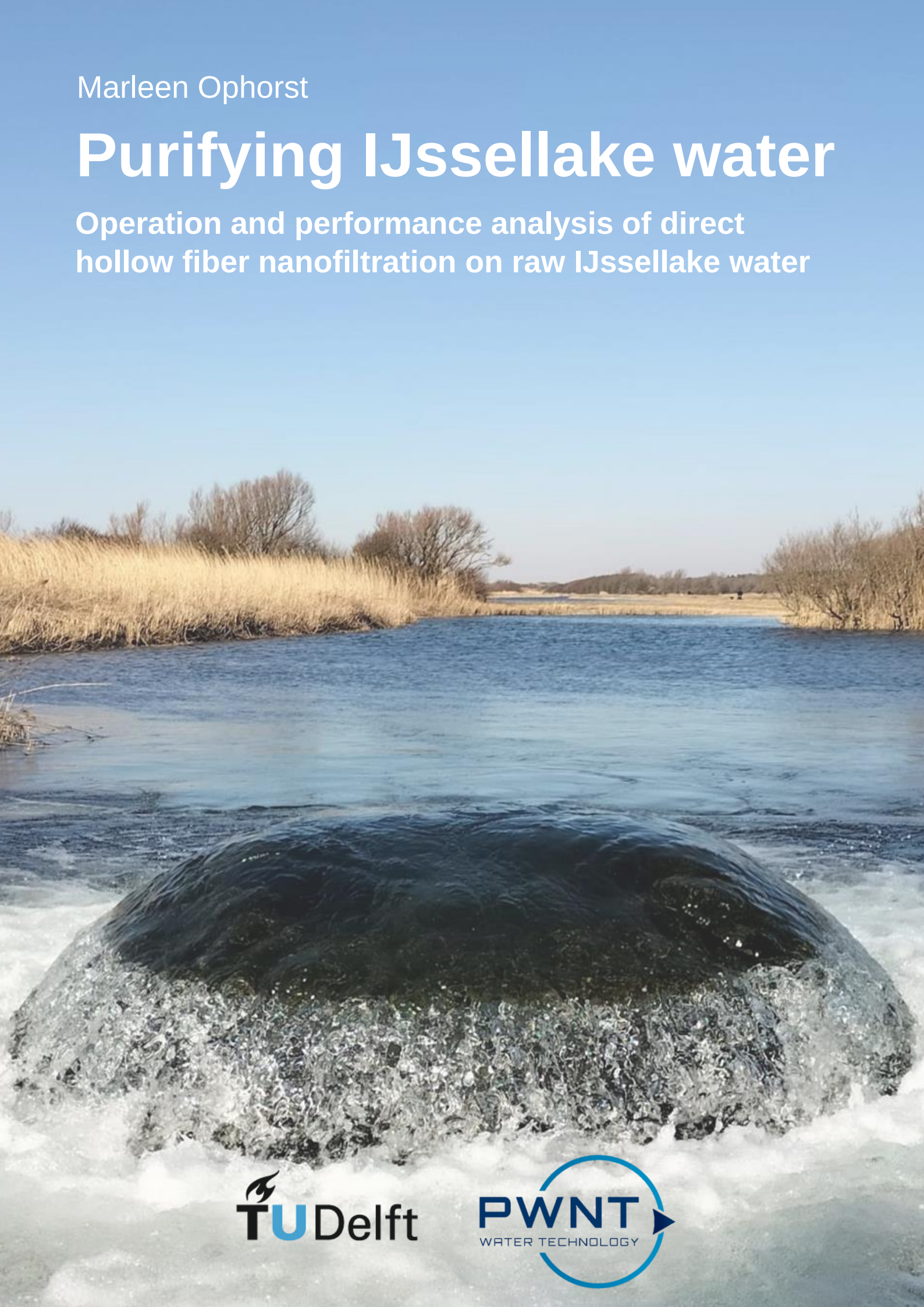

TU Delft

PWNT
WATER TECHNOLOGY

Purifying IJssellake water

Operation and performance analysis of direct hollow fiber nanofiltration on raw IJssellake water

by

Marleen Ophorst

in partial fulfillment of the requirements of the degree of

Master of Science
in Civil Engineering

at Delft University of Technology,
to be defended publicly on Monday 11th of July 2022 at 11:00

Student number:	4477154	
Project duration:	September 6, 2021 – July 11, 2022	
Thesis committee:	Dr. ir. S. G. J. Heijman	TU Delft (chair)
	Prof. dr. ir. L. C. Rietveld	TU Delft
	Dr. H. Bazyar	TU Delft
	Prof. dr. ir. J. van Lier	TU Delft
	Dr. ir. M. Jafari	PWN(t)

An electronic version of this thesis is available at http://repository.tudelft.nl/

TU Delft

PWNT
WATER TECHNOLOGY

Acknowledgements

I would like to thank the following people for their support during the completion of my master thesis.

I would like to thank my daily supervisor Dr. ir. Morez Jafari for his ongoing support throughout the duration of my master thesis. His knowledge in membrane technology was a big help to me. Moreover, I would like to thank Morez for his endless, but enjoyable, conversations. I would also like to thank Dr. ir. Bas Heijman for giving me the opportunity to write my master thesis at the company PWNT and for being an approachable chair committee member. A big thanks to the rest of my graduation committee Prof. dr. ir. Luuk Rietveld, Dr. Hanieh Bazyar and Prof. dr. ir. Jules van Lier for their valuable feedback and advise throughout my master thesis.

Furthermore, I would like to thank the company PWNT for welcoming me with open arms. A special thanks to Maria and Jaap Pennekamp for allowing me to stay in their beautiful home in Andijk and to Nicola Elardo for being a great roommate.

Finally, I cannot thank my friends and family enough for the unconditional support and love. I would like to thank my friends for the memories we created during the time spend at TU Delft. I will cherish those forever. A very big thanks to my family for always being there for me and supporting me in every decision I made. I would not be where I am today without them.

Marleen Ophorst
July 2022

Abstract

Ultrafiltration and reverse osmosis (UF-RO) process in Heemskerk is a determinantal part of PWN drinking water production for the region North Holland. UF-RO process provides a high quality water stream which is used for water softening and biological stability of the distribution network. However, UF-RO also has some challenges, such as high energy consumption, high antiscalant costs, the required post conditioning due to permeate transport to pompstation (PS) Bergen via concrete pipeline and relatively high water loss (80% recovery). Therefore, PWN is evaluating an alternative process and/or membrane type to improve the UF-RO process in Heemskerk. Among the possible alternative solutions is the layer-by-layer hollow fiber nanofiltration membranes.

The aim of this research was to evaluate the feasibility of direct hollow fiber nanofiltration membranes for drinking water purposes. The experiments were performed on the dNF40 pilot provided by NXF. The membrane of the dNF40 pilot was prepared by alternating depositing of polyanions and polycations on a charged surface to form polyelectrolyte multilayers. The membrane is negatively charged and has a molecular weight cutoff (MWCO) of 400 Da. The fouling potential and the ion retention of the dNF40 pilot were determined by continuous filtration experiments using raw IJssellake water under different operational conditions. The performances (ion retention and fouling potential) of the dNF40 on raw IJssellake water were compared with the dNF40 performances on pre-treated water from Waterwinstation Prinses Juliana (WPJ) (previously done at PWNT). The WPJ pre-treated water has undergone extensive pre-treatment consisting of drum screens, flocculation, sedimentation, rapid sand filtration (RSF) and granular activated carbon (GAC). The OMP retention of the dNF40 pilot was determined by full recirculation experiments using WPJ pre-treated water under two different operational conditions with elevated concentrations 'spiked solution'.

Limited to no fouling impact was observed on the membrane performance when feeding the pilot with raw IJssellake water. The membrane performance parameters (mass transfer coefficient (MTC), trans membrane pressure (TMP) and normalized pressure drop (NPD)) were stable over time. In addition, limited to no fouling impact was observed on the membrane when feeding the pilot with WPJ pre-treated water. However, membrane performance (i.e. MTC) was better for raw IJssellake water (1 year old membrane) compared to WPJ pre-treated water (virgin membrane). The temperature corrected MTC value of raw IJssellake water was 8.5 LMH/bar as opposed to the temperature corrected MTC value of 6.9 LMH/bar for WPJ pre-treated water at 70% recovery, 20 LMH flux and 0.2 m/s crossflow velocity. This implies that the active outer layer of the membrane has undergone a change in properties leading to these higher MTC values. These changes in the properties of the membrane have potentially been caused by excessive chemical cleaning or insufficient flushing between high pH and low pH cleaning.

An increase in recovery, flux and crossflow velocity resulted in a decrease in ion retention. However, a decrease in ion retention with elevated crossflow velocity is unusual. Higher crossflow velocities should actually lead to an increase in ion retention due to reduced ion build-up next to the membrane surface (i.e. lower concentration polarization effect). However, the lower ion retention can be attributed to the elevated MTC during experiments. The removal of natural organic matter (NOM) was consistently above 90% and was not influenced by a change in operational condition. Ion retention was higher for WPJ pre-treated water (virgin membrane) compared to raw IJssellake water (1 year old membrane). This can be attributed to the increase in MTC of 1.5 LMH/bar in raw IJssellake water (compared to WPJ pre-treated water) potentially caused by a change in the properties of the active outer layer.

For determining the OMP retention of the dNF40 membrane, a spiked solution containing per- and polyfluoroalkyl substances (PFAS) and pharmaceutical compounds was analyzed. The PFAS compounds of the spiked solution were retained very well (above 80%). The PFAS compounds of the measured background PFAS were retained less than the PFAS compounds of the spiked solution, although the measured background PFAS had a smaller molecular weight (MW). As expected, the retention increased with increasing MW. The adsorption percentage of PFAS was between 40%-90% and mostly

related to hydrophobic and electrostatic interaction. The pharmaceutical retention was around 30%, although all pharmaceuticals analyzed had a MW below the MWCO of the membrane. As expected based on membrane surface charge, the negative charged pharmaceuticals were retained better by the membrane than the positive and neutral charged pharmaceuticals.

A 5-stage full-scale dNF40 plant was designed based on a permeate flow of 15 M m^3/year, a total hardness concentration in the permeate stream below 1.4 mmol/L and a recovery percentage of 85%. Based on the 5-stage full-scale dNF40 plant an economical analysis was performed and compared to the full-scale UF-RO in Heemskerk. The operational cost (OPEX) included the energy cost, chemical cost, membrane replacement cost and pre-treatment cost. The capital cost (CAPEX) included the equipment and installation cost and pre-treatment cost. The total cost (OPEX and CAPEX) were cheapest for the full-scale dNF40 plant fed with raw IJssellake water (11 ct/m^3), followed by the dNF40 plant fed with WPJ pre-treated water (31 ct/m^3) and most expensive for the UF-RO plant (35 ct/m^3). The major factors in the OPEX was the membrane replacement cost for the dNF40 plant and the energy and chemical cost for the UF-RO plant.

The experiments on the dNF40 pilot fed with WPJ pre-treated water and raw IJssellake water imply that HF NF membranes were not a suitable candidate for direct drinking water production or for the replacement of the UF-RO process in Heemskerk, at least under the tested conditions. This was mainly related to the low pharmaceutical retention and the high total hardness concentration in the permeate. However, the retention of pharmaceuticals and total hardness can potentially be increased by membrane modification, hybrid processes or a full-scale system with a membrane lifetime of 3.8 years. Even though the drinking water quality standards were not yet achieved by the use of HF NF membranes, it does not mean that HF NF membranes cannot be used at all. The high NOM and PFAS retention of the dNF40 pilot show that within PWN, HF NF membranes can be a promising candidate for WPJ RO pre-treatment, conventional and novel pre-treatment and RO concentrate treatment.

Contents

Nomenclature

δ	boundary layer thickness	[nm]
μ	fluid viscosity	[Pa.s]
$\Delta\pi$	osmotic pressure difference	[Pa]
ρ	density	[kg/m^3]
Ψ	electrical potential	[mV]
c_{i}	concentration of i	[mg/L]
Cf_{c}	chemical cleaning cost	€/ton
Cf_{e}	electricity cost	€/kWh
Cf_{module}	module price	€/module
D	diffusion coefficient	[m^2/s]
d_{h}	hydraulic diameter	[m]
F	Faraday constant	[96485.3321 sA/mol]
J	permeate flux	[LMH]
k	mass transfer coefficient	[m]
$K_{\mathrm{i,c}}$	convective coupling coefficient	[-]
$log(K_{\mathrm{ow}})$	octanol-water partitioning coefficient	[-]
$log(P)$	octanol-water partitioning coefficient	[-]
L	length of the tube	[m]
N_{module}	number of modules	[-]
P	pressure	[bar]
pKa	acid dissociation constant	[-]
Q_{f}	feed flow	[m^3/h]
R	gas constant	[8.314 J/K/mol]
R	recovery	[%]
$R\%$	retention	[%]
R_{i}	irreversible resistance	[m^{-1}]
R_{m}	clean membrane resistance	[m^{-1}]
R_{r}	reversible resistance	[m^{-1}]
R_{t}	total resistance	[m^{-1}]
Re	Reynolds number	[-]
Sc	Schmidt number	[-]
Sh	Sherwood number	[-]
t	operational time	[h]
T	temperature	[∘C]

U_c	crossflow velocity	[m/s]
$V_{chemical}$	volume of the chemical	[m^3]
X	charge density of the membrane	[-]
z_i	valence of i	[-]

Abbreviations

BB	building blocks
BP	biopolymers
CAPEX	capital cost
CBA	cost-benefit analysis
CIP	cleaning in place
CF	concentration factor
CP	concentration polarization
DCC	direct cell count
dNF	direct nanofiltration
DOC	dissolved organic carbon
ENP	extended Nernst-Planck equation
GAC	granular activated carbon
HF	hollow fiber
HOC	hydrophobic organic carbon
HS	humic substances
HWL	het Waterlaboratorium
LbL	layer-by-layer
MF	microfiltration
MTC	mass transfer coefficient
MW	molecular weight
MWCO	molecular weight cutoff
NF	nanofiltration
NOM	natural organic matter
NPD	normalized pressure drop
NXF	NX Filtration
OMP	organic micropollutant
OPEX	operational cost
PAA	poly(acrylic acid)
PAH	poly(allylaminehydrochloride)
PDADMAC	poly(diallyldimethylammonium chloride)
PE	polyelectrolyte
PEM	polyelectrolyte multilayer
PEMM	polyelectrolyte multilayer membranes
PEQ	PFOA-equivalent
PES	polyethersulfone

PFAS	per- and polyfluoroalkyl substances
PFCA	perfluoroalkyl carboxylic acid
PFHxS	perfluorohexanesulfonic acid
PFNA	perfluorononanoic acid
PFOA	perfluorooctanoic acid
PFOS	perfluorooctane sulfonate
PFSA	perfluoroalkyl sulphonic acid
P&ID	piping and instrumentation diagram
POC	particulate organic carbon
PS	pompstation
PSS	polystyrene sulfonate
PVC	polyvinyl chloride
RIVM	Rijksinstituut voor Volksgezondheid en Milieu
RO	reverse osmosis
RSF	rapid sand filtration
SKK	Spiegler-Kedem-Katchalsky
SW	spiral wound
TC	temperature corrected
TFC	thin-film composite
TMP	trans membrane pressure
TOC	total organic carbon
UF	ultrafiltration
WPJ	waterwinstation Prinses Juliana

List of Figures

List of Tables

1

Introduction

Membrane processes can be used in a variety of different fields, namely fresh water treatment, municipal wastewater treatment and industrial wastewater treatment [1]. In fresh water treatment, such as the production of drinking water, membrane processes are essential as they provide an absolute barrier to contaminants. Application of membrane processes in drinking water production includes, among others, organic micropollutant (OMP) removal, providing biological stability to the drinking water network and reducing hardness.

There are four different types of membrane processes; microfiltration (MF), ultrafiltration (UF), nanofiltration (NF) and reverse osmosis (RO). Membranes are used to separate contaminants from the water based on size and charge. Figure 1.1 shows the contaminant removal based on pore size of the membrane, with biggest pores in MF (20 - 1000nm) followed by UF (5-20nm) and NF (1-5nm) and smallest pores in RO (< 1nm) [2].

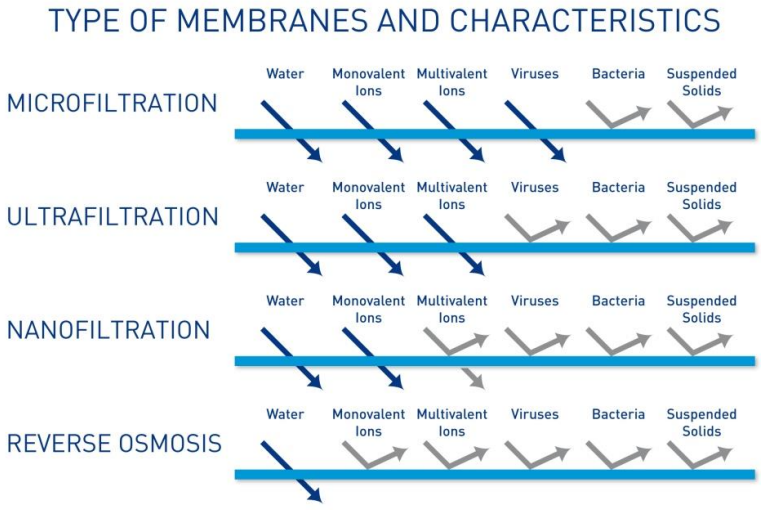

Figure 1.1: Type of membranes and rejection of contaminants by each membrane.

At the moment, UF and RO are typically incorporated by utility companies for drinking water production. UF-RO process in Heemskerk is a determinantal part of PWN drinking water production for the region North Holland. The advantage of UF-RO is that it provides a high quality water stream which is used for water softening and biological stability of the distribution network. The produced water stream from the UF-RO process in Heemskerk is transported to pompstation (PS) Bergen where it is mixed with Bergen dune water in a mixing ratio of roughly 40%-60% to produce the required water for drinking water purposes.

On the contrary, UF-RO also has some challenges. Important challenges are high energy consumption to operate the UF-RO installation (specially RO unit) and high antiscalant cost to prevent fast scaling on the membranes. Moreover, the water produced by the UF-RO process in Heemskerk requires post conditioning in order to transport the water to PS Bergen due to low pH values and low bicarbonate concentrations in the permeate. This post conditioning consists of dosing caustic soda and CO_2. Lastly, the RO unit has a recovery of 80% which results in a relatively high water loss.

Therefore, PWN is evaluating alternative processes and/or membrane types to improve the UF-RO process in Heemskerk. The alternative technologies are, among others, NF and/or open RO membrane (bigger pore size) to achieve lower energy consumption and to decrease the post-conditioning cost by avoiding unnecessary bicarbonate removal, while still providing a good OMP retention. Moreover, minimizing the water loss and fouling potential on the membrane are also important criteria for PWN.

Surface water filtration for drinking water companies are lately cautious towards OMPs and other emerging contaminants. OMPs include a large range of chemicals, such as household products, cosmetics, pesticides and PFAS [3]. This last sub-category is on the spotlight in the drinking water industry, as they are found in a wide range of consumer products used daily [4]. Their harmfulness resides in the frequency exposure, but also in their ability to accumulate and stay in human organisms for long periods of time [5]. They have been linked to low infant birth weights, effect on the immune system, cancer and thyroid hormone dysfunction [5]. Regulatory standards on the concentrations of OMPs in drinking water are tightening.

NF membranes combine unique separation properties with reduced operating pressures compared to conventional RO membranes [6]. NF membranes are used for applications such as reducing hardness due to their high retention towards multivalent ions over monovalent ions and can potentially achieve high retention towards small OMPs [1]. There are several NF membrane configurations available, namely spiral wound (SW) membranes, hollow fiber (HF) membranes and tubular membranes. SW membranes are characterized by their high packing density and low module cost [1]. However, SW membranes do not allow for hydraulic cleaning and therefore require extensive pretreatment to limit fouling potential on the membrane [1]. Tubular membranes, on the other hand, allow for hydraulic cleaning and require less pretreatment [7]. However, they are characterized by their low packing density and high module cost [7]. The HF membrane compares the benefits of both SW and tubular membranes [6]. HF membranes have a low fouling potential due to their effective hydraulic cleaning possibilities [1], which enables the filtration of fouling prone feed waters (e.g., raw surface water).

The layer-by-layer (LbL) method is a versatile method for the preparation of HF NF membranes. The LbL is prepared by alternating depositing of polyanions and polycations on a charged surface to form polyelectrolyte multilayers (PEMs) [8]. These PEMs create an ultrathin separation layer in the nanometer range. This creates a chemical and physical stable membrane with various retention properties [8].

Among the possible alternatives is the LbL HF NF membranes by the company NX Filtration (NXF). Recent research on bench scale LbL HF NF membranes (dNF40 Mexplorer) has been done by Arun [9] with synthetic water and by van der Poel [10] with raw surface water. However, there is a gap in knowledge on filtration performance of LbL HF NF membranes at commercially relevant scale and conditions (dNF40 Mexpert). Direct treatment of surface water specifically with LbL HF NF membranes on pilot scale have not been reported in literature. Moreover, due to the increased cautiousness to OMPs in raw surface water bench-scale testing on the removal of OMP by LbL HF NF membranes (dNF40 Mexplorer) have been done recently as well [11, 10]. However, performance of LbL HF NF membranes to OMP removal at commercially scale (dNF40 Mexpert) is not well understood yet. This research will focus on a pilot-scale study using LbL HF NF membranes for the direct treatment of surface water with regards to fouling potential, ion retention and OMP retention.

This research is a collaborative project between PWNT, PWN, NXF and TU Delft. PWNT has previously studied the feasibility of direct HF NF membranes on pre-treated water from WPJ using the dNF40 pilot from NXF. This research showed promising results with regards to fouling on the membrane and retention of multivalent ions due to the low MWCO of the membrane (400 Da). Therefore, PWN is interested to evaluate dNF40 performance fed with raw IJssellake water to evaluate fouling potential and their potential application for direct use (without/minimal pre-treatment). Especially for isolated parts within North Holland this can be of interest. The objective of this study is to evaluate the feasibility

of direct HF NF (dNF40 pilot) on raw IJssellake water. To answer this objective, the following research questions will be answered:

1. To what extent do the operating conditions influence the performance parameters (ion retention, MTC, TMP and NPD) of the dNF40 pilot fed with raw IJssellake water?
2. To what extent does the dNF40 pilot remove selected OMP compounds under elevated conditions 'spiked solution' with WPJ pre-treated water?
3. To what extent do the different water matrices (raw IJssellake water and WPJ pre-treated water) impact the dNF40 performance and the membrane fouling potential?
4. To what extent is the full-scale dNF40 plant economic feasible with respect to WPJ pre-treated water, raw IJssellake water and a comparison with UF-RO in Heemskerk?

2

Theoretical Background

2.1. Hollow fiber nanofiltration membranes

For NF membranes there are several different membrane configurations available. The traditional SW membranes have been dominated the market for the last decades, but recently HF membranes have made an appearance [1]. The advantages of HF membranes over SW membranes are that HF membranes have a low fouling tendency and effective hydraulic cleaning possibilities [1]. This makes it possible to handle feed streams with much higher suspended solid concentrations. At the moment, HF membranes are used in multiple applications in freshwater treatment, municipal wastewater treatment and industrial treatment for the removal of NOM, OMPs, sulfate or for the softening of water by removing multivalent ions.

2.1.1. Configuration of hollow fiber nanofiltration membranes

The configuration of a HF NF module consists out of four components, namely the HF membrane bundle, the housing, the tubesheets and the end caps [12], see Figure 2.1. The HF membrane bundle contains thousands of long, porous membrane fibers with a diameter of 0.7 mm [13]. These membrane fibers are often made from the material polyethersulfone (PES). The membrane fibers are arranged parallel and are protected by the housing which is often made from the material polyvinyl chloride (PVC). The membrane bundle divides the module into two compartments, the lumen side which is the space enclosed by the membrane fibers and the shell side which is the space between the outer surface of the membranes and the housing [12]. The tubesheets on both sides of the membrane fibers form a fluid-tight seal between the fibers to separate the fluid which is flowing through the lumen and the shell side of the membrane [12]. Everything is connected and kept together by the end caps on both sides of the membrane module. Inlet and outlet ports on the end caps allow fluid inflow to or outflow from the lumen side of the membrane bundle and inlet and outlet ports on the housing allow fluid inflow to or outflow from the shell side of the membrane bundle.

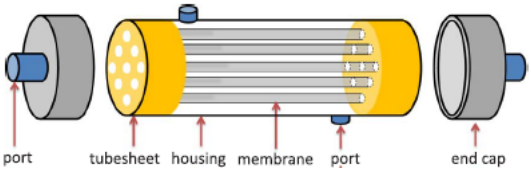

Figure 2.1: The design of a HF NF membrane module [12].

In HF NF membranes the module can be operated in axial flow or crossflow mode [12]. Most HF NF membranes are operated in crossflow mode, which means that the fluid flows tangential to the membrane. During crossflow mode the feed stream fed into the pilot is divided into two streams, the permeate stream and the concentrate stream. Within crossflow mode, the fluid flows through the membrane either from the inside to the outside or from the outside to the inside [12]. During inside-out operation mode, the feed stream enters the membrane on the lumen side and the permeate stream is collected on the shell side. During outside-in operation mode, the feed stream enters the membrane on the shell side and the permeate stream is collected on the lumen side. During inside-out operation the lumen side is the active layer, while during outside-in operation the shell side is the active layer.

2.1.2. Preparation of hollow fiber nanofiltration membranes

Most NF membranes used for water treatment are thin-film composite (TFC) membranes in which an ultra-thin polyamide selective membrane layer is attached on top of a highly permeable support layer [8]. This ultra-thin selective layer can be prepared with different preparation methods, such as phase inversion, grafting, coating, polymerization and self-assembly [1]. A promising method for the preparation of this ultra-thin selective layer using the preparation method self-assembly is the layer-by-layer (LbL) structure [1]. The LbL structure can be explained by the deposition of charged polyelectrolytes (PEs) on top of each other to form PE multilayers (PEMs). PEs are polymers with charged or chargeable groups within the monomer repeat units, whereby these ion pairs can dissociate in water, leaving the charges on the polymer while releasing the counter ions in solution [8]. Figure 2.2 shows the preparation of these PEM membranes (PEMM) by alternating depositing of polyanions and polycations, positively and negatively charged polyelectrolytes, on a charged surface sometimes followed by a rinsing step to remove excess PE. This process is repeated until the PEMM has the required thickness. The charge of the membrane is determined by the charged or chargeable groups from the polymer of the terminal layer and can thus be either positively charged or negatively charged [14].

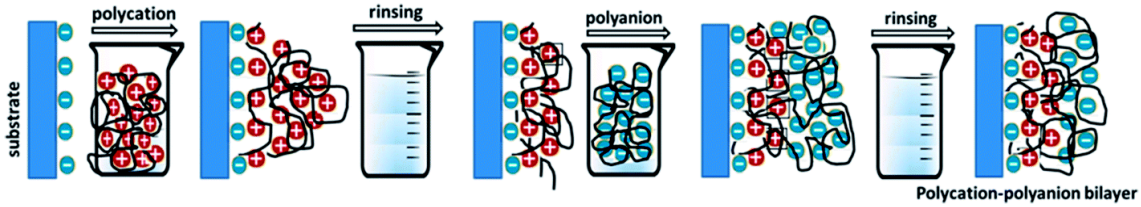

Figure 2.2: Preparation of polyelectrolyte membranes by alternating deposition of polyanions and polycations on a charged surface followed by a rinsing step to remove the counterions [8]

The type of PEs should be chosen carefully since they will influence the PEM formation and will determine the PEM growth mechanism and the PEM properties, such as thickness, roughness, porosity, hydrophilicity, swellability and mechanical properties [8]. Available polyelectrolytes that are used for LbL assembly are for example poly(allylaminehydrochloride) (PAH), poly(diallyldimethylammonium chloride) (PDADMAC), poly(acrylic acid) (PAA) and polystyrene sulfonate (PSS) [15]. The former two are polycations and have a positive charge, while the latter two are polyanions and have a negative charge.

2.2. Water quality and emerging contaminants

2.2.1. Natural organic matter (NOM)

Most natural surface waters contain NOM, which is a complex mixture of organic molecules with different MW, charge densities and hydrophobicities [16]. NOM enters the environment through the excretions of living matters or the decomposition of dead animals, plants and microorganisms. NOM can give problems in drinking water treatment and supply, by forming disinfection by-products or promoting regrowth of bacteria in the distribution system which can change the color, taste and odor of the

water [17]. Moreover, NOM can cause fouling on the membrane resulting in a decrease in flux or an increase in TMP [16].

NOM in the water is indicated by the total organic carbon (TOC) and the dissolved organic carbon (DOC). The fractions of NOM (acids, biopolymers (BP), building blocks (BB), hydrophobic organic carbon (HOC), humic substances (HS), neutrals and particulate organic carbon (POC)) are measured using the LC-OCD analysis [18]. The TOC is subdivided into the fractions acids, BP, BB, HOC, HS, neutrals and POC. The DOC is subdivided into the fractions acids, BP, BB, HOC, HS and neutrals.

2.2.2. Organic Micropollutants (OMP)

The concentration of OMPs in the aquatic environment is increasing every year and becoming more a concern. OMPs, also called emerging contaminants, are synthetic or natural compounds such as pharmaceuticals, personal care products, steroid hormones, industrial chemicals (e.g. PFAS, which will be explained in more detail in Chapter 2.2.3) and pesticides [3] with different MW, charge densities and hydrophobicities [19]. They are present in the environment in concentrations in between the range from a few ng/L to several μg/L. OMPs enter the environment through industrial wastewater, runoff from agriculture, livestock and aquaculture, landfill leachates and domestic and hospital effluents [20]. They have been monitored in the recent years for their potential harmful effect on the aquatic environment and human health [21].

The pKa of an OMP and the pH of the water determine the positive, negative or neutral state of the OMP in that same water. The pKa indicates how likely an OMP wants to keep its proton [H^+]. To calculate the state of the OMP in the water with a certain pH, the Henderson-Hasselbalch equation can be used. This equation is derived from the equilibrium equations of the acid or base. For an acid the Henderson-Hasselbalch equation can be written as:

$$pH = pKa + log\frac{[A^-]}{[HA]} \tag{2.1}$$

with [A^-] the conjugated base and [HA] the acid. For a base the Henderson-Hasselbalch equation can be written as:

$$pH = pKa + log\frac{[B]}{[BH^+]} \tag{2.2}$$

with [B] the base and [BH^+] the conjugated acid.

For acid OMPs, when the concentration [A^-] is larger than the concentration [HA], the OMP is negatively charged in the water and when the concentration [A^-] is smaller than the concentration [HA], the OMP is neutrally charged in the water. For base OMPs, when the concentration [B] is larger than the concentration [BH^+], the OMP is neutrally charged in the water and when the concentration [B] is smaller than the concentration [BH^+], the OMP is positively charged in the water.

2.2.3. Perfluoroalkyl and polyfluoroalkyl substances (PFAS)

PFAS are human made substances which structure consist out of a long carbon (alkyl) chain in which the hydrogen atoms have been replaced with fluor atoms [22]. Perfluoroalkyl substances have only fluorine atoms and no hydrogen atoms in their structure, while polyfluoroalkyl substances have partially hydrogen and partly fluorine atoms in their structure. The most well known and most researched PFAS compounds are perfluorooctanoic acid (PFOA) and perfluorooctane sulfonate (PFOS). Their structure can be found in figure 2.3. These are not the only two compounds which exist and recently more research has also been done to this other PFAS compounds [23]. As of today, more than 4000 long and short chain PFAS compounds exist and are used worldwide [4]. PFAS compounds can either have a carboxylic head or a sulphonic head attached to their carbon chain. Perfluoroalkyl carboxylic acids (PFCAs) have a carboxylic head, while perfluoroalkyl sulphonic acids (PFSAs) have a sulphonic head. Their hydrophobic fluorinated alkyl chain, hydrophilic functional head and strong carbon-fluorine bond gives PFAS unique physical and chemical properties which makes PFAS suitable for everyday products resistant to stain, heat, oil, grease and water [4]. PFAS is used to make products such as

lubricants, food packaging materials, extinguishing foam, non-stick coatings of pans, clothing, textiles and cosmetics.

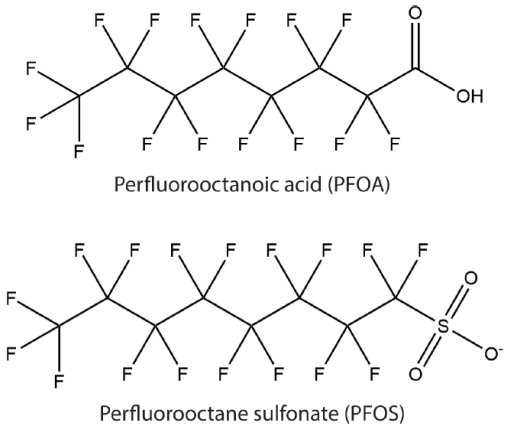

Figure 2.3: Structure of PFOA and PFOS [23].

PFAS enters the environment through wastestreams discharged from facilities that work with PFAS, through the use of extinguishing foam or through leachate from products which contain PFAS [23]. The Rijksinstituut voor Volksgezondheid en Milieu (RIVM), in collaboration with Germany, Denmark, Sweden and Norway, is working on an European project to banish the use and production of PFAS and to limit the discharge of PFAS in the environment. However, PFAS will remain in the environment for years to come due to their strong carbon-fluorine bond, which makes it difficult to degrade PFAS [22]. This persistence against degradation will have severe effects on the drinking water sources for generations to come [23].

Humans are exposed to PFAS either through food, drinking water or PFAS containing environments [5]. PFAS can be a risk for human health since it is known to accumulate in our bodies and can cause cancers, birth defects, infertility, thyroid disease and more [5]. Whether PFAS actually is a risk for human health depends, among other things, on how much PFAS people ingest over time. A research done by the RIVM (2021) shows that the Dutch population is exposed to too much PFAS through food and drinking water [24]. At the moment, there is no strict guideline on the amount of PFAS in drinking water. The RIVM, however, proposes a future drinking water guideline for four PFAS compounds (PFOS, PFOA, perfluorononanoic acid (PFNA) and perfluorohexanesulfonic acid (PFHxS)) of 4.4 ng/L PFOA-equivalent (PEQ) assuming a body weight of 70 kg and a daily water consumption of 2 liters per day.

2.3. Retention mechanisms in nanofiltration

The retention mechanism of solutes in NF is complex since it relies on both sieving and non-sieving mechanisms [14]. The main retention mechanisms in NF are Donnan (charge) exclusion, size (steric) exclusion [25] and retention influenced by concentration polarization (CP). Donnan (charge) exclusion is a non-sieving retention mechanism which is depended on the charge of the membrane, while size (steric) exclusion is a sieving retention mechanism which is depended on the size of a solute. CP is the build-up of solutes near the membrane surface, which can influence the retention. When the membranes are operated in feed-and-bleed mode, the installation retention of solutes can be calculated from [25]:

$$R_{\text{installation}} = (1 - \frac{c_{\text{p}}}{c_{\text{f}}}) * 100\% \tag{2.3}$$

with c_{f} and c_{p} the concentrations of solutes in the feed stream to the system and the permeate stream respectively. When the membranes are operated in feed-and-bleed mode, the membrane retention of solutes can be calculated from:

$$R_{\text{membrane}} = (1 - \frac{c_{\text{p}}}{c_{\text{c}}}) * 100\% \tag{2.4}$$

with c_{c} the concentrations of solutes in the concentrate stream.

2.3.1. Size (steric) exclusion

Neutral solutes are primarily retained by size (steric) exclusion [14]. Retention takes place based on a sieving mechanism in which solutes are prevented to pass through a pore size smaller than the solute itself. The MWCO of the membrane is used to characterize the pore size of the membrane. The MWCO of NF membranes ranges from 200 Da to 500 Da and is defined by the MW in which 90% of the solute is retained [26]. Although determining the MW of a solute is fairly easy, it does not provide enough information on the retention of solutes based on size since the geometry of a solute is not taken into account in the MW parameter [27]. Molecular size parameters which can be better indicators than MW are for example molecular length, Stokes radii and mean molecular size [27]. In addition, adsorption, CP, feed concentration and solubility effects can also affect the retention of solutes based on size [14].

2.3.2. Donnan (charge) exclusion

Charged solutes are primarily retained by Donnan (charge) exclusion [14]. Retention takes place based on electrostatic interaction between the charged solute and the charged membrane. The charge of the membrane determines which solute passes through the membrane and which not. The membrane charge is mostly depended on the dissociation of functional groups on the membrane, but can change due to adsorption of solutes from the solution on the membrane [28]. For a negative charged membrane, the negative charged solutes have a higher concentration in the solution, while the positive charged solutes have a higher concentration near/in the membrane [29]. This difference in concentration between solution and membrane generates a potential difference at the interface between the membrane and the solution to maintain electrochemical equilibrium between the membrane and the solution [29]. This potential difference is called the Donnan potential, which retains the negative charged solutes and attracts the positive charged solutes for a negative charged membrane. This distribution of ions in the solution and near the membrane results in a so called electrical double layer. The positive charged solutes which are attracted towards the negative charged membrane form a positive layer on top of the membrane, the so called Stern layer [30]. Between the bulk solution and the stern layer, there is the diffusive layer in which solutes can move around freely [30]. The zeta-potential is the electrical potential at the slipping plane and determines if a solute stays in the fluid phase or is attached to the membrane.

The retention of negative charged solutes due to the Donnan potential results also in the retention of positive charged solutes due to the electroneutrality condition [31]. The electroneutrality condition states that within the feed solution, the CP boundary layer, the membrane and the permeate solution, the net charge should be zero [31]. Within the membrane, the electroneutrality condition can be written as [32]:

$$\sum_i z_i c_i + X = 0 \tag{2.5}$$

with z_i the valence of i, c_i the concentration of i and X the charge density of the membrane. Within the feed solution, the CP boundary layer and the permeate solution, the electroneutrality condition can be written as [32]:

$$\sum_i z_i c_i = 0 \tag{2.6}$$

with c_i the concentration of i in the feed solution, CP boundary layer or the permeate solution. To maintain electroneutrality, the retention of negative charged solutes on the feed side will result in the retention of positive charged solutes on the feed side as well. However, if positive charged solutes pass through the membrane, negative charged solutes will pass through the membrane as well to maintain electroneutrality on the permeate side [31].

2.3.3. Concentration polarization

CP is the process in which retained solutes build up in the membrane boundary layer and was firstly discovered by Sherwood [33]. Figure 2.4 shows a schematic representation of CP near the membrane in which a convective flow brings the solutes into the boundary layer and a slower back diffusion removes the solutes from the boundary layer back into the bulk solution [34]. This slower back diffusion creates a higher solute concentration in the boundary layer than in the bulk solution. The build-up of retained solutes in the boundary layer results in an increase in the effective osmotic pressure ($\Delta\pi$) at the membrane surface compared to the bulk solution [33]. This increase in $\Delta\pi$ leads to a decrease in the water flux or an increase in the TMP to obtain a given permeate flux. The effect of CP can have an influence on both fouling and retention. Fouling in the form of precipitation and scaling on the membrane can occur if the concentration of ions in the boundary layer exceeds the solubility limit of certain ions [33]. The retention of ions can decrease since the increase of ions at the membrane surface result in an increase in diffusive transport of ions through the membrane to the permeate side [33], see Equation 2.11.

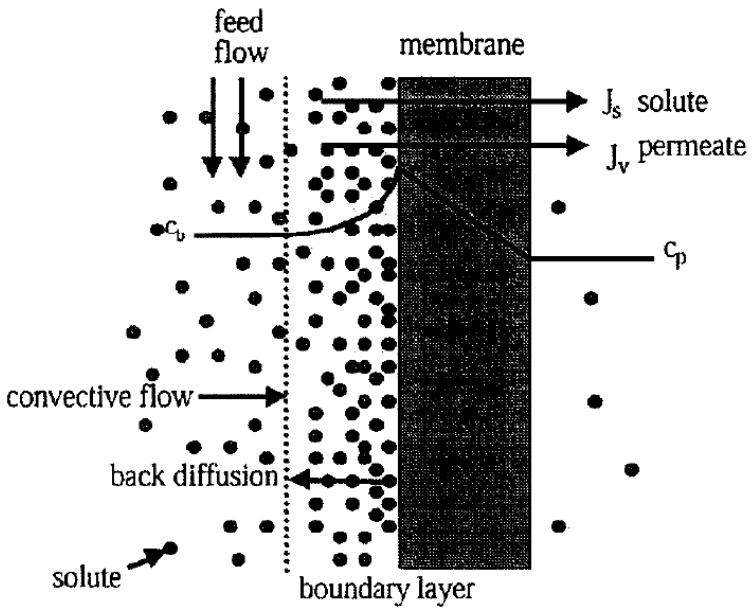

Figure 2.4: A schematic representation of concentration polarization near the membrane [34].

The flux decline due to CP can be calculated using the film theory model. Under steady-state conditions, a solute mass balance in the boundary layer can be written as:

$$J * c = D\frac{dc}{dy} + J * c_{\mathrm{p}} \tag{2.7}$$

with J the permeate flux, c the solute concentration in the boundary layer, c_{p} the solute concentration in the permeate stream and D the diffusion coefficient of the solute in the solvent [35].

After integrating Equation 2.7 over the boundary layer thickness δ, with the boundary conditions $c(y = \delta) = c_{\mathrm{b}}$ and $c(y = 0) = c_{\mathrm{m}}$, the following equation can be derived:

$$J = k_{\mathrm{s}} * ln\frac{(c_{\mathrm{m}} - c_{\mathrm{p}})}{(c_{\mathrm{b}} - c_{\mathrm{p}})} \tag{2.8}$$

with c_{m} the solute concentration at the membrane surface, c_{b} the solute concentration in the bulk solution and $k_{\mathrm{s}} = \frac{D}{\delta}$ the solute mass transfer coefficient in the boundary layer [35].

However, it is impossible to measure the concentration of ions near the membrane surface inside the boundary layer. That is why a distinction is made between the observed retention (R_o) and the real retention (R_r) [36]. The observed retention can be calculated with:

$$R_o = 1 - \frac{c_p}{c_f} * 100\% \tag{2.9}$$

with c_f the solute concentration in the feed stream. The real retention can be calculated with:

$$R_r = 1 - \frac{c_p}{c_m} * 100\% \tag{2.10}$$

The relation between R_o, R_r and permeate flux can be described as:

$$ln\frac{1 - R_o}{R_o} = ln\frac{1 - R_r}{r} + \frac{J}{k_w} \tag{2.11}$$

with k_w the solvent mass transfer coefficient depended on the Reynolds number.

The mass transfer coefficient is usually obtained from semi empirical Sherwood correlation and vary with flow regime and membrane module [35]. The semi empirical Sherwood correlation for HF membranes operated under laminar flow conditions can be described as:

$$Sh = \frac{k_s d_h}{D} = 1.62 Re^{0.33} Sc^{0.33} (\frac{d_h}{L})^{0.33} \tag{2.12}$$

with Sh the Sherwood number ($Sh = \frac{k d_h}{D}$), Re the Reynolds number ($Re = \frac{\rho d_h U_c}{\mu}$), Sc the Schmidt number ($Sc = \frac{\mu}{\rho D}$) [37], d_h the hydraulic diameter of the membrane cell, ρ the density of the water, U_c the crossflow velocity, D the diffusivity of the solute in bulk solution and L length of the tube.

The CP layer can be reduced using NF in crossflow mode rather than dead-end mode. In crossflow mode the water flows tangential to the membrane sweeping away trapped solutes and thus limiting the build-up of solutes near the membrane [34].

2.4. Transport mechanism in nanofiltration

The solute transport through the pores of a membrane is usually determined by the rejection mechanisms described in Chapter 2.3 [38]. In NF, different models can describe this solute transport. The first model was proposed by Spiegler and Kedem and is called the Spiegler-Kedem-Katchalsky (SKK) model which is based on irreversible thermodynamics [39]. Since this model does not take into account the characterization of the electrical and structural properties of the membrane and the charge of the solutes [39], Walther Nernst and Max Planck proposed the Nernst film model.

In the Nernst film model the extended Nernst-Planck equation (ENP) describes the flux of a charged solute i through the pores of a membrane [29]. These solute fluxes are described based on diffusion due to a concentration gradient across the membrane, convection due to a pressure difference over the membrane and electromigration due to a potential gradient across the membrane [40]. It assumes the water transport to be one-dimensional and laminar within the boundary layer [33]. The solute flux of solute i through the pores of the NF membrane can be written as [29]:

$$J_i = -D_i^m (\frac{dc_i^m}{dx} + c_i^m \frac{z_i F}{RT} \frac{d\Psi^m}{dx}) + K_{i,c} J_v c_i^m \tag{2.13}$$

with D the diffusion coefficient of i, c the concentration of i, x the coordinate in the flow direction, z the valency of i, F the Faraday constant, Ψ the electrical potential, R the gas constant, T the temperature, J_v the solvent flux and $K_{i,c}$ the convective coupling coefficient. The superscript m refers to the membrane phase.

In Equation 2.13, the first term describes the fluxes based on diffusion, the second term the fluxes based on electromigration and the third term the fluxes based on convection. For neutral solutes the second term which describes the fluxes based on electromigration can be neglected and the solute flux of solute i through the pores of the NF membrane can be written as [41]:

$$J_{\mathrm{i}} = -D_i^m \frac{dc_i^m}{dx} + K_{i,c} J_v c_i^m \tag{2.14}$$

2.5. Membrane performance parameters

The membrane performance parameters determine the efficiency of the membrane. Solute and solvent transport across and alongside the membrane is depended on the membrane performance parameters, as well as the fouling potential on the membrane. The membrane performance parameters are the MTC, TMP and NPD.

2.5.1. Mass transfer coefficient

The MTC is the ability of the the membrane to allow water to be transported to the permeate side and is depended on the surface properties of the membrane, the porosity and the pore size [42]. The higher the MTC, the easier it is for water to permeate to the other side of the membrane. When fouling occurs on the membrane, the MTC decreases due to a higher TMP to maintain a certain flux.

NXF calculates the MTC based on the following formula:

$$MTC = \frac{J}{TMP} \tag{2.15}$$

with J the permeate flux through the membrane and TMP the trans membrane pressure over the membrane.

2.5.2. Trans membrane pressure

The TMP is the amount of pressure needed to transport the solvent through the membrane and is depended on the MTC of the membrane. Membrane fouling can result in a decrease in MTC which consequently results in an increase in TMP, since more pressure is needed to transport the solvent through the membrane, see Equation 2.15.

NXF calculates the TMP based on the following formula:

$$TMP = \frac{P_{\mathrm{f}} + P_{\mathrm{c}}}{2} - P_{\mathrm{p}} + static\ height\ correction \tag{2.16}$$

with P_f, P_c and P_p the pressure in the feed, concentrate and permeate stream respectively.

2.5.3. Normalized pressure drop

The NPD is the loss of pressure alongside the membrane system and is depended on the crossflow velocity and the amount of fouling on the membrane. The NPD increases with increasing crossflow velocity and with increased fouling formation on the membrane, since more energy is required for feed circulation.

NXF calculates the NPD based on the following formula:

$$NPD = P_{\mathrm{f}} - P_{\mathrm{c}} - static\ height\ correction \tag{2.17}$$

with P_f and P_c the pressure in the feed and concentrate stream respectively.

2.6. Membrane fouling in nanofiltration

The limited factor when using membrane separation techniques, such as NF, for the treatment and purification of drinking water is fouling of the membrane [43]. Membrane fouling is the attachment, accumulation or adsorption of solutes on the pores, inside the pores or on the membrane surfaces and is characterized by a loss of membrane performance [43]. Membrane fouling is normally identified by a decrease in permeate flux when the system is operated under constant pressure or an increase in TMP to maintain a given permeate flux [43]. Membrane fouling can also be distinguished as reversible fouling and irreversible fouling in which the distinction is depended on the cleaning operation of the membrane. During reversible fouling the permeate flux can be restored by hydraulically or chemically cleaning the membrane [34]. During irreversible fouling the permeate flux can only partially be restored by chemically cleaning the membrane or in worst case scenario replacing the membrane [44].

There are four types of fouling which can occur in NF, namely (i) scaling, (ii) organic fouling, (iii) colloidal fouling and (iv) biofouling [43]. Scaling is defined as the formation of mineral deposits precipitating from the feed stream to the membrane surface when the solubility limit of one or more poor soluble salts is exceeded. Organic fouling is the adsorption of organic foulants on the membrane surface and is depended on the nature of the organic foulants and the type and charge of the membrane surface. Colloidal fouling is the deposition of suspended or colloidal particles on the membrane surface. Biofouling is the growth of biological species on the membrane surface .

Membrane fouling is caused by complex physical, chemical and biological interactions between the various fouling constituents in the feed water and between these constituents and the membrane surface [43]. Factors such as feed water composition, the concentration of the major fouling constituents, water chemistry, membrane properties, temperature, mode of operation and hydrodynamic conditions determine fouling on the membrane [43]. Since raw surface water can contain a wide range of fouling constituents it is difficult to determine the type of fouling in real-life applications as different fouling types can occur at the same time [45].

Due to the different constituents in the feed water, different fouling mechanisms lead to membrane fouling [43]. There are three fouling mechanisms which can be distinguished, namely (i) pore blocking, (ii) the formation of a cake or gel layer on the membrane surface or (iii) adsorption that is strengthened by CP [46]. Cake layer formation is an examples of reversible fouling, while adsorption, pore plugging and gel layer formation are examples of irreversible fouling.

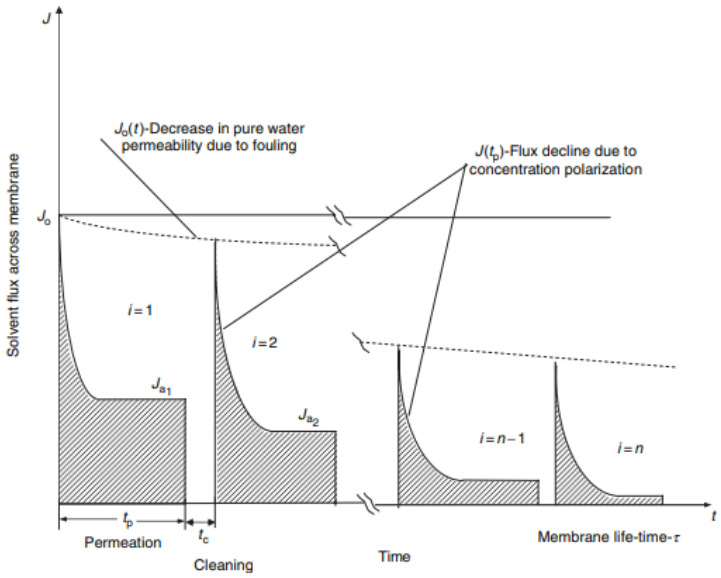

Figure 2.5: Permeate flux decline over time due to concentration polarization and fouling. J_a is the average permeate flux under steady-state concentration, $J_o(t)$ is the permeate flux decrease due to fouling and $J(t_p)$ is the permeate flux decrease due to concentration polarization [34].

The difference between reversible and irreversible fouling is also explained in Figure 2.5 [34]. The figure shows a membrane system which operate in cyclic mode in which filtration cycles are alternated with chemical cleaning cycles. Within a filtration cycle, the permeate flux decreases over time due to CP ($J(t_p)$) until an average permeate flux under steady-state concentration (J_a) is reached. During the entire filtration period, the permeate flux for pure water ($J_o(t)$) decreases over time due to irreversible fouling on the membrane. In addition, J_a also decreases from filtration cycle to filtration cycle due to irreversible fouling.

The permeate flux parameter can tell us something about the fouling on the membrane. The permeate flux of pure water under laminar conditions through a porous barrier can be described as:

$$J = \frac{TMP}{\mu * R_m} \tag{2.18}$$

with J the pure water flux, μ the fluid viscosity and R_m the clean membrane resistance.

When a different feed solution than pure water is used, additional resistances will contribute to the decrease of the permeate flux during filtration. The permeate flux decrease due to fouling can be described using the resistance in serie model [47]. In this model the membrane resistance is replaced by the total resistance (R_t). The permeate flux can, therefore, be described as:

$$J = \frac{TMP}{\mu * R_t} \tag{2.19}$$

with R_t the sum of R_m, the reversible resistances (R_r) and the irreversible resistances (R_i) as seen in the following equation:

$$R_t = R_m + R_r + R_i \tag{2.20}$$

The permeate flux decrease due to fouling can also be described using the osmotic pressure model as described in equation:

$$J = \frac{TMP - \Delta\pi}{\mu * R_m} \tag{2.21}$$

with $\Delta\pi$ the osmotic pressure difference across the membrane.

3

Methodology

3.1. Experimental set-up

The experimental set-up, shown in Figure 3.1 and used for the experiments, was the fully automated Mexpert dNF40 pilot installation of NXF. The set-up consists of a feed tank, an anti-scalant tank, three tanks for chemicals, a permeate tank, a micron cartridge filter, a membrane model, valves, pumps, piping and pressure gauges.

Figure 3.1: dNF40 pilot provided by NXF

The dNF40 pilot was operated remotely via the Mexpert interface of Jotem, see Figure 3.2. This online program gave the possibility to remotely change the operational conditions of the pilot, to start and stop filtration and to start and stop hydraulic or chemical cleaning of the membrane. During the experiments, the pilot did not always ran smoothly and would sometimes turn off. Through the pilot interface it was possible to track down what was wrong due to alarms shown on the interface. The problem could then easily be solved in order to continue the experiments. Figure 3.2 also shows the piping and instrumentation diagram (P&ID) of the Mexpert dNF40 pilot installation. A better readable version of this P&ID diagram can be found in Appendix A.

The pilot was fed 24/7 with water stored in the feed tank (00-T-01). A centrifugal pump (00-P-01) pumped water with a certain flow (depended on the flux) towards a 125-micron cartridge filter (00-F-01). This 125-micron cartridge filter was able to filter out particles which could block the fibers of the HF NF membrane. After the 125-micron cartridge filter, a centrifugal pump (01-P-01) transported the water to the 1.428m height membrane model. The direction of the feed flow rate could be changed during operation by either closing or opening the valves 01-AV-01 and 01-AV-04 and closing or opening the valves 01-AV-02 and 01-AV-03. During the filtration experiments, the feed flow direction of the water

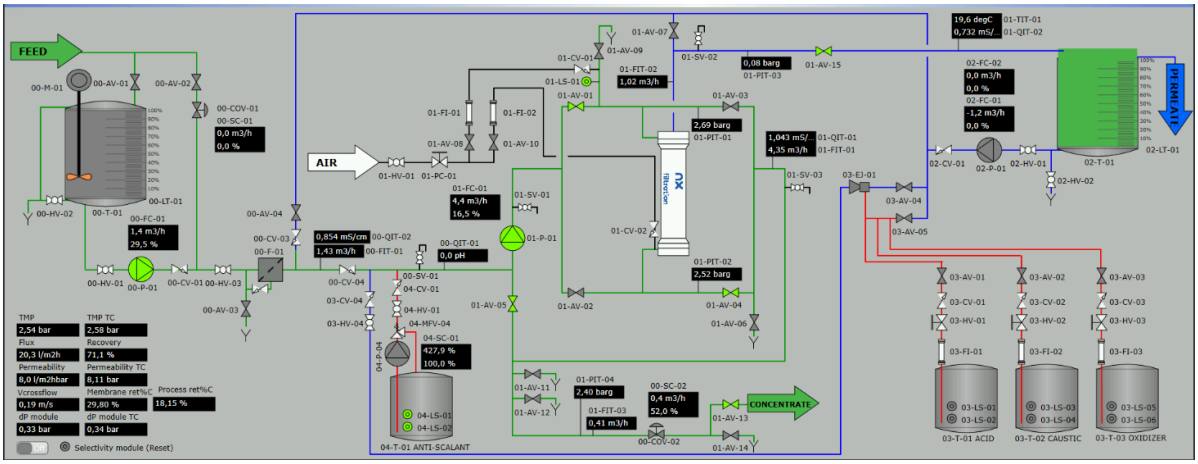

Figure 3.2: Mexpert dNF40 pilot interface available via Jotem

through the membrane model was from top to bottom, which meant that valves 01-AV-01 and 01-AV-04 were open and valves 01-AV-02 and 01-AV-03 closed. The membrane separated the feed stream into a permeate and concentrate stream. The concentrate stream was partially discharged (depending on the applied recovery) and partially combined with fresh feed water and recycled to the membrane module feed side (feed-and-bleed mode). Dependent on the experiments, either the permeate stream was collected in the blue tank which is called the permeate tank (02-T-01) and the concentrate was discharged to the sewerage (continuous filtration) or the permeate and concentrate were both collected in the permeate tank (full recirculation filtration). The permeate tank held an overflow for excess water to be discharged to the sewerage.

The membrane model, provided by NXF, was a dNF40 HF LbL membrane in which polycations and polyanions were LbL deposited on a porous media to form a PEM. The terminal PE layer is negatively charged. The membrane specifications of the dNF40 membrane and their operational limits given by NXF are listed in Table 3.1.

Table 3.1: dNF40 membrane specifications and their operational limits

Parameters	Values
Membrane parameters	
Module length [mm]	1428
External diameter [mm]	200
Module Material (housing-membrane)	PVC-Modified PES
Membrane area [m^2]	43
Membrane MWCO	400
Membrane charge	Negative at pH 7
Membrane rejection ($MgSO_4$) [%]	91
Fiber inner diameter [mm]	0,7
Membrane operational limits	
Max temperature [°C]	40
Operating pH	2-12
Cleaning pH	1-13
Crossflow velocity [m/s]	0,1-2
Max TMP [bar]	6
Max backwash pressure [bar]	6
Max active chlorine concentration [ppm]	500 at pH > 10

3.2. Experimental procedure

Two different experiments were carried out with two water matrices at different operational conditions. The different water matrices were pre-treated water from Waterwinstation Prinses Juliana (WPJ) and raw IJssellake water. The operational conditions recovery, flux and crossflow velocity were changed during each experiment. Depending on the experiment, the results obtained were the membrane performance, ion retention, NOM removal and/or OMP retention. Table 3.2 gives a summary of the two experiments. This table shows which feed water is used, the general pilot operation and pilot settings and the outcome (membrane performance and retention) of the experiments.

The aim of the first experiment was to determine the membrane performance and ion retention of the dNF40 pilot operated at different operational conditions with WPJ pre-treated water and raw IJssellake water. The main focus was on the experiment with raw IJssellake water. The performance (membrane performance and ion retention) of the dNF40 on raw IJssellake water were compared with the dNF40 performance on pre-treated water (previously done in PWNT). During these experiments, the dNF40 pilot was operated in continuous filtration mode which indicated that the permeate stream was collected in the permeate tank and the concentrate stream was discharged to the sewerage. For simplicity, this experiment will be denoted as ”continuous filtration”.

The aim of the second experiment was to determine the OMP retention of the dNF40 pilot operated at different operational conditions with spiked WPJ pre-treated water. During this experiment, the dNF40 pilot was operated in full recirculation filtration mode which indicated that the permeate stream and concentrate stream were both collected in the permeate tank. Full recirculation was needed to prevent any potential leakage of harmful OMP in the environment. For simplicity, this experiment will be denoted as ”full recirculation filtration”.

Table 3.2: Summary of the feed water, general pilot operation, pilot settings, membrane performance and sampled compounds of the continuous filtration experiment and the full recirculation experiment.

	Continuous filtration experiment	**Full recirculation filtration experiment**
Aim	Membrane performance parameters Ion retention and NOM removal	OMP retention under elevated conditions
Feed solution	Raw IJssellake water	Spiked WPJ pre-treated water
General pilot operation	Continuous operation Filtration cycle: 2h	Full recirculation operation Filtration cycle: 2h
Pilot settings	Top-bottom flow direction Air scouring + BW (every 1 filtration cycle) CIP between each round No antiscalant dose	Top-bottom flow direction CIP between each round No antiscalant dose
Operational Conditions	See table 3.3	See table 3.5
Membrane performance	MTC, TMP, NPD	N.A.
Retention	Ions and NOM	OMP under elevated conditions

3.2.1. Continuous filtration experiment

Two different feed solutions were tested during the continuous filtration experiment. An earlier study done at PWNT used the feed solution from the drinking water treatment plant at WPJ just before the water is transported to the UF-RO at the water treatment plant in Heemskerk. For simplicity, this feed solution will be denotes as ”WPJ pre-treated water”. This feed solution has already undergone different treatment steps, such as drum screens, flocculation, sedimentation, RSF and GAC, see Figure 3.3. The study in this report focused mainly on the feed solution from the WPJ reservoir. For simplicity, this feed solution will be denoted as ”raw IJssellake water”, see Figure 3.3.

This section explains the methodology for the experiment with raw IJssellake water. The same methodology was also used for the experiment with WPJ pre-treated water, but more changes in operational conditions were researched, see Appendix D.

A pump installed in the reservoir next to the IJssellake transported 24/7 the feed solutions to the feed tank. The feed tank was able to store 1000L of water and held an overflow for excess water. This excess water was discharged to the sewerage.

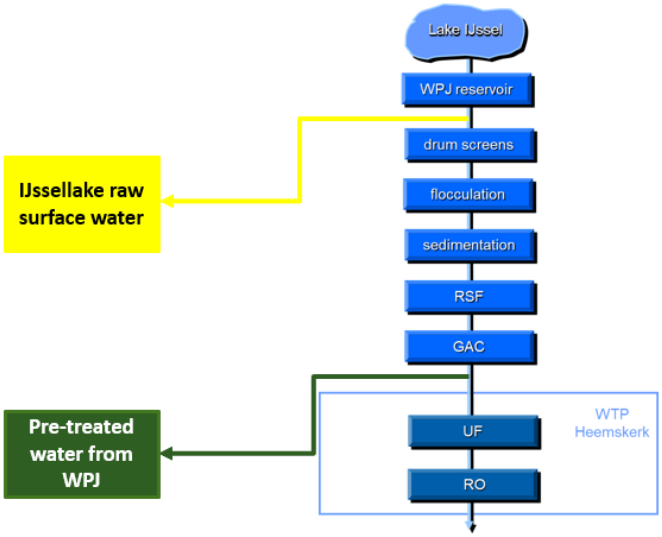

Figure 3.3: Feed solutions for the continuous filtration experiment.

The dNF40 pilot was operated in continuous filtration mode under different operational conditions (round A/B/C/D/E), see table 3.3. These operational conditions were chosen to test the extremes of the pilot within the system limits provided by NXF. Every round was tested for a week before changing to the next round. During the filtration experiments, the pilot operated in cyclic mode in which filtration cycles of 120 minutes were alternated with hydraulic cleaning cycles. After each filtration cycle of 120 minutes a hydraulic cleaning cycle of 60 seconds consisting of backwash and air scour occurred to hydraulically clean the membrane. This hydraulic cleaning protocol was recommended by NXF to remove contaminants from the membrane and to decrease the fouling formation. The flow direction of the backwash water was reversed from the feed flow direction. The air scour was combined with a forward flush and was from bottom to top. Air scour is done to increase turbulence during the forward flush which should increase efficiency of cleaning. In addition, air scour also helps in removing particulate matter which might block fibers. The backwash water and air scour water were discharged to the sewerage. After the backwash and air scour cycle, a 50 seconds venting step was performed to vent the dNF40 pilot and to restart the filtration cycle.

Table 3.3: Summary of operational conditions used during continuous filtration experiment.

	Water type	Recovery [%]	Flux [LMH]	Crossflow velocity [m/s]
Round A		70	20	0.2
Round B		80	20	0.2
Round C	Raw IJssellake water	90	20	0.2
Round D		70	25	0.2
Round E		70	20	0.5

On the last day of each round, ion and NOM samples were collected in duplo at 09:00h for the installation retention calculations. The ion samples of round A/B/C/D/E and the NOM samples of round A were collected from the feed stream, permeate stream and concentrate stream. The NOM samples of round B/C/D/E were collected from the feed stream and permeate stream. The sample bottles were provided by Het Waterlaboratorium (HWL). The analysis of the samples was also done by HWL.

3.2.2. Full recirculation experiment

The OMP retention tests were performed on spiked WPJ pre-treated water. To cover a wide range of OMPs, a multi-element solution containing PFAS, negatively charged, neutral and positively charged pharmaceuticals was provided by HWL. Each spiking solution was made by diluting a 1L multi-element solution sent by HWL in the 1000L NXF tank with WPJ pre-treated water. Concentrations of the spiking solution can be found in table 3.4.

Table 3.4: PFAS and pharmaceutical compounds in the spike solution, their molecular weight and the concentration

Category	Compound	MW [g/mol]	Concentration in spike solution [μg/L]
PFAS	PFOS	500	0.1
	PFNA	464	0.02
	PFOA	414	0.1
	PFHxS	400	0.1
Negatively charged pharmaceuticals	Diclofenac	296	2
	Sulfamethoxazole	253	2
Neutral charged pharmaceuticals	Carbamazepine	236	2
	Gabapentin	171	2
	Benzotriazole	119	2
	Pyrazol	68	2
Positively charged pharmaceuticals	Sotalol	272	2
	Metoprolol	267	2
	Metformin	129	2
	Melamine	126	2

The dNF40 pilot was operated under two different operational conditions (round C1/C2), see table 3.5. The idea behind the operational conditions was minimizing the water loss of the dNF40 pilot and minimizing the fouling potential on the dNF40 membranes. The 90% recovery was chosen to minimize the water loss and the 20 LMH flux was chosen to minimize the fouling potential on the membrane. However, results from a previous study done at PWNT with WPJ pre-treated water showed that with 90% recovery, the norm set by PWN drinking water of 1.4 mmol/L for total hardness in the permeate was not met, see Appendix G. Only with a recovery below 80% this norm was met. For this reason the recovery was lowered to 70% for the second operational condition interval. To compensate for the greater water loss with 70% recovery, the flux was increased to 30 LMH.

In each round, the pilot was in operation for 2h to reach the permanent regime of filtration and maximum PFAS adsorption. After 2h, OMP samples were taken from the feed, permeate and concentrate stream for the installation retention calculations. To improve the comparison of the results for the 2 different sets of operational conditions, a new and identical spiking solution was prepared for each test. At the end of each test, the spiked WPJ pre-treated water was collected in an IBC and picked up by a third party company for safe disposal.

Table 3.5: Summary of operational conditions used during full recirculation filtration experiment.

	Recovery [%]	Flux [LMH]	Crossflow velocity [m/s]
Round C1	90	20	0.2
Round C2	70	30	0.2

3.2.3. Membrane performance parameters normalization

The membrane performance parameters were measured every round in both experiments. The membrane performance parameters included the MTC, TMP and NPD, see Chapter 2.5. The membrane performance parameters were generated from the Mexpert interface and normalized to a temperature of 20°C to comply with the temperature effect. The equations used to normalize the membrane performance parameters to a temperature of 20°C were given by NXF, see Equation 3.1, 3.2, 3.3 and 3.4 for TMP TC, NPD TC, flow TC and MTC TC respectively in which TC is temperature corrected and T is the temperature of the permeate water. The osmotic pressure, which is also dependent on the temperature, is not taken into account in these formulas.

$$TMP\_TC = TMP * 497 * (42.5 + T)^{-1.5} \tag{3.1}$$

$$NPD\_TC = NPD * 0.02582 * 10^{\frac{247.8}{T+133}} \tag{3.2}$$

$$NPD_{flow}\_TC = |NPD\_TC - static\ height\ correction| \tag{3.3}$$

$$MTC\_TC = MTC * \frac{0.02414 * 10^{\frac{247}{T+273-140}}}{0.02414 * 10^{\frac{247.8}{20+273-140}}} \tag{3.4}$$

3.2.4. Chemical cleaning of the membrane

Between every change in operational condition, a chemical cleaning of the membrane took place using the CIP protocol recommended by NXF. During the continuous filtration experiment, the CIP solution was discharged to the sewerage. During the full recirculation filtration experiment, the CIP solution was collected in an IBC and picked up by a third party company for safe disposal due to OMP concentrations in the CIP solution.

CIP was performed manually to avoid any risk such as leakages. The CIP was performed with a high pH solution (pH≈12) followed by a low pH solution (pH≈3). The protocol recommended by NXF was as follow:

1. Dosing high pH solution: NaOCl / NaOH 30 ppm $(NaOH)^+$ 130 ppm (NaOCl), 1.5 minutes dosing.
2. Soaking high pH solution: 30 minutes soaking.
3. Rinsing high pH solution: 1 minute rinsing with permeate water.
4. Dosing low pH solution: citric acid 3200 ppm, 1.5 minutes dosing.
5. Soaking low pH solution: 30 min soaking.
6. Rinsing low pH solution: 1 minute rinsing with permeate water.

3.2.5. Safety measures

PFAS is a compound which can be very harmful for the environment and health. To minimize the contact between the researcher and the spiked solution gloves, safety goggles and a lab coat should be worn during all experiments. Not only PFAS is harmful for the scientist health, but also the chemical solution used during the CIP and the chemical solution stored in some of the sample bottles. It was advised to wear gloves, a lab coat and safety goggles at all times.

3.3. Economic analysis

For the economic analysis, a full-scale dNF40 plant fed with WPJ pre-treated water and raw IJssellake water was compared with the full-scale UF-RO plant in Heemskerk. A projection report of a full-scale dNF40 plant had been made available based on the results of the experiments with the dNF40 pilot. This projection report contained plant specifications such as the amount of modules, the feed flow, the

total recovery percentages and the average applied pressure. Based on these specifications a cost-benefit analysis (CBA) was done to compare the economic feasibility of a full-scale dNF40 plant to the full-scale UF-RO plant in Heemskerk. The plant specifications for the UF-RO in Heemskerk were obtained from PWN data. The CBA has been simplified to OPEX and CAPEX. The OPEX included the energy cost, chemical cost, membrane replacement cost [48] and pre-treatment cost, see Equation 3.5. The waste disposal cost and labour cost have been considered out of the scope of these calculations. This is due to the fact that information on waste disposal cost for NF is missing and labour cost for NF and UF-RO are considered identical. The CAPEX include the equipment & installation cost [48] and pre-treatment cost, see Equation 3.6. Other possible CAPEX, such as land acquisition, planning and construction of buildings were excluded, since those cost factors are highly case dependent and subjective.

$$€_{\text{OPEX}} = €_{\text{energy}} + €_{\text{chemical}} + €_{\text{membrane}} + €_{\text{pre-treatment}} \tag{3.5}$$

$$€_{\text{CAPEX}} = €_{\text{equipment \& installation}} + €_{\text{pre-treatment}} \tag{3.6}$$

The energy cost, chemical cost and membrane replacement cost were calculated with Formula 3.7, 3.8 and 3.9 respectively, in which P_f is the average applied pressure (including feed pump, recirculation pumps and hydraulic cleaning pumps), Q_f is the feed flow, $V_{chemical}$ is the volume of the chemical, t is the operational time and N_{module} is the number of modules. The other relevant cost factors for the OPEX calculations can be found in table 3.6.

$$€_{\text{energy}} = \frac{Cf_e}{\eta} * P_f * Q_f \tag{3.7}$$

$$€_{\text{chemical}} = \Sigma(Cf_c * V_{\text{chemical}}) \tag{3.8}$$

$$€_{\text{membrane}} = \frac{Cf_{\text{module}}}{t} * N_{\text{module}} \tag{3.9}$$

The equipment and installation cost were calculated based on the number of membrane modules and the price of each membrane module (Cf_{module}). For the auxiliary components (pipes, pumps, valves, etc.) a price similar to the membrane price was used. The equipment and installation cost were calculated with Formula 3.10.

$$€_{\text{equipment \& installation}} = 2 * Cf_{\text{module}} * N_{\text{module}} \tag{3.10}$$

Table 3.6: Cost factors for the OPEX calculations.

Cost factor	Symbol	Unit	Value
Power supply efficiency	η	[-]	0.8
Electricity cost	Cf_e	€/kWh	0.10
UF membrane module price	Cf_{module}	€/module	1200
NF membrane module price	Cf_{module}	€/module	2500
RO membrane module price	Cf_{module}	€/module	800
Chemical cleaning cost	Cf_c		
NaOH (30%)		€/ton	300
NaOH (50%)		€/ton	300
NaOCl (12.5%)		€/ton	240
Citric acid (50%)		€/ton	1500
HCl (33%)		€/ton	240
CO_2		€/ton	78
Antiscalant ”2mg/l”		€/ton	690

4

Results and Discussion

4.1. Membrane performance

Fouling is one of the major challenges in the use of NF as an application for the direct filtration of raw surface water [43]. To determine the fouling potential of the dNF40 pilot, the membrane performance parameters (MTC, TMP and NPD) were evaluated under different operational conditions on raw IJssellake water. These experiments were done in continuous filtration mode in which the permeate, concentrate and backwash stream were discharged to the sewerage. The impact of operational conditions on the membrane performance parameters are discussed and presented in this chapter.

4.1.1. Performance parameters: impact of operational conditions

The membrane performance parameters MTC, TMP and NPD were measured during raw IJssellake water continuous filtration experiments to evaluate the fouling potential of the membrane. Figure 4.1 shows the MTC in LMH/bar of each filtration round, Figure 4.2 the TMP in bar and Figure 4.3 the NPD in bar. The red line is the temperature of the feed water. The MTC, TMP and NPD were corrected to a temperature of 20°C to enable fair comparison among performance parameters. The impact of the operational parameters on the fouling potential were evaluated by either increasing recovery, flux or crossflow velocity while keeping the other two operational conditions constant.

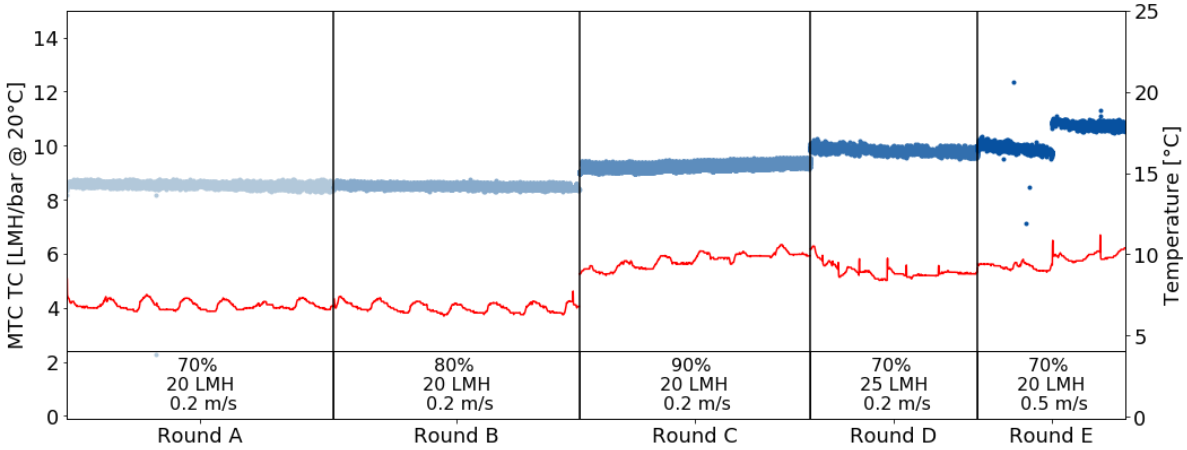

Figure 4.1: Mass transfer coefficient temperature corrected according to Equation 3.4 during different filtration rounds with raw IJssellake water. The red line indicates the temperature of the feed water.

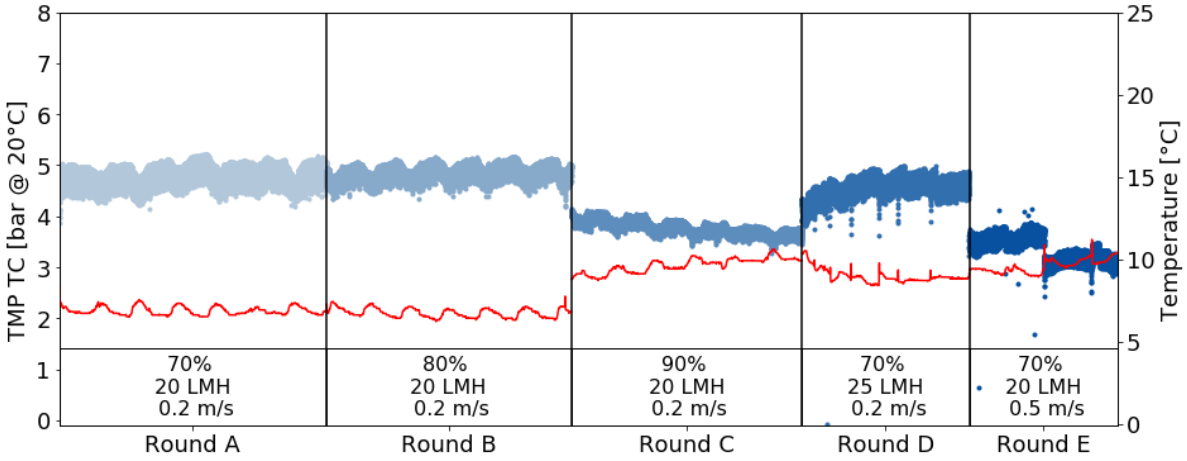

Figure 4.2: Trans membrane pressure temperature corrected according to Equation 3.1 during different filtration rounds with raw IJssellake water. The red line indicates the temperature of the feed water.

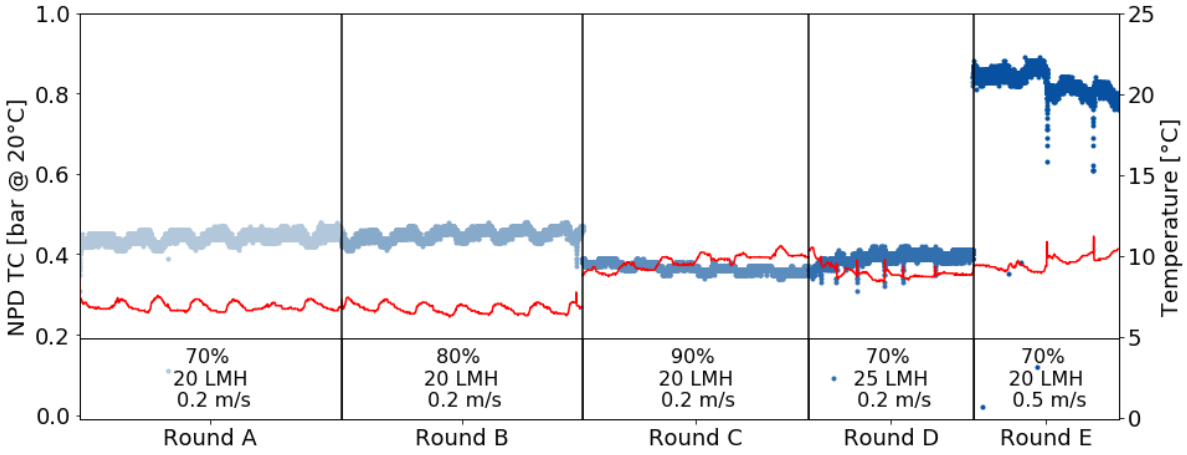

Figure 4.3: Normalized pressure drop temperature corrected according to Equation 3.2 during different filtration rounds with raw IJssellake water. The red line indicates the temperature of the feed water.

A smaller operation interval was observed in round D and E compared to round A, B and C. Throughout round D the pilot had difficulties operating at a flux of 25 LMH. Due to low feed water temperature, high flux and low recovery, the feed pump was running near its maximum capacity. Nearly everyday the pilot stopped running and when noticed restarted again. Throughout round E the pilot did not have access to the feed water during the weekend and turned off. After the weekend, when the pilot was turned on without performing a CIP a jump in MTC and drop in TMP and NPD was observed.

Within each constant operational condition interval the MTC, TMP and NPD were stable over time, see Figure 4.1, 4.2 and 4.3. This means that no fouling impact on MTC, TMP and NPD was observed when the pilot was fed with raw IJssellake water. The regular backwash and air scour cleaning (every filtration cycles) and weekly CIP might have helped to limit fouling formation on the membrane.

The impact of recovery on the membrane performance parameters was evaluated by increasing recovery from 70% (round A) to 80% (round B) to 90% (round C). Song et.al. [49] showed that with SW NF membranes using seawater as feed water, an increase in recovery resulted in a slight flux decline. This can be explained that when recovery increased more proportion of NF concentrate was recycled back to the NF feed stream (feed-and-bleed system). Consequently, this caused an increase of salt concentration in the NF feed stream resulting in a slight flux decrease. However, on the dNF40 pilot (feed-and-bleed system) a flux decline due to a decrease in MTC or increase in TMP was not observed,

see Figure 4.1 and 4.2. This might suggest that the increased salt concentration near the HF NF membrane with increasing recovery was not sufficient enough to cause flux decline. Increasing the recovery did show, however, a slight increase in MTC in round C (9.1 LMH/bar) compared to round A and B (8.5 LMH/bar). This change in performance can be related to an increase in feed water temperature, namely 6.9°C in round A and B to 9.6°C in round C. Gedam et.al. [50] using SW RO membranes observed a flux increase with elevated temperatures from 17°C to 40°C. However, in the experiments with SW RO membranes, the performance parameters were not corrected to similar temperature. In the continuous filtration experiment, MTC, TMP and NPD were corrected to a temperature of 20°C to comply with the change in viscosity and density of the different temperature feed waters. The slight change in performance parameters can be explained that not all parameters were considered in the temperature corrected calculations. A change in the membrane material due to a temperature change of the water was not considered. Emamjomeh [51] showed that a higher water temperature resulted in an expansion of the membrane material (bigger pores), while a lower water temperature resulted in a shrinkage of the membrane material (smaller pores). Moreover, temperature correction was performed for 20°C which is well above the average water temperature in the Netherlands. This might have impacted the change in performance parameters. Performance parameters remained stable under different recovery, but were slightly affected by feed water temperature.

The impact of flux on the membrane performance parameters was evaluated by increasing flux from 20 LMH (round A) to 25 LMH (round D). Fouling on the membrane occured when the critical flux is exceeded and the module operates outside the linear relationship regime between flux and TMP [7]. When fouling does not occur TMP should increase with increasing flux [52] resulting in a higher TMP in round D compared to round A. However, increasing flux showed similar TMP values in round A (4.8 bar) compared to round D (4.6 bar). The absence of this TMP increase in round D with higher flux can be explained by the lower feed water temperature in round A (6.9°C) compared to round D (9.0°C). When feed water temperature is lower, a higher TMP is needed to maintain the desired flux due to shrinkage of the membrane material [51]. Similar to recovery, the performance parameters remained stable under different fluxes, but were slightly affected by feed water temperature.

The impact of crossflow velocity on the membrane performance parameters was evaluated by increasing crossflow velocity from 0.2 m/s (round A) to 0.5 m/s (round E). It is known that as crossflow velocity increases, the risk of fouling decreases [53]. However, limited to no fouling was observed when operated at both crossflow velocities. Increasing crossflow velocity only seemed to affect NPD. NPD values were increased by almost a factor 2 in round E (0.83 bar) compared to round A (0.44 bar). This can be explained by the fact that increased crossflow velocities require more energy for feed circulation. Similar to recovery and flux, the performance parameters remained stable under different crossflow velocities, but were slightly affected by feed water temperature.

Limited to no fouling was observed on the membrane when feeding the dNF40 pilot with raw IJssellake water. Even little fishes which were pumped together with the raw IJssellake water into the feed tank and abundantly present in the feed tank did not contribute to fouling formation on the membrane. This is different from SW NF membranes and RO membranes. Frank et.al. [7] observed a flux decline when using HF and SW NF membranes fed with raw surface water from the river Rhine at Arnhem. It also demonstrated that even though fouling was happening in both membranes, HF NF membranes were less prone to fouling than SW NF membranes due to the possibility of backwash cleaning. In RO the main challenge to reliable membrane performance is membrane fouling, which results in the need of extensive pre-treatment of the feed water and effective and efficient cleaning of the membrane in order to reduce the fouling formation on the membrane [54].

The experiments with raw IJssellake water were performed in March 2022. However, the IJssellake water is subjected to seasonal variations in water quality. These seasonal variations in water quality might have an influence on the fouling formation of the membrane. For example, NOM, one of the important fouling constituents in surface water [55], can vary between 4 - 8 mg/L in raw IJssellake water dependent on the season. High concentrations of algal NOM are found in summer and low concentrations of BP are found in spring. Experiments with the dNF40 pilot on raw IJssellake water should be performed throughout the whole year to determine if seasonal variations play a role in membrane fouling.

4.2. Membrane retention

The dNF40 permeate water quality is important to determine the suitability of the dNF40 pilot for PWN drinking water purposes. In this chapter the ion retention and NOM removal under different operational conditions fed with raw IJssellake water are evaluated. These experiments were done in continuous operation mode in which the permeate stream and the concentrate stream were discharged to the sewerage.

4.2.1. Ion concentration in feed stream

Figure 4.4 shows the initial concentration in mg/L of different ions in the feed stream raw IJssellake water for the operation of the different conditions. These ion concentrations in the feed stream represent the ion concentrations before the feed water enters the membrane module and recirculation loop. The ion concentrations in the feed stream of raw IJssellake water are needed to calculate the installation retention of the ions passing the dNF40 membrane, see Equation 2.3. Therefore, it is favourable to have similar ion concentrations in the feed stream to enable fair comparison between the installation retention of the different rounds. From Figure 4.4 it can be observed that ion concentrations fluctuated only slightly, which results in negligible impact on the ion retention. The ion concentration of barium (Ba^{+}), phosphate (PO_4^{3-}) and iron (Fe^{2+} / Fe^{3+}) were extremely low. These three compounds were not considered when calculating the installation and membrane retention of the dNF40 pilot.

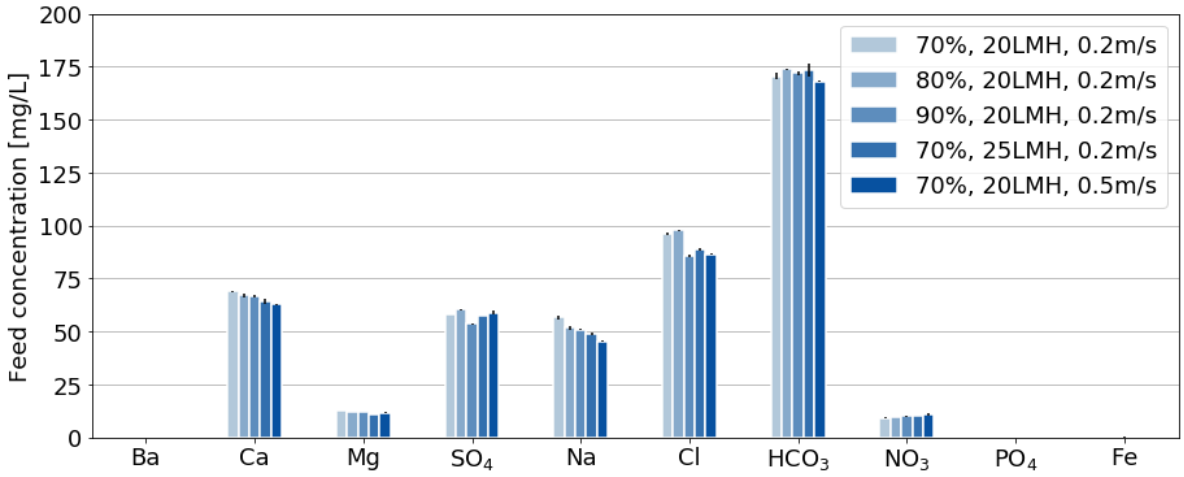

Figure 4.4: Ion concentration in feed stream under different conditions with raw IJssellake water.

4.2.2. Ion installation retention: impact of recovery

Recovery was increased from 70% to 80% to 90% to determine the effect of recovery on ion retention. Figure 4.5 shows the installation retention in % based on ion concentrations measured in the feed stream and the permeate stream of different ions when operated under 70%, 80% and 90% recovery. The flux and crossflow velocity remained constant at 20 LMH and 0.2 m/s. The installation retention was calculated with Equation 2.3. The red numbers above the bars represent the CF of each ion. The installation retention during the different filtration rounds with increasing recovery varied in the range of 2%-85%. The ions Cl^{-} and NO_3^{-} were negatively retained by the membrane. The membrane retention of the ions can be found in Appendix B.

The ion retention of the ions which were partially retained by the membrane decreased with increasing recovery. This is in line with experiments done on the dNF40 pilot with WPJ pre-treated water, see Appendix C. The decrease in ion retention can be explained by the concentration factor (CF), which can be calculated with the following Equation [49]:

$$CF = \frac{1 - R(1 - R_{obs})}{1 - R} \tag{4.1}$$

with R the recovery and R_{obs} the observed ion retention. An increase in recovery leads to an increase in CF for most ions and consequently to a decrease in ion retention. At higher recovery the boundary layer near the membrane is thicker, due to a higher concentration of ions near the membrane. This results in an increase in concentration gradient across the membrane and consequently an increase in diffusive transport of ions to the permeate side, hence a decrease in ion retention. A decrease in ion retention has also been observed by Song et.al. [49] on SW NF membranes with recovery values increasing from 40% to 65% and corresponding increasing CF values from 1.25 to 1.52, although the decrease in retention for especially SO_4^{2-} was less severe.

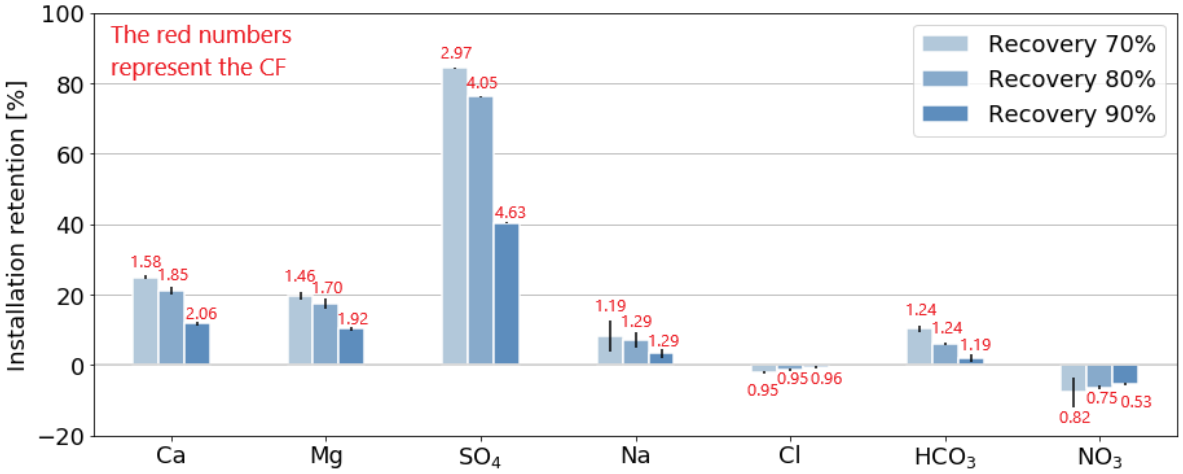

Figure 4.5: Ion installation retention based on concentrations measured in feed stream and permeate stream during filtration with raw IJssellake water at 70%, 80% and 90% recovery - 20 LMH flux - 0.2 m/s crossflow velocity. The ions barium, phosphate and iron were not considered when calculating the ion retention of the dNF40 pilot, due to low concentrations in feed stream (see Figure 4.4). The red numbers above the bars represent the CF of each ion.

The retention mechanisms to retain ions by NF membranes is both due to size (steric) exclusion and Donnan (charge) exclusion [25]. The retention of the divalent ions Ca^{2+}, Mg^{2+} and SO_4^{2-} was higher than the retention of the monovalent ions Na^+, Cl^-, HCO_3^- and NO_3^- due to their larger hydrated size and charge, see Table 4.1 [25]. The negative charged divalent ion SO_4^{2-} had with a retention in the range of 40%-84% the highest retention. This was followed by the positive charged divalent ions Ca^{2+} and Mg^{2+} with a retention in the range of 12%-25%. The positive charged monovalent ion Na^+ and negative charged monovalent ion HCO_3^- had with a retention in the range of 2%-10% the lowest retention.

Cheng et.al. [25] explored the retention of cations with positively charged LbL NF membranes. This research showed that Mg^{2+} is retained better than Ca^{2+} followed by Na^+, due to the difference in hydrated radius and ionic radius. A bigger hydrated radius leads to a stronger size exclusion between the ion and the membrane. Looking at the cations, Mg^{2+} has the biggest hydrated radius followed by Ca^{2+} and then Na^+, see Table 4.1. A higher ionic radius results in a lower ionic charge density leading to weaker electrostatic repulsion between the ion and the membrane surface. Mg^{2+} has the lowest ionic radius followed by Ca^{2+} and then Na^+, see Table 4.1. Comparing the positive charged ions in the raw IJssellake water experiment, Ca^{2+} was retained better than Mg^{2+} which was retained better than Na^+. The better retention of Ca^{2+} over Mg^{2+} is not on line with the hydrated size and ionic charge of these cations. However, this difference in retention between Ca^{2+} and Mg^{2+} was negligible small (25% over 21% at 70% recovery).

The negative terminal layer of the dNF40 membrane showed a typical Donnan exclusion in which higher retention values were observed for the negative multivalent ion SO_4^{2-} compared to the positive multivalent ions Ca^{2+} and Mg^{2+}. Even though size exclusion is the dominant retention mechanism

in nanofiltration, the underlying positive layer can have an effect on the retention of positive ions as well. Inside a polyanion-polycation multilayer, polycations can be excessively present in the multilayer creating a surplus positive charge which rejects the positive ions [56]. Although this rejection of positive ions is hindered by the negative terminal layer on the membrane, hence the lower retention values for Ca^{2+} and Mg^{2+}.

The ions Cl^- and NO_3^- had a negative retention, which meant that the concentration of these two ions was higher in the smaller permeate volume than in the much larger feed volume. Negative retention of ions in NF can be explained by the charge electroneutrality principle [57]. LbL HF NF membranes are mostly developed to reject divalent ions over monovalent ions. The monovalent ions Cl^- and NO_3^- are in competition with the divalent ion SO_4^{2-} and the monovalent ion HCO_3^- (bigger hydrated radius than Cl^- and NO_3^-, see Table 4.1). The membrane permeability with respect to SO_4^{2-} is lower than with respect to Cl^- and NO_3^-. To comply with charge neutrality on both sides of the membrane, the only anions available to neutralize the permeate stream are Cl^- and NO_3^- [58, 59]. This results in a transport of Cl^- and NO_3^- to the permeate side, hence the negative retention of these two ions.

Table 4.1: MW, charge, hydrated radius and ionic radius of the ions.

Ion compound	MW [g/mol]	Charge [-]	Hydrated radius [nm]	Ionic radius [nm]
Ca	40.1	2+	0.412	0.100
Mg	24.3	2+	0.428	0.072
SO_4	96.1	2-	0.379	0.290
Na	23.0	1+	0.358	0.102
Cl	35.5	1-	0.332	0.181
HCO_3	61.0	1-	0.364	0.156
NO_3	62.0	1-	0.335	0.264

Scaling is one of the four fouling types in membrane filtration [43]. Scaling on the membrane can occur if the concentration of ions in the boundary layer exceeds the solubility limit of certain ions [33]. Increasing the recovery results in a higher concentrations of ions near the membrane. This higher concentrations of ions in the boundary layer can promote scaling on the membrane. Lee et.al. [60] observed that once the solubility limit exceeded, a further increase in CF resulted in a flux decline due to $CaSO_4$ scaling on the membrane surface when using SW, tubular and plate and frame NF membranes fed with a supersaturated $CaSO_4$ solution. Chapter 4.1 showed that no fouling layer was formed on the dNF40 membrane. This presumes that the concentration of ions in the boundary layer did not exceed the solubility limit or that the operational conditions and hydraulic cleaning cycles were efficient enough to wash away any scale formation on the membrane surface.

4.2.3. Ion installation retention: impact of flux

Flux was increased from 20 LMH to 25 LMH to determine the effect of flux on ion retention. Figure 4.6 shows the installation retention in % based on ion concentrations measured in the feed stream and the permeate stream of different ions when operated under 20 LMH and 25 LMH flux. The recovery and crossflow velocity remained constant at 70% and 0.2 m/s. The installation retention was calculated with Equation 2.3. The red numbers above the bars represent the CP degree of each ion. The installation retention during the different filtration rounds with increasing flux varied in the range of 7%-84%. The ions Cl^- and NO_3^- were negatively retained by the membrane.

The ion retention of the ions which were partially retained by the membrane decreased with increasing flux. This is not in line with experiments done on the dNF40 pilot with WPJ pre-treated water, see Appendix C. These results showed that the ion retention is not significantly influenced by filtration flux and that the observed slight reduction in ion retention can be correlated to the increase in CP with elevated flux. In addition, two former master students looked at the ion retention with increasing flux on the Mexplorer (lab-scale installation). Van der Poel [10] found an increase in retention with elevated flux for all ions and Arun [9] found an increase in retention with elevated flux for the positive charged monovalent ions and a decrease in retention with elevated flux for the positive charged divalent ions.

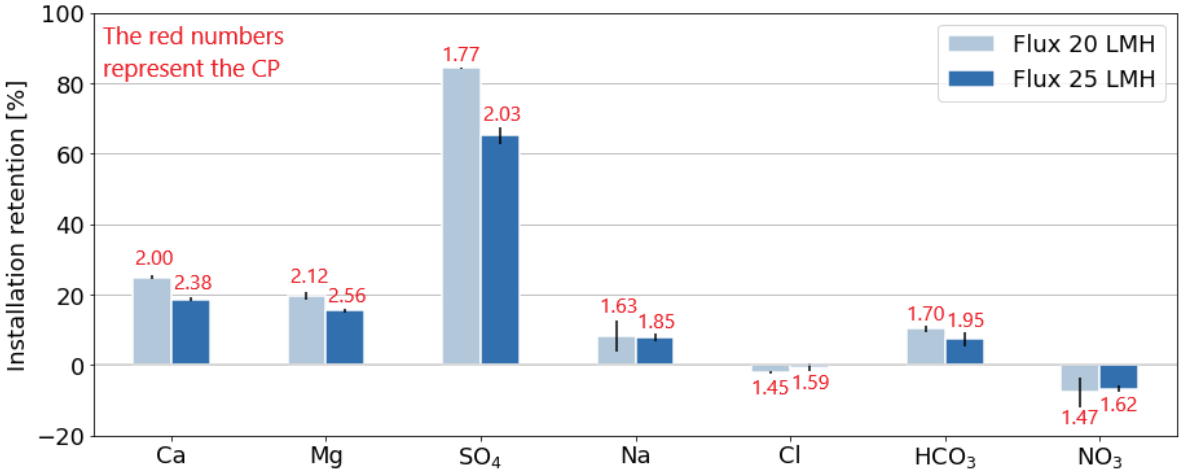

Figure 4.6: Ion installation retention based on concentrations measured in feed stream and permeate stream during filtration with raw IJssellake water at 20 LMH and 25 LMH flux - 70% recovery - 0.2 m/s crossflow velocity. The ions barium, phosphate and iron were not considered when calculating the ion retention of the dNF40 pilot, due to low concentrations in feed stream (see Figure 4.4). The red number above the bars represent the CP degree of each ion.

When flux increases, two phenomena play a role. First of all, the convective transport across the membrane increases with increasing flux and consequently more feed water passes the membrane to the permeate side [61]. The ion concentration will be diluted in a bigger volume of water on the permeate side resulting in a higher retention of ions. Secondly, CP intensifies with increasing flux and a thicker boundary layer near the membrane is formed due to an increase in concentration of ions near the membrane. This results in an increase in diffusive transport of ions to the permeate side, hence a decrease in ion retention [61, 51]. It seemed that in the dNF40 membrane the ion retention is potentially more dominated by diffusive transport instead of convective transport. This can also be observed by the red numbers above the bars which show that the CP degree, calculated with Equation 2.12, increased with elevated flux. That diffusive transport is more dominant can possibly be related to the low crossflow velocity (0.2 m/s) which enhance the effect of CP near the membrane [6]. Another reason for the decrease in ion retention with elevated flux could be the increase in MTC from 8.5 LMH/bar in round A (Flux 20 LMH) to 9.8 LMH/bar in round 4 (Flux 25 LMH), see Figure 4.1. An increase in MTC represents a bigger pore size in the membrane or potentially a decrease in the thickness of the active membrane layer and more ions are able to pass to the permeate side [8].

The negative charged divalent ion SO_4^{2-} had with a retention in the range of 65%-84% the highest retention. This is followed by the positive charged divalent ions Ca^{2+} and Mg^{2+} with a retention in the range of 16%-25%. The positive charged monovalent ion Na^+ and negative charged monovalent ion HCO_3^- had with a retention in the range of 7%-10% the lowest retention. The ions Cl^- and NO_3^- were negatively retained by the membrane. This order in retention was also observed during the filtration rounds with increasing recovery (see Figure 4.5).

The negative retention of the monovalent ions Cl^- and NO_3^- allows the permeate side of the HF NF membrane to have a higher osmotic pressure than the permeate of other NF membranes that partially reject monovalent ions as well as multivalent ions [58]. This gives the advantage of HF NF membranes over other NF membranes to operate with lower applied feed pressures due to the smaller difference in osmotic pressure across the membrane [58].

4.2.4. Ion installation retention: impact of crossflow velocity

Crossflow velocity was increased from 0.2 m/s to 0.5 m/s to determine the effect of crossflow velocity on ion retention. Figure 4.7 shows the installation retention in % based on ion concentrations measured in the feed stream and the permeate stream of different ions when operated under 0.2 m/s and 0.5 m/s crossflow velocity. The recovery and flux remained constant at 70% and 20 LMH. The installation retention was calculated with Equation 2.3. The red numbers above the bars represent the CP degree of each ion. The installation retention during the different filtration rounds with increasing crossflow velocity varied in the range of 5%-84%. The ions Cl^- and NO_3^- were negatively retained by the membrane.

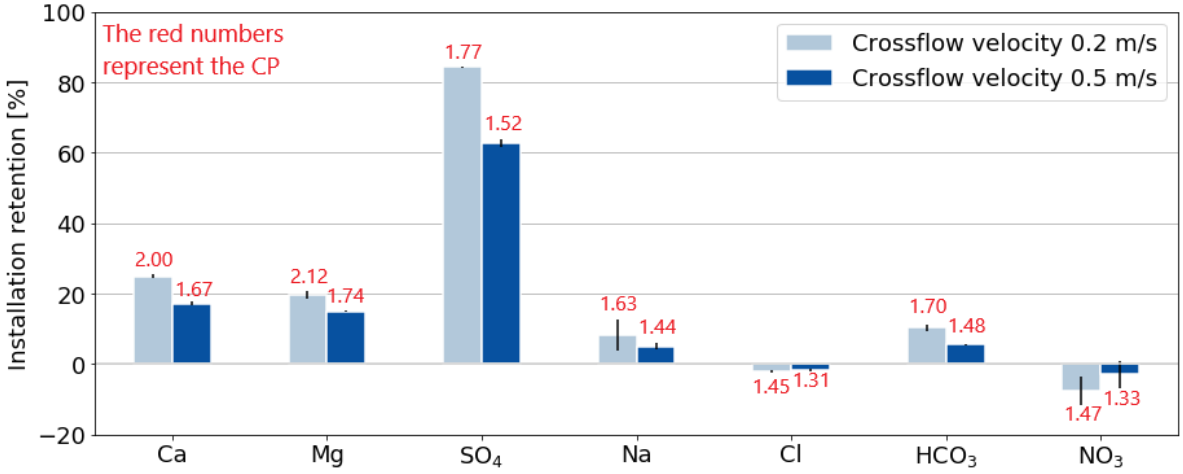

Figure 4.7: Ion installation retention based on concentrations measured in feed stream and permeate stream during filtration with raw IJssellake water at 0.2 m/s and 0.5 m/s crossflow velocity - 70% recovery - 20 LMH flux. The ions barium, phosphate and iron were not considered when calculating the ion retention of the dNF40 pilot, due to low concentrations in feed stream (see Figure 4.4). The red number above the bars represent the CP degree of each ion.

The ion retention of the ions which were partially retained by the membrane decreased with increasing crossflow velocity. This is in line with experiments done on the dNF40 pilot with WPJ pre-treated water, see Appendix C. These results showed that the ion retention decreased with increasing crossflow velocity. However, theoretically it is the contrary, as can also be observed by the red numbers above the bars which show the CP degree with elevated crossflow velocity calculated with Equation 2.12. An increase in crossflow velocity should lead to a decrease in CP and thus a decrease in the thickness of the boundary layer near the membrane surface resulting in a decrease in diffusive transport across the membrane [62, 63], hence an increase in ion retention. An increase in $MgSO_4$ retention with elevated crossflow velocity was observed by Junker et.al. [6] using LbL HF NF membranes. The decrease in ion retention with elevated crossflow velocity on the dNF40 can possibly be explained by the increase in MTC from 8.5 LMH/bar in round A (crossflow velocity 0.2 m/s) to 10.3 LMH/bar in round E (crossflow velocity 0.5 m/s). A higher MTC represent a bigger pore size in the membrane or potentially a decrease in the thickness of the active membrane layer and more ions are able to pass to the permeate side decreasing the retention [8].

During the filtration rounds with increasing crossflow velocity, the same order in retention of the ions was observed compared to the filtration rounds with increasing recovery (see Figure 4.5) and increasing flux (see Figure 4.6). The negative charged divalent ion SO_4^{2-} had with a retention in the range of 63%-84% the highest retention. This was followed by the positive charged divalent ions Ca^{2+} and Mg^{2+} with a retention in the range of 15%-25%. The positive charged monovalent ion Na^+ and negative charged monovalent ion HCO_3^- had with a retention in the range of 5%-10% the lowest retention. The ions Cl^- and NO_3^- were negatively retained by the membrane.

4.2.5. Total hardness removal

Considering the potential application of the dNF40 pilot fed with raw IJssellake water to be used as a one-step treatment process for drinking water purposes, the total hardness in the permeate stream was analyzed. The desired total hardness norm by PWN for drinking water purposes is below 1.4 mmol/L. Figure 4.8 shows the total hardness in mmol/L based on Ca^{2+} and Mg^{2+} concentrations measured in the permeate stream during filtration at 70%, 80% and 90% recovery. The flux and crossflow velocity remained constant at 20 LMH and 0.2 m/s. The red line at 1.4 mmol/L indicates the desired hardness norm of PWN drinking water.

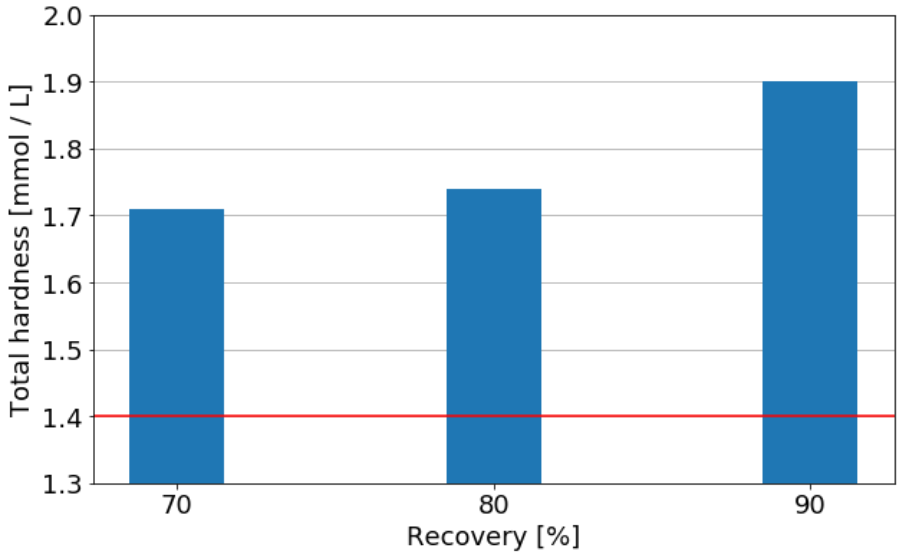

Figure 4.8: Total hardness based on Ca^{2+} and Mg^{2+} concentrations in permeate stream during filtration with raw IJssellake water at 70%, 80% and 90% recovery - 20 LMH flux - 0.2 m/s crossflow velocity. The red line at 1.4 mmol/L represent the norm of PWN drinking water.

All filtration experiments showed much higher total hardness values than the desired 1.4 mmol/L. The total hardness in the dNF40 permeate stream indicate that the dNF40 pilot as a one-step treatment process did not achieve the desired norm set by PWN. With the implementation of a multiple stage system, a total hardness value below 1.4 mmol/L could possibly be achieved. This will be explained in more detail in Chapter 4.8.2. In addition, previous experiments done on the dNF40 pilot fed with WPJ pre-treated water showed that total hardness values in the permeate stream below 1.4 mmol/L were achieved when operated below 80% recovery, see Appendix G. This suggest that the active outer layer of the dNF40 membrane might have undergone a change in properties when operated with raw IJssellake water leading to higher total hardness values in the permeate stream. This will be explained in more detail in Chapter 4.3.

4.2.6. Natural organic matter removal

NOM in water is indicated by the TOC. The importance of the removal of NOM from the water is that NOM can contribute to the formation of disinfection by-products and promote the regrowth of bacteria in the distribution system [17]. TOC concentrations in feed and permeate stream were measured to determine the TOC removal by the dNF40 pilot under different operational conditions using Equation 2.3. The results are presented in Table 4.2. TOC removal was consistently above 90% for every operational condition which indicate that a change in operational condition did not have an effect on the removal of TOC. This is due to the fact that the dNF40 pore size is generally smaller than the size of typical organic compounds. The operational conditions did, however, have an effect on the retention of the ions. These high percentages of TOC removal have also been observed in literature. Haddad et.al. [64] showed that the NOM removal on a lab scale crossflow filtration set-up containing thin-film

HF NF membranes with a MWCO of 200 Da was consistently above 90% regardless of their initial concentration.

Table 4.2: Feed concentration TOC and TOC removal based on concentration measured in feed stream and permeate stream during filtration with raw IJssellake water at different operational conditions.

Operational condition	Feed concentration [mg/L C]	TOC removal [%]
70%, 20 LMH, 0.2 m/s	5.8	95
80%, 20 LMH, 0.2 m/s	6.1	95
90%, 20 LMH, 0.2 m/s	6.3	92
70%, 25 LMH, 0.2 m/s	6.5	95
70%, 20 LMH, 0.5 m/s	6.2	93

NOM consist out of different fractions which can be hydrophobic or hydrophilic and charged or neutral [18]. In addition, every fraction has their different size and thus different molecular weight [18]. The fractions of NOM consist out of acids, BP, BB, HOC, HS, neutrals and POC. The TOC is subdivided into the fractions acids, BP, BB, HOC, HS, neutrals and POC. The properties of the fractions can be found in Table 4.3.

Table 4.3: Properties of the fractions in NOM [18].

Fraction	Hydrophobic / Hydrophilic	Charge	Molecular Weight [g/mol]
Acids	N.A.	-	< 350
Biopolymers	Hydrophilic	0	> 10,000
Building blocks	Hydrophilic	N.A.	300 - 500
HOC	Hydrophobic	0	N.A.
Humic substances	Hydrophilic	N.A.	800 - 1000
Neutrals	Hydrophilic	0	< 350

In order to determine the fraction removal of TOC by the dNF40 pilot, an LC-OCD analysis was performed on round A with operational conditions 70%, 20 LMH and 0.2 m/s. Figure 4.9 shows the concentration in μg/L C of the different fractions in TOC measured in the feed, permeate and concentrate stream during raw IJssellake water filtration. Figure 4.10 shows the removal in % of the different fractions in TOC based on the concentrations measured in the feed stream and the permeate stream.

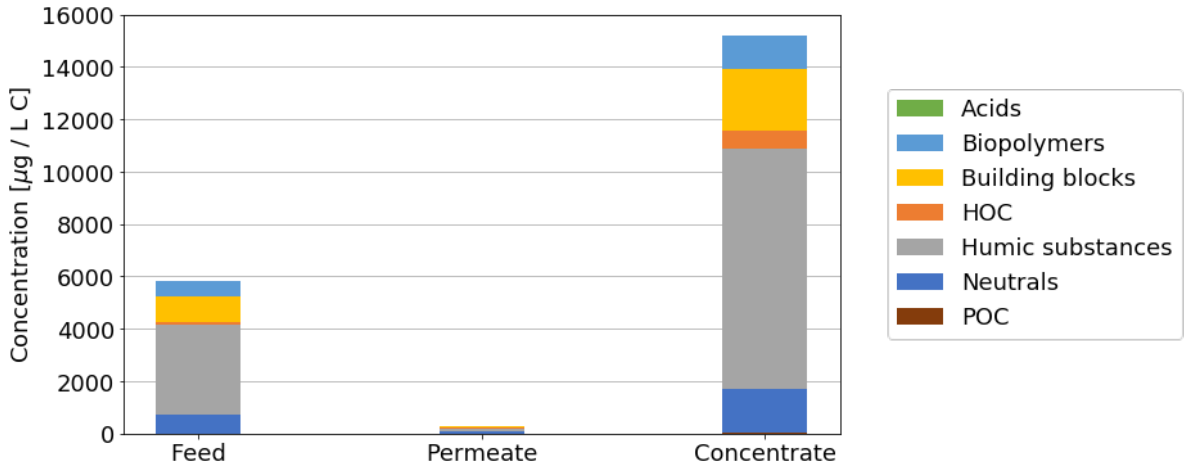

Figure 4.9: The concentration of the fractions of TOC measured in the feed, permeate and concentrate stream during filtration with raw IJssellake water at 70% recovery - 20 LMH flux - 0.2 m/s crossflow velocity.

In the feed stream, the concentration of HS was with 3436 μg/L C the highest, followed by BB with 984 μg/L C. The concentration of BP and neutrals was around 600 μg/L C and the concentration of HOC was 115 μg/L C. Acids and POC had the lowest concentrations in the feed stream. These two fractions were not considered when calculating the removal of the different fractions of the dNF40 pilot. In the permeate stream, the concentration of all fractions was below 80 μg/L C. In the concentrate stream, the concentration of HS was with 9206 μg/L C the highest, followed by BB with 2387 μg/L C. Also here the concentration BP and neutrals was similar, around 1500 μg/L C and the concentration of HOC was 662 μg/L C. Acids and POC had also here the lowest concentration.

The retention mechanisms to remove NOM fractions by NF membranes is both attributed to size (steric) exclusion and Donnan (charge) exclusion [64]. However, due to the large MW of the NOM fractions and considering that most NOM fractions are neutral, size (steric) exclusion will most likely be dominant over Donnan (charge) exclusion [65]. The factions BP, BB and HS had with a removal of above 96% the highest removal percentage. This can be explained by their MW which is much higher than the MWCO of the membrane (400 Da). The neutrals with a removal percentage of 89% were removed less than the fractions BP, BB and HS. The MW of the neutrals is also smaller than the MW of the BP, BB and HS, but still around the MWCO of the membrane. HOC had with a removal percentage of 43% the lowest removal percentage. However, the HOC concentration in the feed and permeate stream of the dNF40 pilot is possibly hindered by the chromatographic column of the LC-OCD analysis. The HOC fraction is adsorbing on the chromatographic column due to its hydrophobic character and is measured by subtracting all NOM fractions from the total DOC (measured from the bypass) [66]. This can possibly give uncertainties in the removal percentage of HOC by the dNF40 membrane.

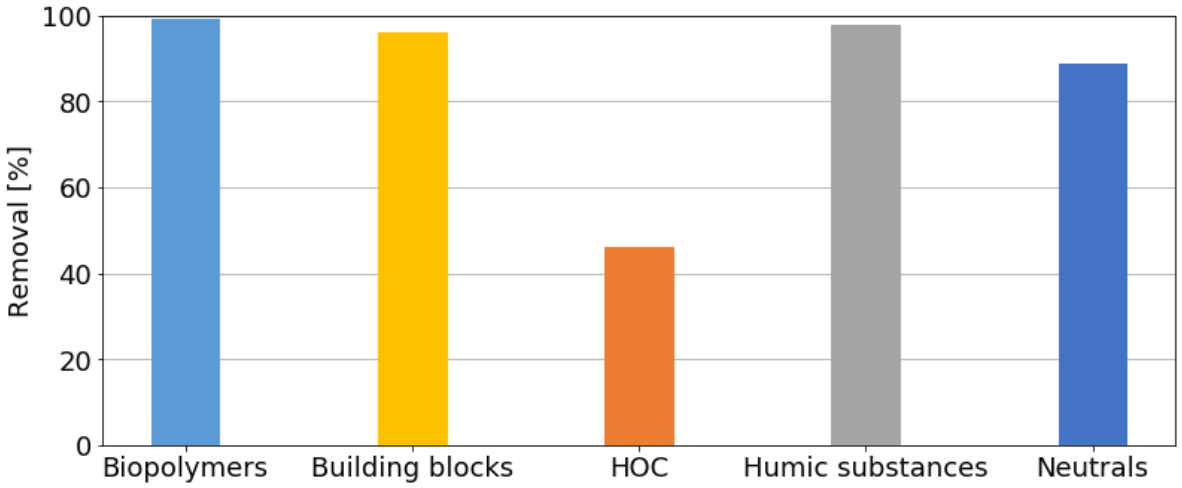

Figure 4.10: NOM removal based on concentrations measured in feed stream and permeate stream during filtration with raw IJssellake water at 70% recovery - 20 LMH flux - 0.2 m/s crossflow velocity. The fractions acid and POC were not considered when calculating the fraction removal of the dNF40 pilot, due to low concentrations in feed stream.

NOM is one of the most important fouling constituents in surface water filtration [55]. Especially in the presence of Ca^{2+}, a compact and highly resistant fouling layer can form on the membrane due to the binding of Ca^{2+} to acidic functional groups of NOM [67]. However, Chapter 4.1 shows that no fouling layer was observed on the membrane. This presumes that, even if, Ca^{2+}-NOM complexes are formed, the operational conditions and hydraulic cleaning cycles are most likely efficient enough to wash away any deposited layer attached to the membrane surface.

4.3. Comparison to WPJ pre-treated water

Previously PWNT conducted a study on the feasibility of the dNF40 pilot on WPJ pre-treated water. This chapter compares the membrane performance parameters and membrane retention of the dNF40 pilot on WPJ pre-treated water and raw IJssellake water. Both experiments were done in continuous operation mode in which the permeate stream and the concentrate stream were discharged to the sewerage.

4.3.1. Performance parameters: comparison to pre-treated water

The limited to no fouling results of the dNF40 pilot with HF NF membranes on raw IJssellake water, presented in Chapter 4.1, show superiority of HF NF membranes over SW NF membranes and RO membranes. However, over the long term operation of the dNF40 pilot unusual results were observed regarding membrane performance. Two studies have been done on the same membrane of the dNF40 pilot. In a previous study done at PWNT, the pilot was fed with WPJ pre-treated water and the dNF40 membrane was new (virgin membrane). This study was done with raw IJssellake water on the same membrane but one year later (1 year old membrane). The previous study, looked into the feasibility of the dNF40 pilot on WPJ pre-treated water under different operational conditions. During these experiments the membrane performance parameters were studied to determine the fouling potential on the membrane. WPJ pre-treated water has undergone extensive pre-treatment steps before the water entered the dNF40 pilot, see Figure 3.3. The operational conditions which were tested during the filtration rounds with WPJ pre-treated water can be found in Appendix D, as well as the membrane performance parameters (MTC, TMP and NPD) of these rounds. Similar to the experiments with raw IJssellake water, limited to no fouling was observed on the membrane with WPJ pre-treated water. The changes in performance parameters during filtration with WPJ pre-treated water were mainly correlated to feed water temperature changes. Since in both experiments (WPJ pre-treated water and raw IJssellake water) the MTC, TMP and NPD were stable within each constant operational condition interval, the values were averaged for comparison. Three rounds with similar operational conditions, but different feed water composition were compared. Table 4.4 shows the operational conditions of which the MTC, TMP and NPD were compared.

Table 4.4: The operational conditions used in both experiments with WPJ pre-treated water and raw IJssellake water. The MTC, TMP and NPD of these rounds can be compared.

Recovery [%]	Flux [LMH]	Crossflow velocity [m/s]
70	20	0.2
80	20	0.2
90	20	0.2

Figure 4.11 shows the average MTC in LMH/bar with increasing recovery of WPJ pre-treated water (green) and raw IJssellake water (blue). Flux and crossflow velocity remained constant at 20 LMH and 0.2 m/s. The filtration rounds with WPJ pre-treated water were performed with a virgin membrane (April 2021) and the filtration rounds with raw IJssellake water were performed when the membrane was one year old (April 2022). The average TMP and NPD with increasing recovery of WPJ pre-treated water and raw IJssellake water can be found in Appendix E. The MTC of raw IJssellake water was on average a value 1.5 LMH/bar higher as opposed to the MTC of WPJ pre-treated water. An increase in MTC over the long-term has not been seen in literature before, since MTC normally decreases over the long-term due to the formation of (irreversible) fouling on the membrane. On the long-term a MTC decrease was observed by Beyer et.al. [68] on NF membranes (5 years of operation) and Jafari et.al. [69] on RO membranes (2 years of operation) due to fouling formation and even a chemical cleaning of the membrane was not able to restore the MTC of these membranes to its original starting values. Though no fouling was observed on the membrane during operation with the dNF40 pilot, an increase in MTC over the long-term is unusual. This might imply that the active outer layer of the dNF40 membrane have undergone a change in properties when operated with raw IJssellake water. In addition, a jump in MTC was observed in round E when the dNF40 pilot fed with raw IJssellake water was not running over

the weekend, as shown in Chapter 4.1.1. This potentially gives another indicator that the properties of the outer active layer of the membrane surface might have changed during round E. An increase in MTC can, however, can give uncertainties in the retention of compounds. A higher MTC represent a bigger pore size in the membrane or a decrease in the thickness of the active membrane layer and more compounds are able to pass to the permeate side [8]. This will be explained in more detail in the next Chapter 4.3.2.

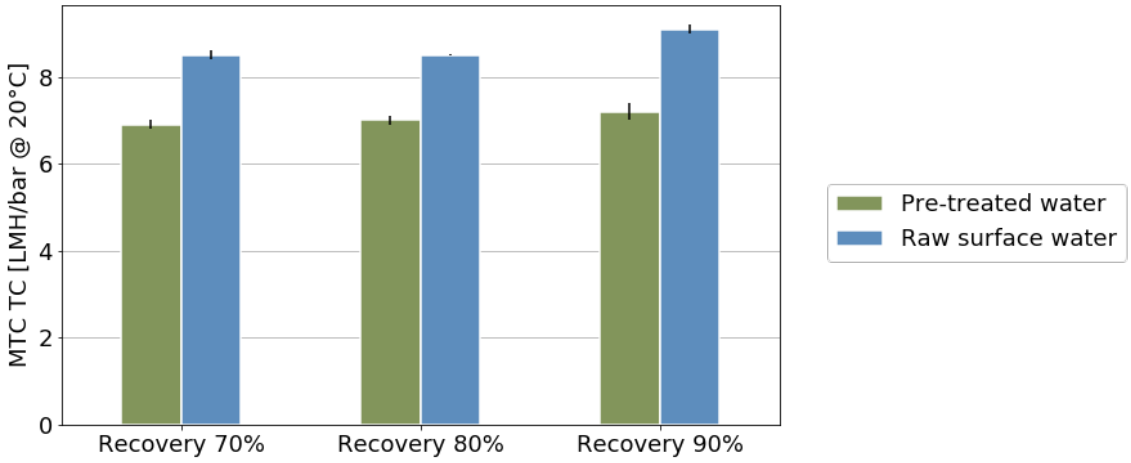

Figure 4.11: Average mass transfer coefficient temperature corrected of WPJ pre-treated water and raw IJssellake water with increasing recovery. Flux and crossflow velocity remained constant at 20 LMH and 0.2 m/s.

4.3.2. Ion installation retention: comparison to pre-treated water

Figure 4.12 shows the installation retention in % based on ion concentrations measured in the feed stream and the permeate stream of different ions when operated with WPJ pre-treated water (green bars) and raw IJssellake water (blue bars). The pilot was operated under 70%, 80% and 90% recovery. The flux and crossflow velocity remained constant at 20 LMH and 0.2 m/s. The installation retention was calculated with Equation 2.3. The installation retention during the different filtration rounds with WPJ pre-treated water varied in the range of 3%-96%. The ion retention of the ion Na^+ was not measured during filtration with WPJ pre-treated water and is not shown in the graph. The installation retention during the different filtration rounds with raw IJssellake water varied in the range of 2%-84%.

During the filtration rounds with WPJ pre-treated water the ion retention of the ions which were partially retained by the membrane decreased with increasing recovery. This was also observed during the filtration rounds with raw IJssellake water. Filtration rounds with raw IJssellake water showed a lower retention for the different ions than filtration rounds with WPJ pre-treated water. The ion retention during raw IJssellake water was lower than expected. Especially during filtration round with 90% recovery and raw IJssellake water, the SO_4^{2-} was retained only by 40% which is low compared to literature. This big difference in retention can be explained by the increase in MTC of 1.5 LMH/bar in raw IJssellake water (compared to WPJ pre-treated water) caused by a change in properties of the active membrane layer, as shown in Figure 4.11. A higher MTC represent a bigger pore size in the membrane or a decrease in the active membrane layer and more ions are able to pass to the permeate side reducing the retention [8].

An increase in MTC and consequently a lower retention of ions by the dNF40 membrane has its advantages and disadvantages. Due to the increase in MTC, less energy is required to press water through the membrane saving on energy cost. In addition, the bicarbonate concentration in the permeate stream is higher which results in a decrease in post conditioning cost. However, the increase in MTC resulted in high concentrations of total hardness in the permeate exceeding the desired norm by PWN for drinking water purposes, see Chapter 4.2.5. This can result in an increase in cost to reduce the total hardness in the permeate.

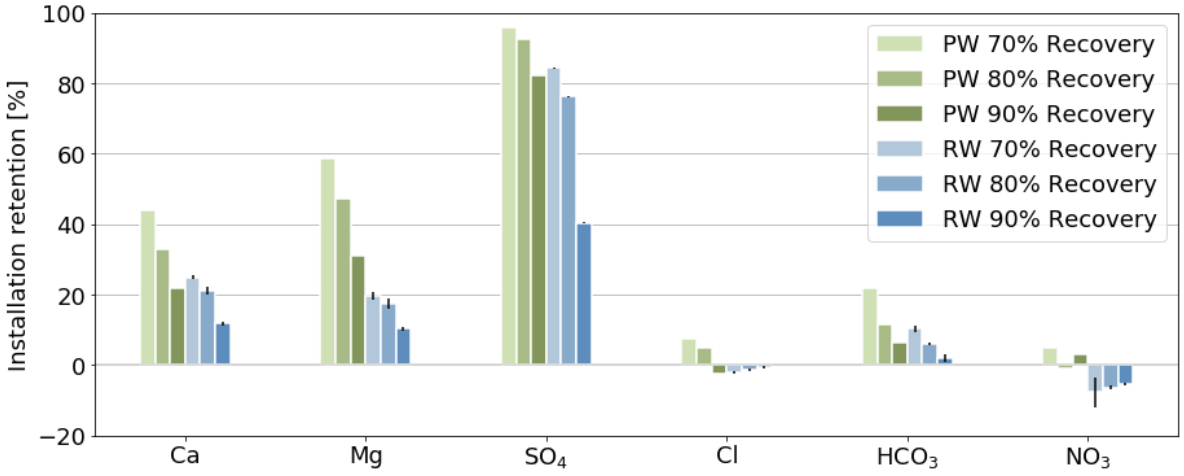

Figure 4.12: Ion installation retention based on concentrations measured in feed stream and permeate stream during filtration with WPJ pre-treated water (green bars) and raw IJssellake water (blue bars) at 70%, 80% and 90% recovery - 20 LMH flux - 0.2 m/s crossflow velocity. PW stands for pre-treated water and RW stands for raw surface water. Na^+ is not shown, because it was only measured during the experiments with raw IJssellake water.

The water matrix might also have an influence on the rejection of ions from the water. Haddad et.al. [64] observed that the ions Ca^{2+} and Mg^{2+} are able to bind to the sulphonic groups of the dNF40 membrane weakening the negative charge of the membrane. This weakens the rejection by Donnan (charge) exclusion between the negative ion SO_4^{2-} and the negative charged membrane and more SO_4^{2-} ions are able to pass to the permeate side decreasing the retention. However, the ion concentration of Ca^{2+} and Mg^{2+} in WPJ pre-treated water was similar to the concentration in raw IJssellake water, see Appendix F. The compound NOM might also be able to alter the charge of the membrane. Especially in the presence of Ca^{2+}, NOM can adsorb on negative membrane surfaces decreasing the negative surface charge of the membrane and decreasing the retention of negative ion compounds [67]. The NOM concentration was higher in raw IJssellake water (6 mg/L) compared to WPJ pre-treated water (3mg/L), see Appendix F. However, no fouling was observed on the membrane indicating limited adsorption of Ca^{2+}-NOM compounds on the membrane [70]. It is recommended to perform zeta potential measurements to evaluate if the membrane surface charge was affected by the adsorption of positive charged compounds on the membrane.

4.3.3. Direct cell count

Another reason for the difference in ion retention between WPJ pre-treated water filtration and raw IJssellake water filtration could have been a fiber failure in the membrane. One single leaking fiber in the dNF40 membrane can result in a feed flow passage of around 0.012 m^3/h (2% of the permeate flow) through this leaking fiber to the permeate stream depending on the location of the leak [71]. NF membranes can remove bacteria and viruses up to at least 4-log, while a fiber failure in most cases decreases the removal to less than 2-log [71]. The log-removal of the dNF40 membrane was determined by performing a direct cell count (DCC). Table 4.5 shows the concentration of cells in the feed stream and in the permeate stream in cells/ml with corresponding log-removal.

Table 4.5: The concentration of DCC-living and DCC-total in the feed and permeate stream and the log-removal.

	Feed concentration [cells/ml]	Permeate concentration [cells/ml]	log-removal
DCC-living	830000	40	4.3
DCC-total	1764000	215	3.9

The log-removal of living bacteria and viruses was 4.3 and the log-removal of total bacteria and viruses was 3.9, which is around the 4-log removal representative for NF membranes. This indicate that a broken fiber was not the reason for the decrease in ion retention. In addition, a pressure decay test performed on the membrane showed that broken fibers were not present in the membrane module.

4.3.4. Chemical cleaning in place of the membrane

Figure 4.13 shows the average MTC in LMH/bar as a function of the numbers of CIPs performed on the dNF40 membrane over the 1 year life-span of the membrane. The green bars show the filtration rounds when the dNF40 pilot was fed with WPJ pre-treated water (virgin membrane) and the blue bars show the filtration rounds when the dNF40 pilot was fed with raw IJssellake water (1 year old). The red numbers above the bars represent the feed water temperature of that specific round. Between CIP number 12 and CIP number 16, a different experiment was carried out on the dNF40 pilot from which the results will not be shown in this report. During the testing period with WPJ pre-treated water (April 2021), the MTC increased slightly (6.8 LMH/bar - 8.2 LMH/bar) with every CIPs performed. However, this slight increase in MTC can be explained by the feed water temperature increase (7.2°C - 20.5°C). During the testing period with raw IJssellake water (April 2022), the MTC increased rapidly (8.5 LMH/bar - 10.3 LMH/bar) with every CIP performed, while the feed water temperature did not increase significantly (6.9°C - 10.4°C). Comparing the MTC after 1 CIP (6.8 LMH/bar) and after 16 CIPs (8.5 LMH/bar) there was an increase in MTC of 1.7 LMH/bar, while the temperature was similar (7.2°C compared to 6.9°C). From this can be observed that the CIP restored the MTC to even higher values than its original starting values. This implies that the active outer layer of the dNF40 membrane might have undergone a change in properties when operated with raw IJssellake water due to frequent chemical cleaning of the membrane.

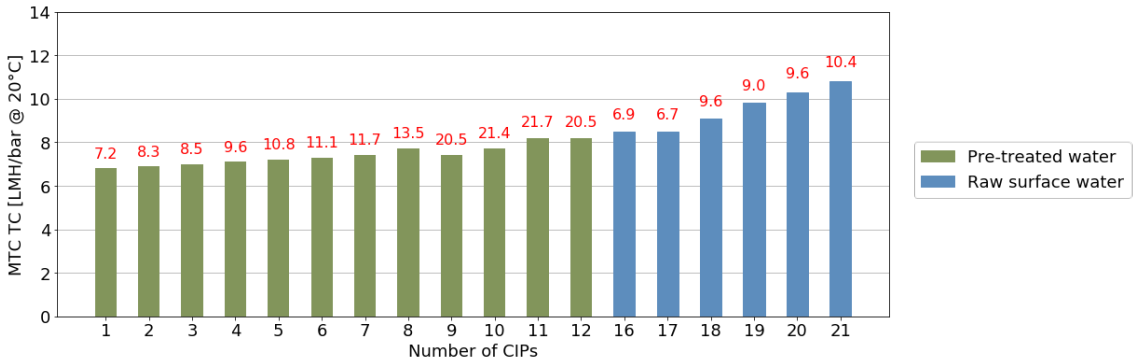

Figure 4.13: Average mass transfer coefficient temperature corrected as a function of number of CIPs performed on the same membrane. The numbers above the bars represent the feed water temperature of that round. The green bars show the filtration rounds fed with WPJ pre-treated water when the membrane was new. The blue bars show the filtration rounds fed with raw IJssellake water when the membrane was one year old.

A CIP was performed by first soaking the membrane in a high pH solution NaOCl/NaOH and second a low pH solution citric acid, see Chapter 3.2.4. When looking at the long-term performance of the dNF40 pilot when fed with raw IJssellake water, the MTC increased with every CIP performed. Several reasons can potentially be the cause of this MTC increase. One of the reasons can possibly be the excessive chemical cleaning of the dNF40 pilot. Over the last year of operation, the dNF40 membrane was cleaned 21 times, while a full-scale dNF40 plant has a CIP frequency of 13 CIPs/year [13]. Moreover, during the filtration experiments with WPJ pre-treated water and raw IJssellake water on the dNF40 pilot, CIP occurred nearly every week. Normally, at full-scale operation CIP only occurs when a TMP increase is observed due to fouling of the membrane. Another potential reason for the increased MTC could be an insufficient flushing time of the module in between a high pH and low pH cleaning resulting in the production of chemical species that may have affected the membrane layers. NaOCl/NaOH, if not flushed away completely, can react with citric acid and produce free residual chlorine [72]. This free

residual chlorine can be dangerous for membrane properties. When an RO membrane is exposed to free residual chlorine, irreversible changes in the active layer structure occurs resulting in an increase in water flux and decrease in salt retention [73]. However, more research needs to be done to determine if the excessive cleaning or insufficient flushing time might have affected the properties of the membrane.

4.4. Regulations on drinking water

The criteria to use dNF40 membranes for drinking water production at PWN are minimizing water loss (high recovery) and fouling potential and a desired total hardness value in the permeate stream below 1.4 mmol/L. When the pilot was operated with WPJ pre-treated water, a recovery below 80% was needed to achieve a total hardness value in the permeate stream below 1.4 mmol/L, see Appendix G. The optimal operational conditions when using WPJ pre-treated water are, therefore, 80% recovery, 20 LMH flux and 0.2 m/s crossflow velocity. When the pilot was operated with raw IJssellake water, the total hardness did not reach below 1.4 mmol/L in the permeate stream, see Chapter 4.2.5. Limited difference in total hardness values was observed when the pilot was operated at 70% (1.71 mmol/L) or 80% (1.74 mmol/L) recovery using raw IJssellake water. To comply with the criteria of limited water loss, the optimal operational conditions when using raw IJssellake water are, therefore, 80% recovery, 20 LMH flux and 0.2 m/s crossflow velocity. The permeate quality of these two operational conditions were compared with the legal drinking water guidelines in the Netherlands, see table 4.6. The drinking water guidelines were obtained from het Drinkwaterbesluit [74]. Except for the total hardness in the permeate stream when the dNF40 pilot was fed with raw IJssellake water, all other values meet the drinking water guidelines. The higher total hardness value in the permeate stream when the dNF40 pilot was fed with raw IJssellake water can be attributed to the potential change in the properties of the active outer layer of the membrane.

Table 4.6: Concentration of ions in permeate stream of the dNF40 pilot compared to the legal drinking water guidelines set in het Drinkwaterbesluit.

Compound	Unit	Pre-treated water	Raw surface water	Drinkwaterbesluit
Ca	mg/L	44.7	53.0	
Mg	mg/L	6.1	10.0	
SO4	mg/L	4.7	14.3	<150
Na	mg/L	N.A.	47.8	<150
Cl	mg/L	131.2	99.1	<150
HCO3	mg/L	132.8	163.9	>60
NO3	mg/L	10.5	10.5	<50
Total hardness	mmol/L	1.37	1.74	<1.4

4.5. PFAS retention

More and more research is done to the harmfulness of PFAS to the environment and health. A recent news article (2021) showed that the PFAS concentration in fish in de Westerschelde is 800 times higher than the Dutch norm [75]. It is important to reduce PFAS concentrations in the drinking water to low concentrations to minimize the harmfulness to human health. This chapter discusses the PFAS adsorption and PFAS retention with spiked concentrations on WPJ pre-treated water. These experiments were done in full recirculation mode in which the permeate stream, the concentrate stream and the backwash stream were fed back into the feed tank.

4.5.1. PFAS retention

The suitability of the dNF40 pilot to retain PFAS was evaluated by performing experiments with WPJ pre-treated water with spiked concentrations. The concentrations of PFAS in the spiked solution can be found in Table 3.4. Figure 4.14 shows the PFAS retention in % based on PFAS concentrations measured in the feed stream and the permeate stream of different PFAS compounds when operated

under two different operational conditions. The PFAS retention was calculated with Equation 2.3. The lighter bars is PFAS retention based on background PFAS concentration in WPJ pre-treated water. The darker bars is PFAS retention based on the spiked solution added to the WPJ pre-treated water. The concentrations of PFAS in the spiked solution can be found in Table 3.4. The numbers in between the brackets under the name of the PFAS compound on the x-axis represent the MW of the PFAS compound. The PFAS compounds are sorted based on MW. The PFAS retention during the two different filtration rounds varied in the range of 41%-100%.

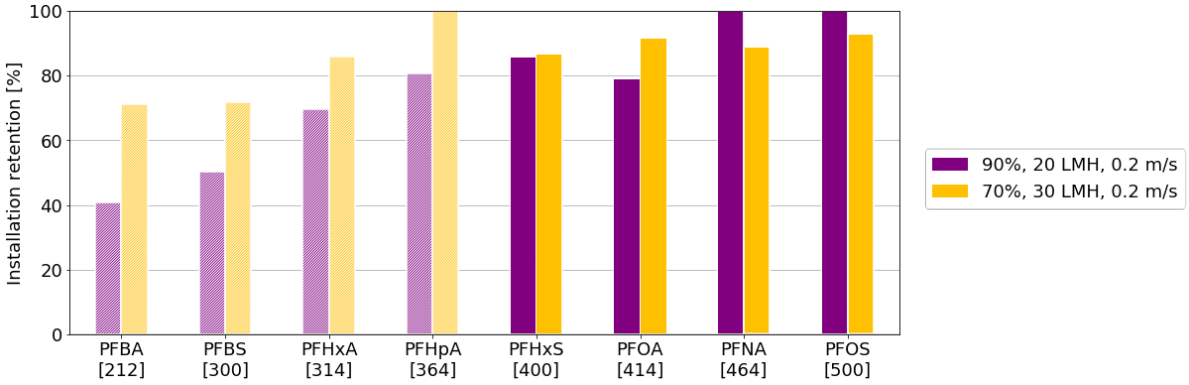

Figure 4.14: PFAS retention during filtration with WPJ pre-treated water at two different operational conditions. The lighter bars show PFAS retention based on background PFAS concentrations in WPJ pre-treated water. The darker bars show PFAS retention based on spiked concentrations in WPJ pre-treated water. The number between the brackets is the MW of the PFAS compounds. The PFAS compounds are sorted based on MW.

Research showed that, especially for high MW PFAS compounds, size (steric) exclusion is the dominant retention mechanism over Donnan (charge) exclusion [76, 77]. The experiment with spiked WPJ pre-treated water showed an increase in retention values with increasing MW due to size exclusion. An increase in retention values with elevated MW was also observed by Liu et.al. [78] using SW NF membranes and Appleman et.al. [79] using flat-sheet NF membranes. In the experiments with spiked WPJ pre-treated water, the retention values for low MW PFAS compounds (<300 g/mol) were quite low (<70%) compared to the studies described above which showed retention values consistently above 90% for all PFAS compounds including low MW PFAS compounds. This difference in retention values can be explained by the higher MWCO of the dNF40 membrane which is 400 Da compared to the MWCO of the membrane used in Liu et.al. study which is 180 Da and the MWCO of the membrane used in Appleman et.al. study which is between 150-200 Da. Moreover, the concentrations measured in the permeate stream of the low MW PFAS compounds, including the PFAS compounds PFHxA and PFHpA, were below the detection limit of the measurement device. These bars only indicate the minimum retention of these PFAS compounds. Wang et.al. [76] showed retention values of above 80% for the high MW PFAS compounds PFOA and PFOS using negative LbL HF NF membranes. Similar results were obtained in the experiment with spiked WPJ pre-treated water.

Liu et.al. [78] showed that changing operational conditions, recovery and flux, did not have an impact on PFAS retention as PFAS retention was consistently above 90% for all operational conditions. This was also observed in the experiment with spiked WPJ pre-treated water when looking at the spiked PFAS compounds, where a decrease in recovery and an increase in flux did not have a significant influence on the PFAS retention. The background PFAS compounds, however, showed a higher retention with lower recovery and higher flux, although it is difficult to determine if this was the effect of recovery or flux since both parameters were changed. A lower recovery percentage results in reduced CP and a decrease in the thickness of the boundary layer and consequently a decrease in diffusive transport of PFAS compounds to the permeate side, hence an increase in PFAS retention. When flux is increased, the convective transport across the membrane increases which results in more feed water passage through the membrane diluting the concentration of PFAS compound on the permeate side, hence an increase in PFAS retention. However, looking at the ion retention of this research, see Chapter 4.2.3, it seemed that with elevated flux diffusive transport was potentially more dominant than convective trans-

port resulting in a decrease in ion retention. More research is needed to determine if the operational conditions have an impact on low MW PFAS retention.

4.5.2. PFAS adsorption

Figure 4.15 shows the PFAS adsorption in % of the four spiked PFAS compounds during filtration with WPJ pre-treated water at the two different operational conditions. Adsorption was calculated based on feed water samples taken after 2h of pilot operation and the initial concentration in the spiked solution. The number between the square brackets is the MW of the PFAS compound. The PFAS adsorption varied in the range of 33%-90%. Noticeable is the 0% adsorption of PFOA with condition 70%, 30 LMH and 0.2 m/s crossflow velocity. During this round the PFOA concentration measured in the feed stream was higher than the initial concentration added with the spiked solution. This can be related to measurement uncertainty.

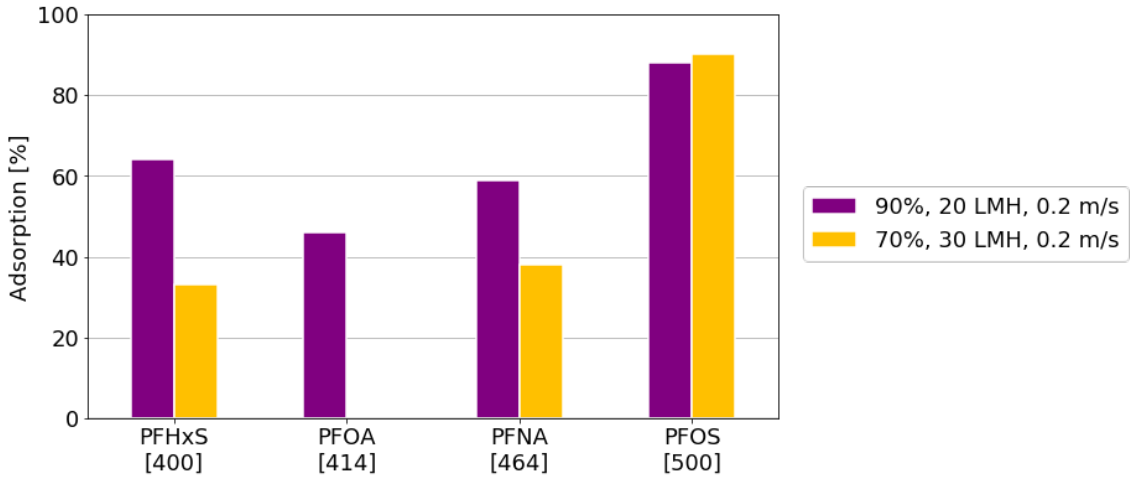

Figure 4.15: PFAS adsorption during filtration with WPJ pre-treated water at two different operational conditions. The number between the brackets is the MW of the PFAS compounds. The PFAS compounds are sorted based on MW.

The main driving forces for adsorption of PFAS on adsorbent materials are hydrophobic interactions and electrostatic interactions [80, 81]. Table 4.7 shows the chemical and physical properties of the four spiked PFAS components. The most hydrophobic PFAS compound, PFOS (highest log(K_{ow}) value) had with 90% the highest adsorption percentage, while PFHxS, PFOA and PFNA had adsorption percentages below 60%. Liu et.al. [78] observed the same results in a pilot study using SW NF membranes in which the two most hydrophobic PFAS compounds, PFOS and PFHpS, had the highest adsorption percentage. These compounds are able to form strong hydrophobic bonds due to their low solubility in water (high log(K_{ow}) values) and their long carbon tails (high number of C-atoms).

Within the spiked WPJ pre-treated water experiment, PFNA has with 8 carbon atoms an equally long tail as PFOS, while the adsorption percentage of PFNA was 30% less than PFOS. This can partially be explained by the lower log(K_{ow}) value for PFNA. However, this difference in log(K_{ow}) is small, indicating that both compounds are strongly hydrophobic. In addition, PFHxS is less hydrophobic than PFOA and PFNA, but had similar adsorption percentage compared to PFNA and higher adsorption percentage compared to PFOA. It seemed that PFAS compounds with a sulphonic head were adsorbed better on the membrane than PFAS compounds with a carboxylic head. This might suggest that sulphonic head groups interact differently with the membrane as opposed to the carboxylic head groups, although a broader PFAS cocktail should be studied to validate this.

Liu et.al. [78] showed greatest adsorption on membrane elements compared to the membrane system. An increase in PFAS adsorption on the membrane elements should eventually lead to a decrease in permeate flux passing through the membrane due to PFAS fouling formation [82]. The membrane performance data shown in Appendix H when the dNF40 pilot was operated with spiked WPJ pre-

treated water showed no decrease in MTC suggesting that PFAS adsorption on the membrane was limited. However, feed sampling was done 2 hours after the start of the experiment which might not be long enough to observe flux decline due to PFAS adsorption. In addition, Li et.al. [83] showed that the adsorption of PFAS compounds on the membrane was less for negative charged membranes compared to neutral charged membranes due to electrostatic repulsion between the negative PFAS compound and the negative membrane. The high PFAS adsorption percentages, shown in Figure 4.15, might suggest that PFAS is able to adsorb to other components within the pilot as well and not only on the membrane elements. Llorca et.al. [84] showed that PFAS was able to adsorb on plastics, which could result in higher PFAS adsorption percentages within the dNF40 pilot. More research is needed to evaluate where PFAS adsorption is taking place within the dNF40 pilot and what the long-term effect (months) is of PFAS adsorption on membrane performance.

Table 4.7: Chemical and physical properties of PFAS compounds in the spiked solution. The values are obtained from PubChem.

Compound	MW [g/mol]	Head group	C-atoms	log(K_{ow}) [-]
PFHxS	400	Sulphonic	6	5.17
PFOA	414	Carboxylic	7	5.30
PFNA	464	Carboxylic	8	5.92
PFOS	500	Sulphonic	8	6.30

4.5.3. Regulations on PFAS

NF is suitable for the removal of PFAS from PFAS containing water. The challenge, however, is that NF does not destroy PFAS compounds but rather produce a concentrate stream with higher PFAS concentrations compared to the feed stream. Limited research has been done to concentrate management of PFAS containing waters.

At the moment, a real regulation on PFAS discharge in the environment is missing. It is proposed by the RIVM that companies should prevent discharging PFAS into the environment. If that is not possible, they must limit their discharge as much as possible. However, this will most likely change in the near future since more and more research is done to the harmfulness of PFAS on the environment and human health and the support for a real guideline is increasing. Therefore, there is a need to manage the concentrate stream in order to destruct the PFAS compounds before it enters the environment.

Technologies that may be suitable for PFAS concentrate management are PFAS defluorination or sequestration [85]. Technologies to destruct PFAS compounds by defluorinating the PFAS compounds are available, but these applications do not cover the whole PFAS compound spectrum and little is known about the expenses on full-scale treatment [85]. A concern of these applications is that during destruction of PFAS the C-F bond should be destroyed and not the C-C bond, otherwise smaller chain PFAS compounds are generated. To date, it is unclear if these smaller chain PFAS compounds are more toxic and persistent than longer chain PFAS compounds. PFAS sequestration can be done by either injecting PFAS in a deep well or store PFAS in landfills [85]. However, on the long-term this might not be an efficient solution due to possible contamination of the environment around the deep well or landfill. Further research is needed to improve the state of the art in PFAS destruction before a strict guideline is set on reducing the discharge of PFAS in the environment.

Up until now, there is not a strict guideline on the amount of PFAS in drinking water. A proposed guideline by the RIVM is 4,4 ng/L PEQ for the four PFAS compounds PFOS, PFOA, PFNA and PFHxS [24]. The expectation is that this guideline will be implemented in the near future. In the experiments with spiked WPJ pre-treated water, the PEQ of the two filtration rounds was 26 ng/L and 38 ng/L for 90%, 20 LMH, 0.2 m/s and 70%, 30 LMH, 0.2 m/s respectively. This is far above the proposed guideline by the RIVM. However, it must be noted that these four PFAS compounds had spiked concentrations in the feed stream which resulted in higher concentrations in the permeate stream. Research should be done to the background concentrations of these four PFAS compounds in WPJ pre-treated water to determine if the PEQ will be below the 4.4 ng/L.

4.6. Pharmaceutical retention

The concentration of pharmaceuticals in the aquatic environment is increasing every year and becoming more a concern. To limit the exposure of pharmaceuticals to human health, it is important to reduce the pharmaceutical concentrations in the drinking water to low concentrations. This chapter discusses the pharmaceuticals retention with spiked concentrations fed with WPJ pre-treated water. These experiments were done in full recirculation mode in which the permeate stream, the concentrate stream and the backwash stream were fed back into the feed tank.

4.6.1. Pharmaceutical retention

The suitability of the dNF40 pilot to retain pharmaceuticals was determined by performing experiments with WPJ pre-treated water with spiked concentrations. The concentrations of pharmaceuticals in the spiked solution can be found in Table 3.4. To cover a broad range of pharmaceuticals a cocktail was prepared consisting of positive, neutral and negative pharmaceuticals.

Figure 4.16 shows the pharmaceutical retention in % based on pharmaceutical concentrations measured in the feed stream and the permeate stream of different pharmaceuticals when operated under two different operational conditions. The pharmaceutical retention was calculated with Equation 2.3. The symbols in between the round brackets represent the charge of the pharmaceutical. The number between the square brackets is the MW of the pharmaceutical. The pharmaceuticals are sorted based on charge and within the charged groups based on MW. The pharmaceutical retention during the two different filtration rounds varied in the range of -33%-79%.

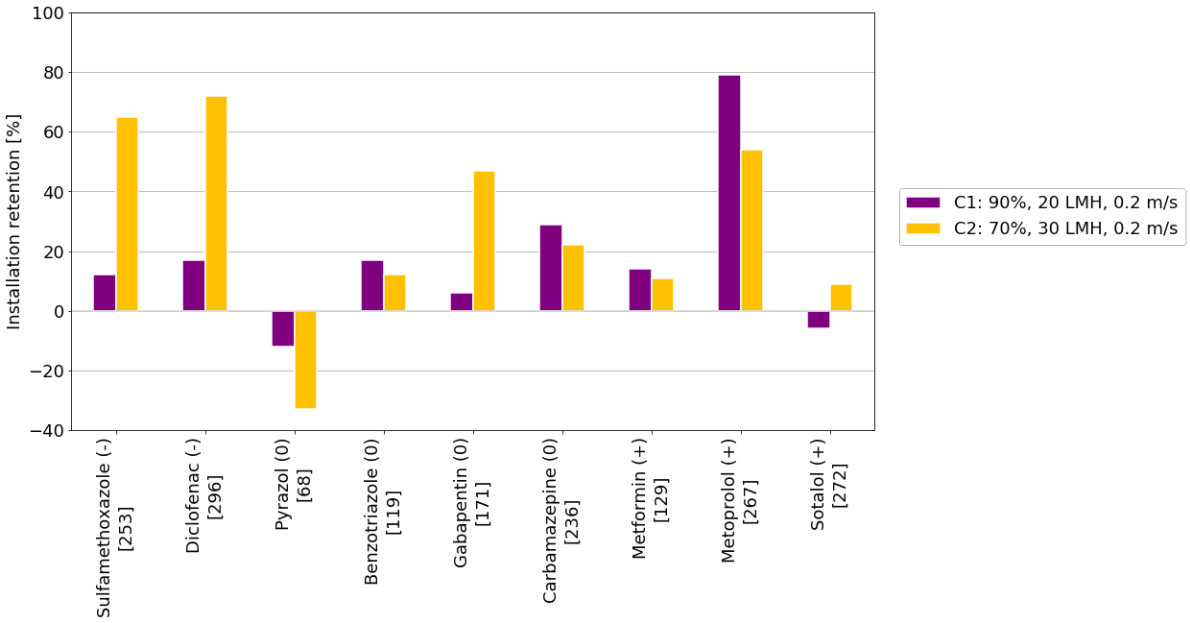

Figure 4.16: Pharmaceutical retention during filtration with WPJ pre-treated water at two different operational conditions. The symbol between the round brackets represent the charge of the pharmaceutical, in which - is negative, 0 is neutral and + is positive. The number between the square brackets is the MW of the pharmaceutical. The pharmaceuticals are sorted based on charge and within the charged groups based on MW.

The retention of uncharged pharmaceuticals is predominantly caused by size (steric) exclusion, while the retention of charged pharmaceuticals is a combination between size (steric) exclusion and Donnan (charge) exclusion. All pharmaceuticals measured have a MW below the MWCO of the dNF40 membrane which is 400 Da. Therefore, it is difficult to find a relationship between the MW and the retention of a certain pharmaceutical.

The compound pyrazol was negatively retained by the membrane, which can be explained by the small MW of this compound, which is 68 g/mol. In addition, pyrazol has a neutral charge and is, therefore, only retained by size (steric) exclusion and not by Donnan (charge) exclusion.

The positively charged compound sotalol, however, with a MW of 272 g/mol showed negative retention in round C1 and low retention (9%) in round C2. While the positively charged compound metoprolol, with a lower MW than sotalol, had a much higher retention (79% and 54%). This difference in retention can be explained by their log(P) value, shown in Table 4.8, which is 0.24 for Sotalol and 1.88 for Metoprolol. The low log(P) value for sotalol shows that this compound is very soluble in water and therefore difficult to retain by the membrane than the more hydrophobic compound metoprolol. Abtahi et.al. [86] also observed that the more hydrophobic a compound, the higher the retention. In addition, Abtahi et.al. [86] observed that during longer operation time (> 31h of operation) of the pilot, the pharmaceutical retention decreased. The hydrophobic pharmaceutical had the largest decrease in retention over longer operation time. This can be explained by the adsorption of hydrophobic pharmaceuticals on the membrane until a certain breakthrough is reached leading to a higher amount of pharmaceuticals passing through the membrane. The operation time during the experiments with spiked WPJ pre-treated water was only 2h. This was potentially not long enough for pharmaceuticals to adsorb on the membrane and to reach this breakthrough event.

Looking at round C2, it was observed that the negative pharmaceuticals were retained better by the membrane than the neutral and positive pharmaceuticals. This can be explained by the negative outer layer of the membrane which repelled negative pharmaceuticals and attracted positive pharmaceuticals. A higher retention of negative pharmaceuticals was also observed by De Grooth et.al. [11] using HF NF membranes with a negative charge terminal layer and a MWCO of 400 Da.

In round C1, a strong decrease in retention values of 53%, 55% and 41% was observed for the pharmaceuticals sulfamethoxazole, diclofenac and gabapentin respectively compared to round C2. Furthermore, the retention values of the negative pharmaceuticals sulfamethoxazole (12%) and diclofenac (17%) were even lower than the retention values of the neutral pharmaceutical carbamazepine (29%) and the positive pharmaceutical metoprolol (79%) in round C1. Considering the negative charge of the membrane this is unusual. In addition, diclofenac is also the most hydrophobic compound in this OMP solution, which should result in a high retention [86], see Table 4.8. Cuhorka et.al. [87] showed that by increasing the flux, the retention of diclofenac increased due to the dilution effect on the permeate side of the membrane. Although, this increase was limited to 1%-2% with a flux increase from 30 LMH to 70 LMH. Decreasing the recovery from 90% to 70% results in less CP near the membrane, decreasing the thickness of the boundary layer, resulting in a decrease in diffusive transport of pharmaceuticals to the permeate side and increasing the retention. However, this strong decrease in retention is too big to be caused by the change in operational conditions. Also considering that the retention values of other pharmaceuticals such as benzotriazole, carbamazepine and metoprolol are higher in round C1 than round C2. This suggest that these low retention values of sulfamethoxazole, diclofenac and gabapentin in round C1 were probably related to measurement errors.

Even though there are no regulations yet on the concentration of pharmaceuticals in drinking water, the rising concern of these compounds to human health will result in the implementation of stricter guidelines in the near future. It might be that in the future the dNF40 pilot, at least under tested conditions, is not a suitable candidate for OMP removal. However, this can potentially be improved by modifications of the membrane or a hybrid system, as explained in Chapter 4.7.

Table 4.8: Chemical and physical properties of pharmaceuticals in the spiked solution. The values are taken from the source of Embrahimzadeh et.al. [19]. The log(P) values are obtained from PubChem.

Name	Harmfulness	MW [g/mol]	pKa [-]	Charge	log(P) [-]
Pyrazol	Pyrazol is mainly clinically used as a non-steroidal anti-inflammatory drugs.	68	2.48	0	0.26
Benzotriazole	Benzotriazole is a type of corrosion inhibitors widely detected in aquatic environments and is persistent. It may affect endocrine systems and neurotoxicity in fish.	119	8.6	0	1.44
Metformin	Metformin is an oral medication that helps manage the effects of type 2 diabetes. The common side effects are bloating, gas, constipation.	129	12.33	+	-2.60
Gabapentin	Gabapentin is an anticonvulsant medication that can cause side effects that include blurred vision, cold or flu-like symptoms, delusions, dementia, lack or loss of strength, swelling of the hands, feet, or lower legs, unsteadiness and uncontrolled eye movements.	171	4.63	0	-1.10
Carbamazepine	Carbamazepine is used to treat epilepsy, nerve pain or bipolar disorder and may cause unusual bleeding or bruising, suicidal thoughts, severe rash of blisters, ulcers, yellowing skin or eyes, pain in joints, muscles and lungs.	236	15.96	0	2.45
Sulfamethoxazole	Sulfamethoxazole is a bacteriostatic antibiotic used in the medication bactrim that may cause blood disorders, liver damage, or lung injury.	253	6.2	-	0.89
Metoprolol	Metoprolol is used to lower high blood pressure, to reduce chest pain but may cause blurred vision, chest pain, confusion faintness, slow heartbeat, sweating.	267	14.09	+	1.88
Sotalol	Sotalol is used in medicine as a treatment for life-threatening ventricular arrhythmia's and may cause breathing issues, blurred vision, sweating and swelling.	273	10.07	+	0.24
Diclofenac	Diclofenac is considered as an emerging environmental pollutant and is mainly produced as an anti-inflammatory drug.	296	4.15	-	4.51

4.6.2. Pharmaceutical retention: compared to Mexplorer and NXF

An extensive research was done by Van der Poel [10] to OMP retention on the Mexplorer (bench-scale) with similar dNF40 membranes. Both the dNF40 membrane of the Mexplorer, as well as the dNF40 membrane of the Mexpert should have a MWCO of 400 Da [13]. However, van der Poel [10] observed during a MWCO-experiment that the MWCO of the dNF40 membrane on the Mexplorer was 200 Da. Higher retention values (an average of 88%) were observed on the Mexplorer with a module length of 0.3m compared to the Mexpert using spiked WPJ pre-treated water with a module length of 1.5m. This could partially be explained by the lower MWCO of the Mexplorer. Another reason for the higher retention values could possibly be the module length. Junker et.al. [6] researched the difference in module length on the retention of $MgSO_4$. A decrease in $MgSO_4$ retention of 10% was observed with increasing module length from 0.3m to 1.5m operated at 20 LMH flux and 0.1 m/s crossflow velocity. An

increase in module length results in varying process parameters along the fiber length, a higher water recovery and an increased CP at similar operational conditions [6] which can influence the retention. The difference in pharmaceutical retention on the Mexplorer compared to the Mexpert was, however, more than 10%. Another possible reason for the lower retention values could be the recovery. The pharmaceutical experiments on the Mexplorer were conducted with recovery values of 1%-2%, while the pharmaceutical experiments on the Mexpert were conducted with recovery values of 70%-90%. As observed with the ion retention, an increase in recovery decreased the retention of the ions due to concentration build-up near the membrane. The low recovery values used on the Mexpert could have contributed to the high pharmaceutical retention values. More research needs to be done to the low pharmaceutical retention values measured on the Mexplorer with spiked WPJ pre-treated water.

4.7. Practical implication

The results of this research implied that HF NF membranes are, at least under tested conditions, not a suitable candidate for direct drinking water production (i.e. one-step filtration) from IJssellake water. This was mainly related to the low pharmaceutical retention and the high total hardness concentration in the permeate exceeding the 1.4 mmol/L. Although, the high permeate hardness can be related to the potential change in properties of the outer active layer possibly caused by extensive CIP events. Moreover, the results from HF NF on pre-treated IJssellake water demonstrated that these system are also not a suitable candidate for the replacement of the current UF-RO in Heemskerk. This was mainly related to the low pharmaceutical retention by the dNF40 pilot. The total hardness concentration in the permeate stream when fed with WPJ pre-treated water was sufficient (below 1.4 mmol/L) when a recovery below 80% was chosen, see Appendix G. However, a recovery below 80% is not an improvement to minimizing water loss considering the UF-RO recovery of 80%.

Even though the drinking water quality standards were not yet achieved by the use of HF NF membranes, the feasibility study in this research showed that HF NF membranes have potential advantages such as limited to no fouling formation on the membrane, high NOM removal (above 90% regardless of operational condition) and sufficient PFAS removal (above 80%). Therefore, it is interesting to evaluate potential adjustments or combinations which can facilitate applications of HF NF for drinking water production from raw/pre-treated IJssellake water. Figure 4.17 shows an overview of all the drinking water treatment processes at PWN.

Membrane modification. If HF NF membranes are to be used as a one-step treatment process or as an alternative for the UF-RO process in Heemskerk adaptation to the membrane can potentially obtain the permeate water quality that meets the standard for drinking water purposes at PWN. Modifying the membrane by increasing the numbers of PEM layers result in a decrease in the permeability of the membrane and thus a higher selectivity towards ions and pharmaceuticals than the membrane used in this study [8]. This can potentially increase Ca^{2+} and Mg^{2+} retention as well as pharmaceutical retention. However, such membranes with LbL configuration and a MWCO below 400 Da are not commercially available yet on pilot or full-scale level [1].

Hybrid processes. Hybrid processes in which HF NF membranes are combined with another process can potentially result in the obtained permeate water quality that meets the standard for drinking water purposes. An additional step consisting of GAC could increase the pharmaceutical removal, although this additional step is at the expense of the CAPEX and OPEX. Heijman et.al. [70] found that the pharmaceuticals which are poorly removed by SW NF membranes are well removed by GAC, e.g. sotalol which has a removal percentage of 40% in NF and 90% in GAC. Moreover, adding softening as an additional step could increase the total hardness removal, although this is again at the expense of CAPEX and OPEX.

Potential candidate for WPJ RO pre-treatment. At the WPJ facility in Andijk, the combined treatment train drum sieves, coagulation, sedimentation and rapid sand filter and the UF membranes at Heemskerk have similar functionalities as HF NF membranes, namely the removal of NOM. For this reason HF NF membranes might be a suitable potential candidate for WPJ RO pre-treatment. However, there are also risks associated with the use of HF NF membranes as a pre-treatment for the RO process. One of the risks is the substitution of 5 processes into 1 process. If the HF NF plant fails due

to technical problems not sufficient NOM will be removed and raw IJssellake water will be fed directly to the RO process. Another risk is that there is a shortage in suppliers for HF NF membranes which can create a monopoly.

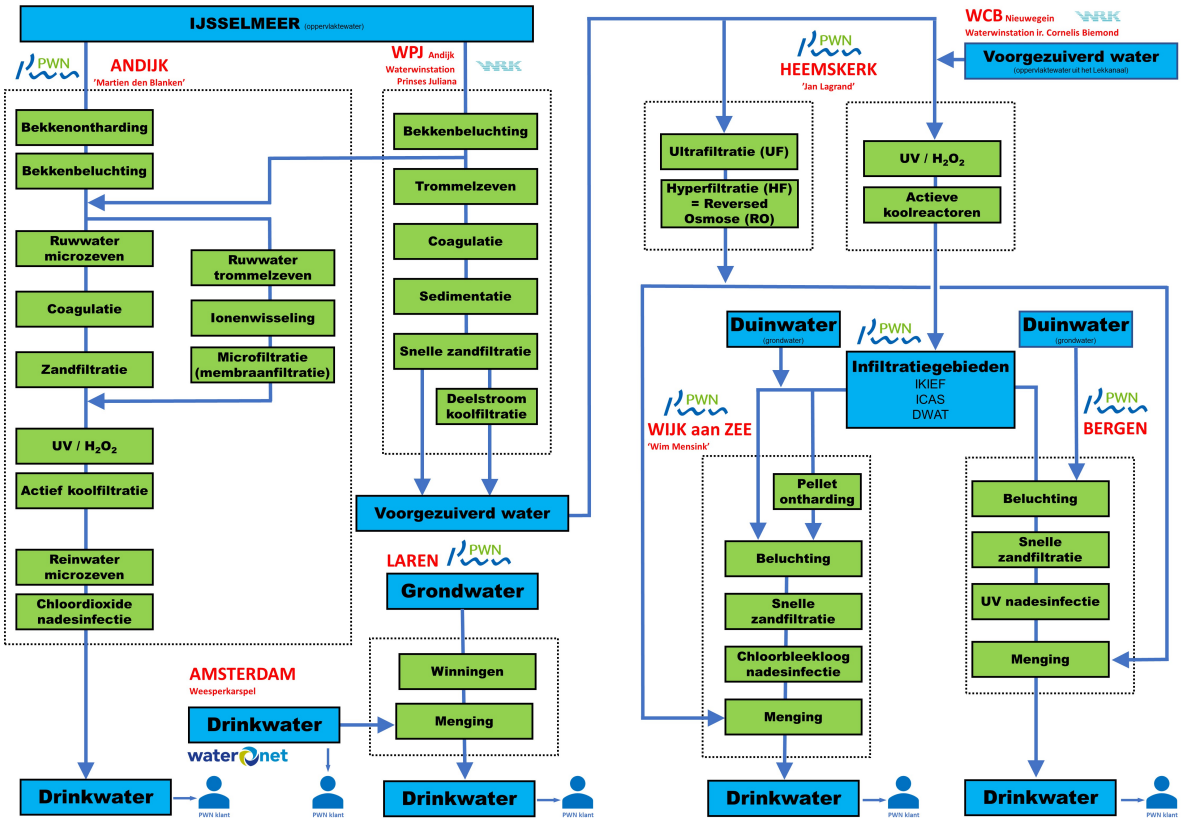

Figure 4.17: Overview of drinking water treatment processes at PWN.

Potential candidate for Andijk conventional and novel pre-treatment. At the Martien den Blanken facility in Andijk, the combined treatment train micro sieves, coagulation and sand filtration and the combined treatment train drum sieves, ion exchange and microfiltration have similar functionalities as HF NF membranes, namely NOM removal. NOM removal is necessary to lower the energy consumption of the UV-lamps, since NOM is able to adsorb UV [88]. Moreover, NOM removal is necessary to decrease the competition between the NOM and pharmaceuticals for available carbon adsorption areas [89]. However, as explained above the same risks associated with the use of HF NF membranes should be considered.

RO concentrate treatment. HF NF membranes can potentially be used as a post-treatment for the RO concentrate at Heemskerk. At the moment, the concentrate of the UF-RO at Heemskerk is discharged in the sea. However, it might be that in the future stricter discharge permission must be met. One of the advantages of using HF NF membranes as a post-treatment for RO concentrate is that the concentrate stream discharged in the sea will be reduced. Moreover, this reduced volume can offer potential solutions for further PFAS treatment in case of stricter discharge permission in the future. Another advantage of the use of HF NF membranes as a post-treatment for RO concentrate is that the recovery of the UF-RO can potentially be increased. By treating the concentrate of the RO process with HF NF membranes, the permeate water from the HF NF membranes can potentially be redirected back to the UF-RO where it will be mixed with the feed stream increasing the recovery of the UF-RO. However, the permeate of the HF NF membranes contain high concentrations of salinity and OMP which should be considered when mixing with the feed stream.

General application PFAS from the water can be removed by multiple processes with the main processes NF membranes or the adsorption on (polymer based) adsorbents. HF NF membranes and

(polymer based) adsorbents are suitable candidates for the removal of long chain PFAS compounds, yet the removal of short chain PFAS compounds is still a challenging task in both processes. Another challenge in the use of (polymer based) adsorbents for PFAS removal is the competition between PFAS and NOM in the water for available adsorption sites, which could affect the adsorption efficiency of PFAS on adsorbents [90]. HF NF membranes are a more suitable potential candidate for the removal of both PFAS and NOM, since it showed promising results towards the retention of PFAS and NOM. One more challenge when using (polymer based) adsorbents is the regeneration of these adsorbents when their adsorption capacity has been reached. PFAS can be removed from the adsorbent by chemical or thermal regeneration, although both have their challenges. Chemical regeneration requires the use of organic solvents which can be harmful for the environment, while thermal regeneration can cause a decline in the adsorption capacity and may release dangerous short-chain fluorinated gases [90]. More research is needed to a feasible and suitable regeneration method. In addition, regenerating the adsorbent generate a waste stream with high PFAS concentrations. When HF NF membranes are used for the removal of PFAS, a similar waste stream with high PFAS concentrations is generated. When stricter discharge permission will be implemented in the future, there is a need to further treat these PFAS containing waste stream. This can be either done by defluorination or sequestration, although the use of these technologies is not feasible yet, see Chapter 4.5.3.

4.8. Economic feasibility

This chapter presents the OPEX and CAPEX calculations of the full-scale dNF40 plant fed with WPJ pre-treated water and raw IJssellake water. These results will be compared to the OPEX and CAPEX of the full-scale UF-RO plant in Heemskerk.

For this study all prices are indicative and highly case dependent. For a representative quotation contact NX Filtration.

4.8.1. Full-scale dNF40 plant: location Heemskerk

A full-scale dNF40 plant has been designed for PWN based on a permeate flow of 15M m^3/year and a total hardness concentration in the permeate stream of below 1.4 mmol/L. A projection report has been generated for the full-scale dNF40 plant, which shows a 5-stage system with a feed flow of 17.7 M m^3/year and a total recovery percentage of 85%. The 5-stage full sale dNF40 plant, see Figure 4.18, was designed based on the feed water matrix of WPJ pre-treated water, although the same system can be used for the feed water matrix of raw IJssellake water. The reason for this is that the only difference in feed water quality of WPJ pre-treated water as opposed to raw IJssellake water was the concentration of NOM, chloride and hydrogen carbonate, see Appendix F. Both the rejection of chloride and hydrogen carbonate was not significantly influenced by the operational conditions, due to the preference of dNF40 membranes to remove multivalent ion compounds over monovalent ion compounds, as seen in Chapter 4.2. The rejection of NOM was not dependent on the operational conditions of the pilot as well, due to the general high MW of these compounds, as seen in Chapter 4.2.6.

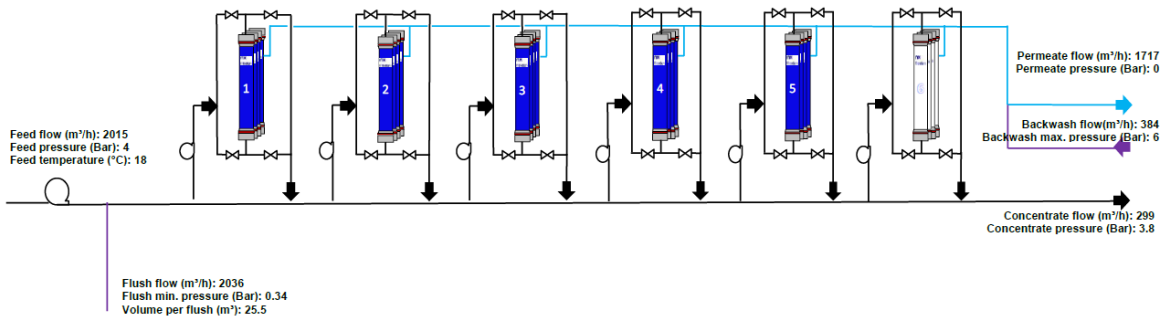

Figure 4.18: 5-stage full-scale hollow fiber nanofiltration plant for location Heemskerk.

4.8.2. Full-scale dNF40 plant: comparison to dNF40 pilot

From the results in this research it was observed that the desired hardness concentration in the permeate stream (<1.4 mmol/L) was not met with the dNF40 pilot when fed with raw IJssellake water, see Chapter 4.2.5. When the dNF40 pilot was fed with WPJ pre-treated water, a recovery below 80% was needed to achieve the desired hardness concentration in the permeate stream, see Appendix G. In a multiple stage full-scale dNF40 plant, the permeate water quality can be improved substantially due to mixing of the permeate streams from the different stages. Every stage in the system has a membrane recovery of 17.3% which adds up to the total installation recovery of the 5-stage system of 85%. The first stage in a full-scale dNF40 plant has the best permeate water quality and the last stage has the worst permeate water quality. This is due to the fact that the concentrate stream of the first stage is transported to the second stage, the concentrate stream of the second stage is transported to the third stage, etc. With every stage, the ion concentration in the concentrate stream is more concentrated and the CP factor more severe. The dNF40 pilot mimics the last stage in a full-scale dNF40 pilot plant, which gives the worst permeate water quality. In addition, the dNF40 pilot operates in a feed-and-bleed mode where part of the concentrate is recirculated back to the feed stream increasing the module recovery, but also the ion concentration in the feed stream.

The 5-stage full-scale dNF40 plant, designed by NXF, has a total installation recovery of 85.2% and a membrane recovery of 17.3% in every stage. This corresponds to a recovery of 66% on the dNF40 pilot. The feed water quality and the permeate water quality of the full-scale dNF40 plant can be found in table 4.9. The total hardness concentration of the full-scale dNF40 plant is 1.24 mmol/L, which is below the norm set by PWN. However, this is the total hardness concentration in the permeate stream measured after 0 year of operation of the full-scale dNF40 plant. After 5 years of operation, the total hardness concentration in the permeate stream exceeds the desired norm by PWN of 1.4 mmol/L. Even with lower recovery values or a 6-stage full-scale system, the total hardness concentration stays above 1.4 mmol/L. The reason for this is that the software which is used to calculate the projection include a safety margin for the longer lifetime of the membrane, hence the decrease in retention. Advised is to decrease the membrane lifetime to 3.8 years in order for the total hardness concentration in the permeate stream not to exceed the 1.4 mmol/L. However, this will be at the expense of the total OPEX of the dNF40 plant.

Table 4.9: Permeate water quality of different ion compounds and TOC of the 5-stage full-scale dNF40 plant.

Parameter	Unit	Feed	Permeate
Ca	mg/L	69.2	39.7
Mg	mg/L	12.7	6.0
Na	mg/L	81.9	81.2
Cl	mg/L	140.0	128.0
SO4	mg/L	58.0	2.5
NO3	mg/L	9.3	8.5
HCO3	mg/L	170.0	139.0
TOC	mg/L	3.3	0.4

4.8.3. Economic cost

The projection report gives information on the full-scale dNF40 plant about the amount of membranes, the applied pressure and the amount of chemicals needed. Based on the data in the projection report, the OPEX and CAPEX of the full-scale dNF40 plant fed with WPJ pre-treated water and raw IJssellake water were calculated. The OPEX and CAPEX of the full-scale dNF40 plant were compared with the OPEX and CAPEX of the full-scale UF-RO plant in Heemskerk. The plant specifications, feed water parameters, performance parameters and chemical information of the full-scale dNF40 plant and the full-scale UF-RO plant in Heemskerk can be found in table 4.10. The membrane lifetime of the dNF40 plant is changed to 3.8 years instead of 5 years to achieve the desired total hardness in the permeate.

Table 4.10: Plant specifications, feed water parameters and performance parameters of the full-scale dNF40 plant fed with WPJ pre-treated water and raw IJssellake water and the full-scale UF-RO plant in Heemskerk fed with WPJ pre-treated water.

Variables	Units	dNF40 pre-treated	dNF40 raw surface water	UF-RO in Heemskerk
Plant characteristics				
Feed water source	[-]	WPJ pre-treated water	Raw IJssellake water	WPJ pre-treated water
Plant product	[-]	Drinking water	Drinking water	Softening for dune water
Pre-treatment steps	[-]	See Figure 3.3	See Figure 3.3	Similar to HF NF pre-treated
Years of operation	years	3.8	3.8	5
Production capacity	m^3/year	15.000.000	15.000.000	14.700.000
Water recovery	%	85	85	UF: 85 RO: 80
Membrane type	[-]	WRC200-dNF40-IRD	WRC200-dNF40-IRD	UF: X-Flow XIGA 40 RO: ESPA3 324S
CIP frequency	CIP/year	13	13	UF: 12 RO: 2
CIP duration	hours/event	1	1	UF: 6-8 RO: 8
Number of stages	[-]	5	5	UF: 4 RO: 8
Number of modules	[-]	1535	1535	UF: 768 RO: 2016
Performance parameters				
Average applied pressure	kWh/m^3	0.19	0.19	UF: 0.065 RO: 0.40
Design flux	LMH	22.3	22.3	UF: 100 RO: 22
Chemical information				
NaOH (30%)	ton/year	0.68	0.68	0
NaOH (50%)	ton/year	0	0	1594
NaOCl (12.5%)	ton/year	1.14	1.14	81.5
Citric acid (50%)	ton/year	6.29	6.29	0
HCl (33%)	ton/year	0	0	5.75
CO_2	ton/year	0	0	587
Antiscalant ”2mg/l”	ton/year	0	0	34.6

OPEX was calculated based on the energy cost, chemical cost, membrane cost [48] and pre-treatment cost, as shown in Equation 3.5. The waste disposal cost and labour cost were considered out of the scope of these calculations. The waste disposal cost was excluded from the OPEX calculations, due to missing information on waste disposal cost for NF. The labour cost was excluded from the OPEX calculations, because of identical labour cost for both NF and UF-RO at PWN.

CAPEX was calculated based on the equipment and installation cost [48] and pre-treatment cost, as shown in Equation 3.6. For the auxiliary components (pipes, pumps, valves, etc.) a price similar to the membrane price was used. Other possible CAPEX, such as land acquisition, planning and construction of buildings were excluded, since those cost factors are highly case dependent and subjective.

The pre-treatment cost cannot be excluded from the OPEX and CAPEX calculations. The full-scale dNF40 plant on raw IJssellake water has no pre-treatment cost, while the full-scale dNF40 plant on WPJ pre-treated water and the full-scale UF-RO plant in Heemskerk have similar extensive pre-treatment steps and thus similar pre-treatment cost, see Figure 3.3. The exact value of the CAPEX and OPEX cost have not been made available. For the calculations a value of 0.10 €/m^3 has been chosen.

Table 4.11 shows the OPEX and CAPEX in €/m^3 permeate flow calculated for the full-scale dNF40 plant on WPJ pre-treated water and raw IJssellake water and the full-scale UF-RO plant in Heemskerk. The OPEX per m^3 permeate flow was higher than the CAPEX, which can be related to the CAPEX investment only once at the beginning of the life span of 20 years, while OPEX are constantly needed [48]. CAPEX, however, only included installation and equipment cost, while land acquisition, planning and construction of buildings were excluded from CAPEX calculations. The inclusion of those factors would increase CAPEX, but are unlikely to exceed OPEX [48].

Table 4.11: OPEX and CAPEX in €/m^3 permeate water of the full-scale dNF40 pilot fed with WPJ pre-treated water and raw IJssellake water and the full-scale UF-RO plant in Heemskerk. The OPEX and CAPEX are divided into the pre-treatment cost and the core treatment cost.

	dNF40 pre-treated	dNF40 raw surface water	UF-RO in Heemskerk
Pre-treatment (€$_{OPEX}$/m^3)	0,10	N.A.	0,10
Pre-treatment (€$_{CAPEX}$/m^3)	0,10	N.A.	0,10
Core treatment (€$_{OPEX}$/m^3)	0,09	0,09	0,13
Core treatment (€$_{CAPEX}$/m^3)	0,03	0,03	0,02
Total OPEX (€/m^3)	0,19	0,09	0,23
Total CAPEX (€/m^3)	0,13	0,03	0,12

The OPEX and CAPEX was cheapest for the dNF40 plant on raw IJssellake water, since no pre-treatment is required. Comparing the dNF40 plant on pre-treated water to the UF-RO plant, which have similar pre-treatment steps, it was observed that the OPEX was 4 ct/m^3 permeate flow cheaper for the dNF40 plant and the CAPEX was 1 ct/m^3 permeate flow more expensive for the dNF40 plant. The lower OPEX can be attributed to the reduced energy and chemical cost in the dNF40 plant as opposed to the UF-RO plant. The higher CAPEX can be attributed to the higher membrane price for HF NF membranes, which is 2500 per membrane as opposed to €1200 per membrane for UF and €800 per membrane for RO, see table 3.6.

The OPEX was divided into cost for energy, chemical, membrane replacement and pre-treatment. Figure 4.19 shows the energy, chemical and membrane replacement cost as a percentage of the total OPEX for the full-scale dNF40 plant for WPJ pre-treated water and raw IJssellake water (left) and the full-scale UF-RO plant in Heemskerk (right). In this graph, the OPEX related to pre-treatment steps is not shown. In the dNF40 plant, the dominant cost contributor in OPEX was the membrane replacement (68%), followed by energy (31%) and chemical (<1%). A different OPEX factor distribution was observed in the UF-RO plant, with the dominant cost contributor the energy (45%), followed by chemical (29%) and membrane replacement (26%). The difference in membrane replacement cost between the dNF40 plant and the UF-RO plant can be attributed to the higher membrane price of HF NF membranes over UF and RO membranes. The difference in chemical cost can be explained by the fact that the UF-RO plant not only uses chemicals to clean the membrane, but also antiscalant to limit the fouling potential on the membrane and chemicals for post conditioning due to permeate stream transport to PS Bergen via concrete pipelines, while the dNF40 plant only uses chemicals to clean the membrane. In addition, the amount of chemicals required for the chemical cleaning of the UF-RO plant is more than the amounts of chemicals required for the chemical cleaning of the dNF40 plant. The difference in energy is due to the higher pressure requirement to transport the feed water through the smaller pores of the RO membrane.

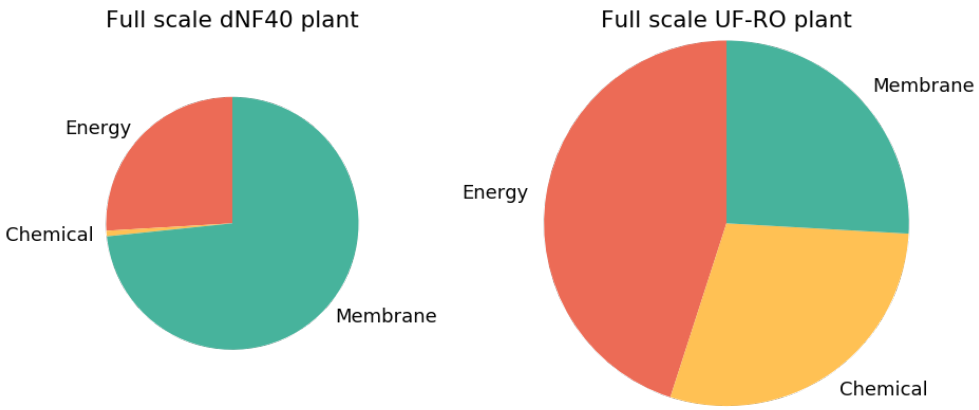

Figure 4.19: The energy, chemical and membrane replacement cost as a percentage of the total OPEX in the full-scale dNF40 plant and the full-scale UF-RO plant.

5

Conclusion

During the one year of operation, the dNF40 pilot was running multiple tests with two different water matrices (WPJ pre-treated water and raw IJssellake water) under different operational conditions (recovery, flux and crossflow velocity). The membrane performance parameters, such as MTC, TMP and NPD and retention of ions, NOM, PFAS and OMPs were evaluated under different operational conditions.

Stable performance parameters were observed during testing periods, both with WPJ pre-treated water and raw IJssellake water, indicating low fouling impact during operation. Within each operational condition interval, the MTC, TMP and NPD remained constant which clearly shows minimal fouling impact. The slight change in MTC, TMP and NPD values within each operational condition interval were associated to corresponding temperature changes.

Generally, dNF40 demonstrated excellent performance regarding fouling potential during testing with WPJ pre-treated water and raw IJssellake water. However, membrane performance (i.e. MTC) was better for raw IJssellake water (1 year old membrane) compared to WPJ pre-treated water (virgin membrane). The temperature corrected MTC value of raw IJssellake water was 8.5 LMH/bar as opposed to the temperature corrected MTC value of 6.9 LMH/bar for WPJ pre-treated water at 70% recovery, 20 LMH flux and 0.2 m/s crossflow velocity, which is an increase of 1.5 LMH/bar. Moreover, during the testing period with raw IJssellake water, the MTC increased rapidly from 8.5 LMH/bar to 10.8 LMH/bar with every CIP performed, while the feed water temperature did not increase substantially (from 6.9°C to 10.4°C). It seemed that during the filtration rounds with raw IJssellake water, the active outer layer of the membrane has undergone a change in properties. These changes in the properties of the membrane have potentially been caused by excessive cleaning or insufficient flushing time between high pH and low pH. An insufficient flushing time can result in the production of chemical species that may have affected the membrane layers.

An increase in operational conditions (recovery, flux or crossflow velocity) resulted in all cases in a decrease in ion retention. Changing the recovery had the biggest influence on the retention of ion compounds in raw IJssellake water. An increase in recovery resulted in a decrease in retention. This was caused by an increase in ion concentration near the membrane surface resulting in a higher diffusive transport of ions to the permeate side. Especially, a recovery of 90% resulted in low retention of the ion compounds Ca^{2+} and Mg^{2+} (around 10%) and SO_4^{2-} (around 40%). Similar to recovery, an increase in flux resulted in a decrease in retention, due to a higher diffusive transport of ions to the permeate side. This observation is, however, different from literature. Literature shows that an increase in flux should lead to an increase in retention caused by an increase in convective transport to the permeate side. Consequently, this results in a bigger volume of water on the permeate side and a dilution of the ion concentration. It seemed that in the dNF40 pilot the diffusive transport was dominant over convective transport, which could possible be explained by the low crossflow velocity (0.2 m/s), which potentially enhances the effect of CP near the membrane. An increase in crossflow velocity also resulted in a decrease in retention. This is unusual since an increase in crossflow velocity should actually result

in a decrease in ion concentrations near the membrane surface due to a lower diffusive transport of ions to the permeate side. The lower ion retention with increasing crossflow velocity can potentially be attributed to the higher MTC in round E, which was 10.3 LMH/bar as opposed to 8.5 LMH/bar in round A. The removal of NOM was consistently above 90% in every round and not influenced by a change in operational conditions, which is due to the high MW values of these compounds.

Comparing the ion retention of raw IJssellake water to the ion retention of WPJ pre-treated water, a lower retention was observed during the operation with raw IJssellake water. This can potentially be attributed to the increase in MTC of 1.5 LMH/bar in raw IJssellake water (compared to WPJ pre-treated water) caused by a change in the membrane properties due to frequent CIP cleaning. A higher MTC represent a bigger pore sizes in the membrane surface or potentially a decrease in the thickness of the active membrane layer. This results in an increase in ion transport to the permeate side. Another potential reason for the decrease in retention could be the higher NOM concentration in IJssellake raw surface water (6 mg/L) compared to WPJ pre-treated water (3 mg/L). NOM is able to form Ca^{2+}-NOM complexes which can potentially adsorb on the membrane surface reducing the negative charge of the active outer layer. However, the membrane performance parameters during pilot operation showed limited adsorption of Ca^{2+}-NOM complexes on the membrane as no fouling impact is observed.

The PFAS compounds in the spiked solution were retained well by the membrane (above 80%). The retention of the background PFAS compounds was lower (between 40%-100%). Especially, PFBA and PFBS with a retention between 40%-70% is low, which can be attributed to the low MW of these PFAS compounds. The retention of PFAS increased with elevated MW. For low MW PFAS compounds (background PFAS compound) a decrease in recovery and increase in flux resulted in a higher PFAS retention. A change in recovery and flux did not have an influence on the spiked PFAS retention. PFAS adsorption took place in the first 2h of the experiment and adsorption percentages of 30%-90% were observed. The most hydrophobic PFAS compound, PFOS had with an adsorption percentage of 90% the highest adsorption.

The retention of the pharmaceuticals in the spiked solution was around 30%. This can be attributed to the low MW of the pharmaceuticals, which were all below the MWCO of the membrane (400 Da). It was, therefore, difficult to find a relation between the MW of the pharmaceutical and the retention. In round C2, the negative charged pharmaceuticals were retained better than the positive and neutral charged pharmaceuticals, due to the negative surface charge of the membrane. In addition, hydrophobic compounds were retained better by the membrane than hydrophilic compounds.

To compare the economical feasibility (OPEX and CAPEX) of the dNF40 membranes with the UF-RO membranes in Heemskerk, a 5-stage full-scale dNF40 plant has been designed based on a permeate flow of 15 M m^3/year, a total hardness concentration in the permeate stream below 1.4 mmol/L and a recovery percentage of 85%. The total cost (OPEX and CAPEX) were cheapest for a full-scale dNF40 plant fed with raw IJssellake water due to the fact that no costs were attributed to pre-treatment steps. This was followed by the total cost for a full-scale dNF40 plant fed with WPJ pre-treated water. The most expensive treatment plant was the UF-RO in Heemskerk, due to the higher contribution of energy and chemical cost in the overall OPEX. In the dNF40 plant, the membrane replacements costs were the dominant contributor to the overall OPEX, due to higher membrane prices for HF NF membranes over UF and RO membranes.

The experiments on the dNF40 pilot fed with WPJ pre-treated water and raw IJssellake water imply that HF NF membranes were not a suitable candidate for direct drinking water production or for the replacement of the UF-RO process in Heemskerk, at least under the tested conditions. This was mainly related to the low pharmaceutical retention and the high total hardness concentration in the permeate. However, the retention of pharmaceuticals and total hardness can potentially be increased by membrane modification, hybrid processes or a full-scale system with a membrane lifetime of 3.8 years. Even though the drinking water quality standards were not yet achieved by the use of HF NF membranes, it does not mean that HF NF membranes cannot be used at all. The high NOM and PFAS retention of the dNF40 pilot show that within PWN, HF NF membranes can be a promising candidate for WPJ RO pre-treatment, conventional and novel pre-treatment and RO concentrate treatment.

6

Recommendations

The results presented in this research showed that the dNF40 pilot has advantages, such as no fouling formation on the membrane during operation, high NOM removal and high PFAS retention. However, the dNF40 pilot permeate stream when operated with raw IJssellake water cannot be used for PWN drinking water purposes, since the total hardness concentration in the permeate stream is above the norm set by PWN. Moreover, the OMP retention is lower than expected. The following recommendations for future research can be provided:

1. From the results it seemed that the outer active layer of the membrane has undergone a change in properties due to the frequent CIP cleaning. This increased the MTC to higher values than the initial values of the virgin membrane. As a result of this higher MTC, the retention of ions, especially Ca^{2+}, Mg^{2+} and SO_4^{2-}, decreased substantially. This decrease in ion retention does have its advantages, such as lower energy cost and post conditioning cost. However, the Ca^{2+} and Mg^{2+} retention was not sufficient enough to achieve the desired total hardness value norm. MWCO-experiments with an uncharged molecule can evaluate if the pore size within the dNF40 membrane has changed during the filtration experiments with raw IJssellake water.
2. The possible change in properties of the outer active layer might be the effect of insufficient flushing in between the high pH cleaning and low pH cleaning. NaOCl/NaOH, if not flushed away completely, can react with citric acid and produce free residual chlorine, which can possibly affect the membrane layers. The flushing time needs to be revised and if necessary an improved CIP procedure needs to be proposed.
3. Similar experiments can be performed on a new dNF40 membrane with the same properties as the membrane used in this study. This experiment can evaluate if the MTC influenced the ion retention. It might be that with the new dNF40 membrane, the total hardness in the permeate water will be sufficient for the production of drinking water at PWN.
4. All filtration tests with raw IJssellake water were done with cold feed water temperatures. In summer, the temperature of the IJssellake is higher resulting in different water quality and more fouling constituents in the water. Pilot operation throughout the whole year should be done to see if a change in water quality has an effect on membrane performance parameters, fouling or retention of compounds.
5. OMP retention tests can be duplicated to determine if the low retention of some OMP compounds are related to measurement uncertainty.
6. In this research, a single dNF40 membrane was tested. From this research, it can be concluded that when the dNF40 pilot is fed with raw IJssellake water, the permeate stream cannot be used for drinking water purposes by PWN. However, this might be different when a multi-stage dNF40 membrane system is tested, since a multi-stage dNF40 membrane system will improve the permeate water quality substantially.

Bibliography

[1] T. Sewerin, M.G. Elshof, S. Matencio, M. Boerrigter, J. Yu, and J. de Grooth. “Advances and Applications of Hollow Fiber Nanofiltration Membranes: A Review”. In: *Membranes* 11 (2021), p. 890. ISSN: 2077-0375. DOI: 10.3390/membranes11110890.

[2] S.S. Madaeni. “The application of membrane technology for water disinfection”. In: *Water Research* 33 (1998), pp. 301–308. DOI: 10.1016/S0043-1354(98)00212-7.

[3] Y. Luo, W. Guo, H.H. Ngo, L.D. Nghiem, F.I. Hai, J. Zhang, S. Liang, and X.C. Wang. “A review on the occurrence of micropollutants in the aquatic environment and their fate and removal during wastewater treatment”. In: *Science of the Total Environment* 473-474 (2014), pp. 619–641. ISSN: 18791026. DOI: 10.1016/j.scitotenv.2013.12.065.

[4] S.P. Lenka, M. Kah, and L.P. Padhye. “A review of the occurrence, transformation, and removal of poly- and perfluoroalkyl substances (PFAS) in wastewater treatment plants”. In: *Water Research* 199 (2021). ISSN: 18792448. DOI: 10.1016/j.watres.2021.117187.

[5] J.L. Domingo and M. Nadal. “Human exposure to per- and polyfluoroalkyl substances (PFAS) through drinking water: A review of the recent scientific literature”. In: *Environmental Research* 177 (2019). ISSN: 10960953. DOI: 10.1016/j.envres.2019.108648.

[6] M.A. Junker, W.M. de Vos, R.G.H. Lammertink, and J. de Grooth. “Bridging the gap between lab-scale and commercial dimensions of hollow fiber nanofiltration membranes”. In: *Journal of Membrane Science* 624 (2021). ISSN: 18733123. DOI: 10.1016/j.memsci.2021.119100.

[7] M. Frank, G. Bargeman, A. Zwijnenburg, and M. Wessling. “Capillary hollow fiber nanofiltration membranes”. In: *Separation and Purification Technology* 22 (2001), pp. 499–506. DOI: 10.1016/S1383-5866(00)00171-4.

[8] N. Joseph, P. Ahmadiannamini, R. Hoogenboom, and I.F.J. Vankelecom. “Layer-by-layer preparation of polyelectrolyte multilayer membranes for separation”. In: *Polymer Chemistry* 5 (2014), pp. 1817–1831. ISSN: 17599962. DOI: 10.1039/c3py01262j.

[9] A. Arun. *Direct Nanofiltration of Surface Water Investigating the fouling and rejection performance of Low MWCO Hollow fiber Nanofiltration Membranes*. 2019. URL: http://repository.tudelft.nl/..

[10] S. Van Der Poel. *Parting ways-removal of salts and organic micropollutants by direct nanofiltration Pretreatment of surface water for the production of dune infiltration water*. 2020. URL: http://repository.tudelft.nl/..

[11] J. de Grooth, D.M. Reurink, J. Ploegmakers, W.M. de Vos, and K. Nijmeijer. “Charged micropollutant removal with hollow fiber nanofiltration membranes based on polycation/polyzwitterion/polyanion multilayers”. In: *ACS Applied Materials and Interfaces* 6 (2014), pp. 17009–17017. ISSN: 19448252. DOI: 10.1021/am504630a.

[12] C.F. Wan, T. Yang, G.G. Lipscomb, D.J. Stookey, and T.S. Chung. “Design and fabrication of hollow fiber membrane modules”. In: *Journal of Membrane Science* 538 (2017), pp. 96–107. ISSN: 18733123. DOI: 10.1016/j.memsci.2017.05.047.

[13] NX Filtration. *WRC200 dNF40 Integrated Rack Design Hollow fiber nanofiltration membrane module for water and wastewater applications*.

[14] N.S. Suhalim, N. Kasim, E. Mahmoudi, I.J. Shamsudin, A.W. Mohammad, F.M. Zuki, and N. Laili-Azua Jamari. “Rejection Mechanism of Ionic Solute Removal by Nanofiltration Membranes: An Overview”. In: *Nanomaterials* 12 (2022), p. 437. ISSN: 2079-4991. DOI: 10.3390/nano12030437.

[15] J. Campbell and A.S. Vikulina. “Layer-by-layer assemblies of biopolymers: Build-up, mechanical stability and molecular dynamics”. In: *Polymers* 12 (2020), pp. 1–30. ISSN: 20734360. DOI: 10.3390/polym12091949.

[16] A.I. Schäfer, A.G. Fane, and T.D. Waite. “Nanofiltration of natural organic matter: Removal, fouling and the influence of multivalent ions”. In: *Desalination* 118 (1998), pp. 109–122. DOI: 10.1016/S0011-9164(98)00104-0.

[17] D. Ghernaout. “Natural Organic Matter Removal in the Context of the Performance of Drinking Water Treatment Processes—Technical Notes”. In: *Open Access Library Journal* 07 (2020), pp. 1–40. ISSN: 2333-9721. DOI: 10.4236/oalib.1106751.

[18] I. Caltran, S.G.J. Heijman, H.L. Shorney-Darby, and L.C. Rietveld. “Impact of removal of natural organic matter from surface water by ion exchange: A case study of pilots in Belgium, United Kingdom and the Netherlands”. In: *Separation and Purification Technology* 247 (2020). ISSN: 18733794. DOI: 10.1016/j.seppur.2020.116974.

[19] S. Ebrahimzadeh, B. Wols, A. Azzellino, B.J. Martijn, and J.P. van der Hoek. “Quantification and modelling of organic micropollutant removal by reverse osmosis (RO) drinking water treatment”. In: *Journal of Water Process Engineering* 42 (2021). ISSN: 22147144. DOI: 10.1016/j.jwpe.2021.102164.

[20] M.O. Barbosa, N.F.F. Moreira, A.R. Ribeiro, M.F.R. Pereira, and A.M.T. Silva. “Occurrence and removal of organic micropollutants: An overview of the watch list of EU Decision 2015/495”. In: *Water Research* 94 (2016), pp. 257–279. ISSN: 18792448. DOI: 10.1016/j.watres.2016.02.047.

[21] C.H. Wei, N. Wang, C. HoppeJones, T.O. Leiknes, G. Amy, Q. Fang, X. Hu, and H. Rong. “Organic micropollutants removal in sequential batch reactor followed by nanofiltration from municipal wastewater treatment”. In: *Bioresource Technology* 268 (2018), pp. 648–657. ISSN: 18732976. DOI: 10.1016/j.biortech.2018.08.073.

[22] M.F. Rahman, S Peldszus, and W.B. Anderson. “Behaviour and fate of perfluoroalkyl and polyfluoroalkyl substances (PFASs) in drinking water treatment: A review”. In: *Water Research* 50 (2014), pp. 318–340. ISSN: 18792448. DOI: 10.1016/j.watres.2013.10.045.

[23] G.B. Post, J.A. Gleason, and K.R. Cooper. “Key scientific issues in developing drinking water guidelines for perfluoroalkyl acids: Contaminants of emerging concern”. In: *PLoS Biology* 15 (2017). ISSN: 15457885. DOI: 10.1371/journal.pbio.2002855.

[24] Rijksinstituut voor Volksgezondheid en Milieu (RIVM). *Analyse bijdrage drinkwater en voedsel aan blootstelling EFSA-4 PFAS in Nederland en advies drinkwaterrichtwaarde*. 2021. URL: https://www.rivm.nl/documenten/analyse-bijdrage-drinkwater-en-voedsel-aan-blootstelling-efsa-4-pfas-in-nederland.

[25] W. Cheng, C. Liu, T. Tong, R. Epsztein, M. Sun, R. Verduzco, J. Ma, and M. Elimelech. “Selective removal of divalent cations by polyelectrolyte multilayer nanofiltration membrane: Role of polyelectrolyte charge, ion size, and ionic strength”. In: *Journal of Membrane Science* 559 (2018), pp. 98–106. ISSN: 18733123. DOI: 10.1016/j.memsci.2018.04.052.

[26] M. Park and S.A. Snyder. “Advanced Treatment Processes”. In: *Contaminants of Emerging Concern in Water and Wastewater: Advanced Treatment Processes* (2019), pp. 177–206. DOI: 10.1016/B978-0-12-813561-7.00006-7.

[27] E.E. Chang, C.H. Liang, C.P. Huang, and P.C. Chiang. “A simplified method for elucidating the effect of size exclusion on nanofiltration membranes”. In: *Separation and Purification Technology* 85 (2012), pp. 1–7. ISSN: 13835866. DOI: 10.1016/j.seppur.2011.05.002.

[28] Z. Ma, M. Wang, X. Gao, and C. Gao. “Charge and separation characteristics of nanofiltration membrane embracing dissociated functional groups”. In: *Frontiers of Environmental Science and Engineering* 8 (2014), pp. 650–658. ISSN: 2095221X. DOI: 10.1007/s11783-013-0605-1.

[29] J.M.M. Peeters, J.P. Boom, M.H.V. Mulder, and H. Strathmann. “Retention measurements of nanofiltration membranes with electrolyte solutions”. In: *Journal of Membrane Science* 145 (1998), pp. 199–209. DOI: 10.1016/S0376-7388(98)00079-9.

[30] S.L. Zhong, Z.M. Dang, W.Y. Zhou, and H.W. Cai. “Past and future on nanodielectrics”. In: *IET Nanodielectrics* 1 (2018), pp. 41–47. ISSN: 25143255. DOI: 10.1049/iet-nde.2018.0004.

[31] Y. Roy, D.M. Warsinger, and J.H. Lienhard. “Effect of temperature on ion transport in nanofiltration membranes: Diffusion, convection and electromigration”. In: *Desalination* 420 (2017), pp. 241–257. ISSN: 00119164. DOI: 10.1016/j.desal.2017.07.020.

[32] S.C. Osorio, P.M. Biesheuvel, J.E. Dykstra, and E. Virga. “Nanofiltration of complex mixtures: The effect of the adsorption of divalent ions on membrane retention”. In: *Desalination* 527 (2022), p. 115552. ISSN: 00119164. DOI: 10.1016/j.desal.2022.115552.

[33] T.K. Sherwood, P.L.T. Brian, R.E. Fisher, and L. Dresner. “Salt concentration at phase boundaries in desalination by reverse osmosis”. In: *Industrial Engineering Chemistry Fundamentals* 4 (1965), pp. 113–118. DOI: 10.1021/i160014a001.

[34] S.S. Sablani, F.A. Goosena, R. Al-Belushi, and M. Wilf. “Concentration polarization in ultrafiltration and reverse osmosis: a critical review”. In: *Desalination* 141 (2001), pp. 269–289. DOI: 10.1016/S0011-9164(01)85005-0.

[35] W.R. Bowen and F. Jenner. “Theoretical descriptions of membrane filtration of colloids and fine particles: an assessment and review”. In: *Advances in Colloid and Interface Science* 56 (1995), pp. 141–200. DOI: 10.1016/0001-8686(94)00232-2.

[36] F. Bi, H. Zhao, L. Zhang, Q. Ye, H. Chen, and C. Gao. “Discussion on calculation of maximum water recovery in nanofiltration system”. In: *Desalination* 332 (2014), pp. 142–146. ISSN: 00119164. DOI: 10.1016/j.desal.2013.11.017.

[37] Z.F. Cui, Y. Jiang, and R.W. Field. “Fundamentals of Pressure-Driven Membrane Separation Processes”. In: *Membrane Technology* (2010), pp. 1–18. DOI: 10.1016/B978-1-85617-632-3.00001-X.

[38] M.C. Ferreira, J.V. Nicolini, H.L.S. Fernandes, and F.V. da Fonseca. “Modeling of ionic transport through nanofiltration membranes considering zeta potential and dielectric exclusion phenomena”. In: *International Journal of Engineering and Technical Research* 7 (2017), pp. 6–14. ISSN: 2321-0869.

[39] A. Ghorbani, B. Bayati, and T. Kikhavani. “Modelling ion transport in an amine solution through a nanofiltration membrane”. In: *Brazilian Journal of Chemical Engineering* 36 (2019), pp. 1667–1677. ISSN: 01046632. DOI: 10.1590/0104-6632.20190364s20190068.

[40] T. Chaabane, S. Taha, M.T. Ahmed, R. Maachi, and G. Dorange. “Coupled model of film theory and the Nernst-Planck equation in nanofiltration”. In: *Desalination* 206 (2007), pp. 424–432. ISSN: 00119164. DOI: 10.1016/j.desal.2006.03.577.

[41] D. Menne, M. Wessling, and N. Benes. “Layer-by-Layer Design of Nanofiltration Membranes Entwicklung von ”Layer-by-Layer” Nanofiltrationsmembranen”. In: *pHd* (2017).

[42] M.U. Siddiqui, A.F.M. Arif, and Salem Bashmal. “Permeability-selectivity analysis of microfiltration and ultrafiltration membranes: Effect of pore size and shape distribution and membrane stretching”. In: *Membranes* 6 (2016). ISSN: 20770375. DOI: 10.3390/membranes6030040.

[43] W. Guo, H.H. Ngo, and J. Li. “A mini-review on membrane fouling”. In: *Bioresource Technology* 122 (2012), pp. 27–34. ISSN: 09608524. DOI: 10.1016/j.biortech.2012.04.089.

[44] T. Fane. “Irreversible Fouling”. In: *Encyclopedia of Membranes* (2015). Ed. by L.D. Enrico and L. Giorno. DOI: 10.1007/978-3-642-40872-4_328-1.

[45] F.C. Silva. “Fouling of Nanofiltration Membranes”. In: (2018). Ed. by Farrukh M.A. DOI: 10.5772/intechopen.75353.

[46] H. Li and V. Chen. “Membrane Fouling and Cleaning in Food and Bioprocessing”. In: *Membrane Technology* (2010), pp. 213–254. DOI: 10.1016/B978-1-85617-632-3.00010-0.

[47] G.D. Arend, K. Rezzadori, L.S. Soares, and J.C.C. Petrus. “Performance of nanofiltration process during concentration of strawberry juice”. In: *Journal of Food Science and Technology* 56 (2019), pp. 2312–2319. ISSN: 09758402. DOI: 10.1007/s13197-019-03659-z.

[48] P. Kehrein, M. Jafari, M. Slagt, E. Cornelissen, P. Osseweijer, J. Posada, and M. van Loosdrecht. “A techno-economic analysis of membrane-based advanced treatment processes for the reuse of municipal wastewater”. In: *Water Reuse* 11 (2021), pp. 705–725. ISSN: 27096106. DOI: 10.2166/wrd.2021.016.

[49] Y. Song, X. Gao, T. Li, C. Gao, and J. Zhou. “Improvement of overall water recovery by increasing RNF with recirculation in a NF-RO integrated membrane process for seawater desalination”. In: *Desalination* 361 (2015), pp. 95–104. ISSN: 00119164. DOI: 10.1016/j.desal.2015.01.023.

[50] V. Gedam, J.L. Patil, S. Kagne, R.S. Sirsam, and P. Labhasetwar. “Performance Evaluation of Polyamide Reverse Osmosis Membrane for Removal of Contaminants in Ground Water Collected from Chandrapur District”. In: *Journal of Membrane Science Technology* 2 (2012). DOI: 10.4172/2155-9589.1000117.

[51] M.M. Emamjomeh, H. Torabi, M. Mousazadeh, M.H. Alijani, and F. Gohari. “Impact of independent and non-independent parameters on various elements’ rejection by nanofiltration employed in groundwater treatment”. In: *Applied Water Science* 9 (2019). ISSN: 2190-5487. DOI: 10.1007/s13201-019-0949-1.

[52] Z. He, D.J. Miller, S. Kasemset, D.R. Paul, and B.D. Freeman. “The effect of permeate flux on membrane fouling during microfiltration of oily water”. In: *Journal of Membrane Science* 525 (2017), pp. 25–34. ISSN: 18733123. DOI: 10.1016/j.memsci.2016.10.002.

[53] H. Choi, K. Zhang, D.D. Dionysiou, D.B. Oerther, and G.A. Sorial. “Influence of cross-flow velocity on membrane performance during filtration of biological suspension”. In: *Journal of Membrane Science* 248 (2005), pp. 189–199. ISSN: 03767388. DOI: 10.1016/j.memsci.2004.08.027.

[54] S. Jiang, Y. Li, and B.P. Ladewig. “A review of reverse osmosis membrane fouling and control strategies”. In: *Science of the Total Environment* 595 (2017), pp. 567–583. ISSN: 18791026. DOI: 10.1016/j.scitotenv.2017.03.235.

[55] A.W. Zularisam, A.F. Ismail, and R. Salim. “Behaviours of natural organic matter in membrane filtration for surface water treatment - a review”. In: *Desalination* 194 (2006), pp. 211–231. ISSN: 00119164. DOI: 10.1016/j.desal.2005.10.030.

[56] D.M. Reurink, E. Te Brinke, I. Achterhuis, H.D.W. Roesink, and W.M. de Vos. “Nafion-Based Low-Hydration Polyelectrolyte Multilayer Membranes for Enhanced Water Purification”. In: *ACS Applied Polymer Materials* 1 (2019), pp. 2543–2551. ISSN: 26376105. DOI: 10.1021/acsapm.9b00689.

[57] A.E. Yaroshchuk. “Negative rejection of ions in pressure-driven membrane processes”. In: *Advances in Colloid and Interface Science* 139 (2008), pp. 150–173. ISSN: 00018686. DOI: 10.1016/j.cis.2008.01.004.

[58] O. Labban, C. Liu, T.H. Chong, and J.H. Lienhard. “Fundamentals of low-pressure nanofiltration: Membrane characterization, modeling, and understanding the multi-ionic interactions in water softening”. In: *Journal of Membrane Science* 521 (2017), pp. 18–32. ISSN: 18733123. DOI: 10.1016/j.memsci.2016.08.062.

[59] M. Reig, N. Pagès, E. Licon, C. Valderrama, O. Gibert, A. Yaroshchuk, and J.L. Cortina. “Evolution of electrolyte mixtures rejection behaviour using nanofiltration membranes under spiral wound and flat-sheet configurations”. In: *Desalination and Water Treatment* 56 (2015), pp. 3519–3529. ISSN: 19443986. DOI: 10.1080/19443994.2014.974215.

[60] S. Lee, J. Kim, and C.H. Lee. *Analysis of CaSO 4 scale formation mechanism in various nanofiltration modules*. 1999, pp. 63–74. DOI: 10.1016/S0376-7388(99)00156-8.

[61] B.A.M. Al-Rashdi, D.J. Johnson, and N. Hilal. “Removal of heavy metal ions by nanofiltration”. In: *Desalination* 315 (2013), pp. 2–17. ISSN: 00119164. DOI: 10.1016/j.desal.2012.05.022.

[62] J. Fernández-Sempere, F. Ruiz-Beviá, P. García-Algado, and R. Salcedo-Díaz. “Experimental study of concentration polarization in a crossflow reverse osmosis system using Digital Holographic Interferometry”. In: *Desalination* 257 (2010), pp. 36–45. ISSN: 00119164. DOI: 10.1016/j.desal.2010.03.010.

[63] R. Bian, K. Yamamoto, and Y. Watanabe. “The effect of shear rate on controlling the concentration polarization and membrane fouling”. In: *Desalination* 131 (2000), pp. 225–236. DOI: https://doi.org/10.1016/S0011-9164(00)90021-3.

[64] M. Haddad, T. Ohkame, P.R. Bérubé, and B. Barbeau. “Performance of thin-film composite hollow fiber nanofiltration for the removal of dissolved Mn, Fe and NOM from domestic groundwater supplies”. In: *Water Research* 145 (2018), pp. 408–417. ISSN: 18792448. DOI: 10.1016/j.watres.2018.08.032.

[65] A.I. Schäfer, A. Pihlajamäki, A.G. Fane, T.D. Waite, and M. Nyström. “Natural organic matter removal by nanofiltration: Effects of solution chemistry on retention of low molar mass acids versus bulk organic matter”. In: *Journal of Membrane Science* 242 (2004), pp. 73–85. ISSN: 03767388. DOI: 10.1016/j.memsci.2004.05.018.

[66] S.A. Huber, A. Balz, M. Abert, and W. Pronk. “Characterisation of aquatic humic and non-humic matter with size-exclusion chromatography - organic carbon detection - organic nitrogen detection (LC-OCD-OND)”. In: *Water Research* 45 (2011), pp. 879–885. ISSN: 00431354. DOI: 10.1016/j.watres.2010.09.023.

[67] S. Lee, J. Cho, and M. Elimelech. “Combined influence of natural organic matter (NOM) and colloidal particles on nanofiltration membrane fouling”. In: *Journal of Membrane Science* 262 (2005), pp. 27–41. ISSN: 03767388. DOI: 10.1016/j.memsci.2005.03.043.

[68] F. Beyer, B.M. Rietman, A. Zwijnenburg, P. van den Brink, J.S. Vrouwenvelder, M. Jarzembowska, J. Laurinonyte, A.J.M. Stams, and C.M. Plugge. “Long-term performance and fouling analysis of full-scale direct nanofiltration (NF) installations treating anoxic groundwater”. In: *Journal of Membrane Science* 468 (2014), pp. 339–348. ISSN: 18733123. DOI: 10.1016/j.memsci.2014.06.004.

[69] M. Jafari, A. D’haese, J. Zlopasa, E.R. Cornelissen, J.S. Vrouwenvelder, K. Verbeken, A. Verliefde, M.C.M. van Loosdrecht, and C. Picioreanu. “A comparison between chemical cleaning efficiency in lab-scale and full-scale reverse osmosis membranes: Role of extracellular polymeric substances (EPS)”. In: *Journal of Membrane Science* 609 (2020). ISSN: 18733123. DOI: 10.1016/j.memsci.2020.118189.

[70] S.G.J. Heijman, A.R.D. Verliefde, E.R. Cornelissen, G. Amy, and J.C. Van Dijk. “Influence of natural organic matter (NOM) fouling on the removal of pharmaceuticals by nanofiltration and activated carbon filtration”. In: *Water Science and Technology: Water Supply* 7 (2007), pp. 17–23. ISSN: 16069749. DOI: 10.2166/ws.2007.131.

[71] A. Lidén, E. Lavonen, K.M. Persson, and M. Larson. “Integrity breaches in a hollow fiber nanofilter – Effects on natural organic matter and virus-like particle removal”. In: *Water Research* 105 (2016), pp. 231–240. ISSN: 18792448. DOI: 10.1016/j.watres.2016.08.056.

[72] P.P. Wright, B. Kahler, and L.J. Walsh. “Alkaline sodium hypochlorite irrigant and its chemical interactions”. In: *Materials* 10 (2017). ISSN: 19961944. DOI: 10.3390/ma10101147.

[73] J.M. Gohil and A.K. Suresh. “Chlorine attack on reverse osmosis membranes: Mechanisms and mitigation strategies”. In: *Journal of Membrane Science* 541 (2017), pp. 108–126. ISSN: 18733123. DOI: 10.1016/j.memsci.2017.06.092.

[74] Overheid. *Drinkwaterbesluit*. 2021. URL: https://wetten.overheid.nl/BWBR0030111/2021-10-13#BijlageA.

[75] H2O actueel. *Onderzoek: veel te veel PFAS in vissen in Westerschelde*. 2021. URL: https://www.h2owaternetwerk.nl/h2o-actueel/onderzoek-veel-te-veel-pfas-in-vissen-in-westerschelde.

[76] Y. Wang, I. Zucker, C. Boo, and M. Elimelech. “Removal of Emerging Wastewater Organic Contaminants by Polyelectrolyte Multilayer Nanofiltration Membranes with Tailored Selectivity”. In: *ACS EST Engineering* 1 (2021), pp. 404–414. ISSN: 2690-0645. DOI: 10.1021/acsestengg.0c00160.

[77] J. Xiong, Y. Hou, J. Wang, Z. Liu, Y. Qu, Z. Li, and X. Wang. “The rejection of perfluoroalkyl substances by nanofiltration and reverse osmosis: Influencing factors and combination processes”. In: *Environmental Science: Water Research and Technology* 7 (2021), pp. 1928–1943. ISSN: 20531419. DOI: 10.1039/d1ew00490e.

[78] C.J. Liu, T.J. Strathmann, and C. Bellona. “Rejection of per- and polyfluoroalkyl substances (PFASs) in aqueous film-forming foam by high-pressure membranes”. In: *Water Research* 188 (2020). ISSN: 18792448. DOI: 10.1016/j.watres.2020.116546.

[79] T.D. Appleman, E.R.V. Dickenson, C. Bellona, and C.P. Higgins. “Nanofiltration and granular activated carbon treatment of perfluoroalkyl acids”. In: *Journal of Hazardous Materials* 260 (2013), pp. 740–746. ISSN: 03043894. DOI: 10.1016/j.jhazmat.2013.06.033.

[80] S. Kancharla, P. Alexandridis, and M. Tsianou. “Sequestration of per- and polyfluoroalkyl substances (PFAS) by adsorption: Surfactant and surface aspects”. In: *Current Opinion in Colloid and Interface Science* 58 (2022). ISSN: 18790399. DOI: 10.1016/j.cocis.2022.101571.

[81] N. Saeidi, F.D. Kopinke, and A. Georgi. “Understanding the effect of carbon surface chemistry on adsorption of perfluorinated alkyl substances”. In: *Chemical Engineering Journal* 381 (2020). ISSN: 13858947. DOI: 10.1016/j.cej.2019.122689.

[82] T. Wang, C. Zhao, P. Li, Y. Li, and J. Wang. “Fabrication of novel poly(m-phenylene isophthalamide) hollow fiber nanofiltration membrane for effective removal of trace amount perfluorooctane sulfonate from water”. In: *Journal of Membrane Science* 477 (2015), pp. 74–85. ISSN: 18733123. DOI: 10.1016/j.memsci.2014.12.038.

[83] M. Li, F. Sun, W. Shang, X. Zhang, W. Dong, Z. Dong, and S. Zhao. “Removal mechanisms of perfluorinated compounds (PFCs) by nanofiltration: Roles of membrane-contaminant interactions”. In: *Chemical Engineering Journal* 406 (2021). ISSN: 13858947. DOI: 10.1016/j.cej.2020.126814.

[84] M. Llorca, G. Schirinzi, M. Martínez, D. Barceló, and M. Farré. “Adsorption of perfluoroalkyl substances on microplastics under environmental conditions”. In: *Environmental Pollution* 235 (2018), pp. 680–691. ISSN: 18736424. DOI: 10.1016/j.envpol.2017.12.075.

[85] E.W. Tow, M.S. Ersan, S. Kum, T. Lee, T.F. Speth, C. Owen, C. Bellona, M.N. Nadagouda, A.M. Mikelonis, P. Westerhoff, C. Mysore, V.S. Frenkel, V. Desilva, W.S. Walker, A.K. Safulko, and D.A. Ladner. “Managing and treating per-and polyfluoroalkyl substances (Pfas) in membrane concentrates”. In: *AWWA Water Science* 3 (2021). ISSN: 25778161. DOI: 10.1002/aws2.1233.

[86] S.M. Abtahi, L. Marbelia, A.Y. Gebreyohannes, P. Ahmadiannamini, C. Joannis-Cassan, C. Albasi, W.M. de Vos, and I.F.J. Vankelecom. “Micropollutant rejection of annealed polyelectrolyte multilayer based nanofiltration membranes for treatment of conventionally-treated municipal wastewater”. In: *Separation and Purification Technology* 209 (2019), pp. 470–481. ISSN: 18733794. DOI: 10.1016/j.seppur.2018.07.071.

[87] J. Cuhorka, E. Wallace, and P. Mikulášek. “Removal of micropollutants from water by commercially available nanofiltration membranes”. In: *Science of the Total Environment* 720 (2020). ISSN: 18791026. DOI: 10.1016/j.scitotenv.2020.137474.

[88] S.R. Sarathy and M. Mohseni. *UV/H2O2 Treatment of Drinking Water: Impacts on NOM Characteristics*. 2009. URL: www.americanairandwater.com.

[89] D.J. de Ridder, A.R.D. Verliefde, S.G.J. Heijman, J.Q.J.C. Verberk, L.C. Rietveld, L.T.J. van der Aa, G.L. Amy, and J.C. van Dijk. “Influence of natural organic matter on equilibrium adsorption of neutral and charged pharmaceuticals onto activated carbon”. In: *Water Science and Technology* 63 (2011), pp. 416–423. ISSN: 02731223. DOI: 10.2166/wst.2011.237.

[90] E. Gagliano, M. Sgroi, P.P. Falciglia, F.G.A. Vagliasindi, and P. Roccaro. “Removal of poly- and perfluoroalkyl substances (PFAS) from water by adsorption: Role of PFAS chain length, effect of organic matter and challenges in adsorbent regeneration”. In: *Water Research* 171 (2020). ISSN: 18792448. DOI: 10.1016/j.watres.2019.115381.

A

P&ID Mexpert dNF40 pilot

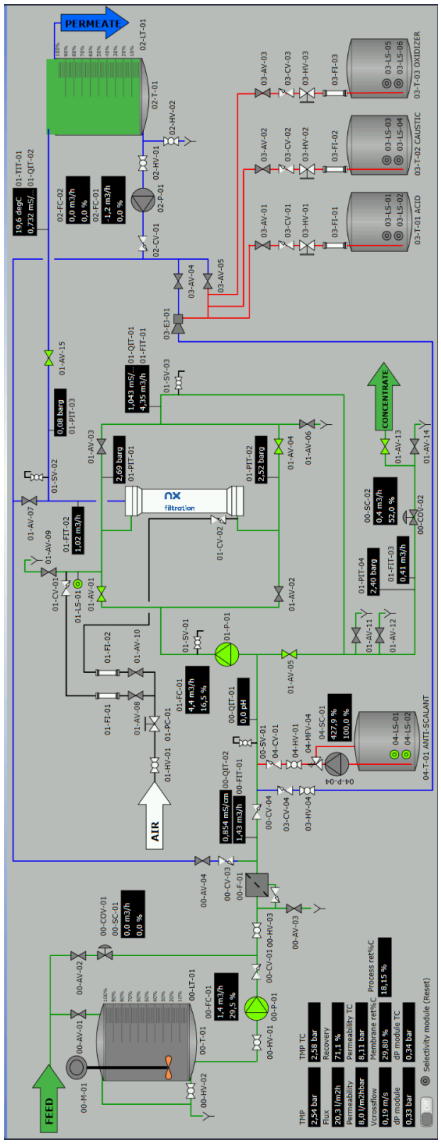

Figure A.1: Enlarged P&ID diagram of the Mexpert dNF40 pilot.

B

Ion membrane retention: impact of recovery

Figure B.1 shows the membrane retention in % based on ion concentrations measured in the permeate stream and the concentrate stream of different ions when operated under 70%, 80% and 90% recovery. The flux and crossflow velocity remained constant at 20 LMH and 0.2 m/s. The membrane retention was calculated with Formula 2.4. The membrane retention during the different filtration rounds with increasing recovery varied in the range of 16%-93%. The ions Cl^- and NO_3^- were negatively retained by the membrane. Those two ions were not shown in the graph.

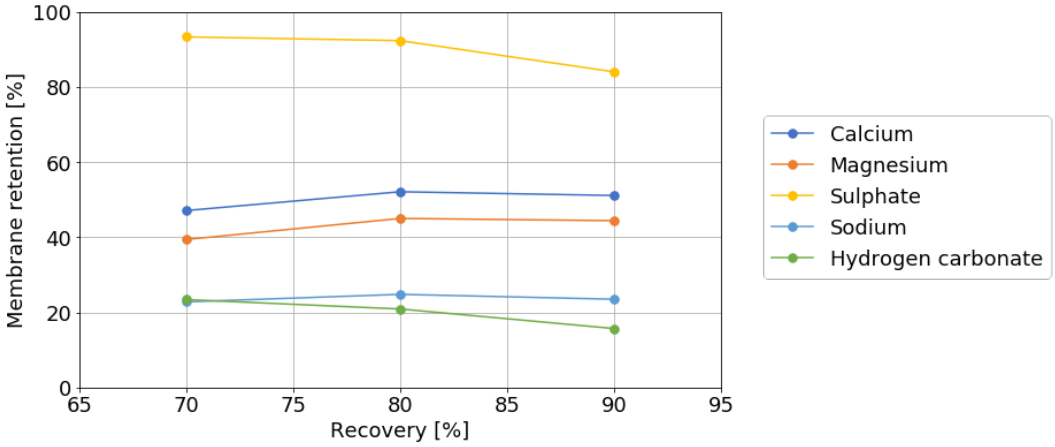

Figure B.1: Ion membrane retention based on ion concentrations measured in permeate stream and concentrate stream during filtration with raw IJssellake water at 70%, 80% and 90% recovery - 20 LMH flux - 0.2 m/s crossflow velocity. The ions barium, phosphate and iron were not considered when calculating the ion membrane retention of the dNF40 pilot due to low concentrations in feed stream, see Figure 4.4. The ions chloride and nitrate had a negative membrane retention and were not shown in this graph.

The divalent ions Ca^{2+}, Mg^{2+} and SO_4^{2-} were retained better by the membrane than the monovalent ions Na^+ and HCO_3^-. In The negative charged divalent ion SO_4^{2-} had with a retention in the range of 84%-93% the highest retention. This was followed by the positive charged divalent ions Ca^{2+} and Mg^{2+} with a retention in the range of 39%-51%. The positive charged monovalent ion Na^+ and the negative charged monovalent ion HCO_3^- had with a retention in the range of 16%-25% the lowest retention. This showed that an increase in recovery did not have an influence on the membrane retention and barely any fouling was observed on the membrane in the applied 70%-90% range.

C

Ion installation retention: pre-treated water

A previous study done at PWNT in March 2021 with the dNF40 pilot on WPJ pre-treated water studied the influence of different operational conditions on ion installation retention of different ion compounds. These results can be found in this Appendix. Figure C.1 shows the installation retention in % with increasing recovery from 60% to 90%. During these experiments the flux and crossflow velocity remained constant at 20 LMH and 0.2 m/s. Figure C.2 shows the installation retention in % with increasing flux from 20 LMH to 38 LMH. During these experiments the recovery and crossflow velocity remained constant at 90% and 0.2 m/s. Figure C.3 shows the installation retention in % with increasing crossflow velocity from 0.1 m/s - 0.3 m/s. During these experiments the recovery and flux remained constant at 90% and 20 LMH.

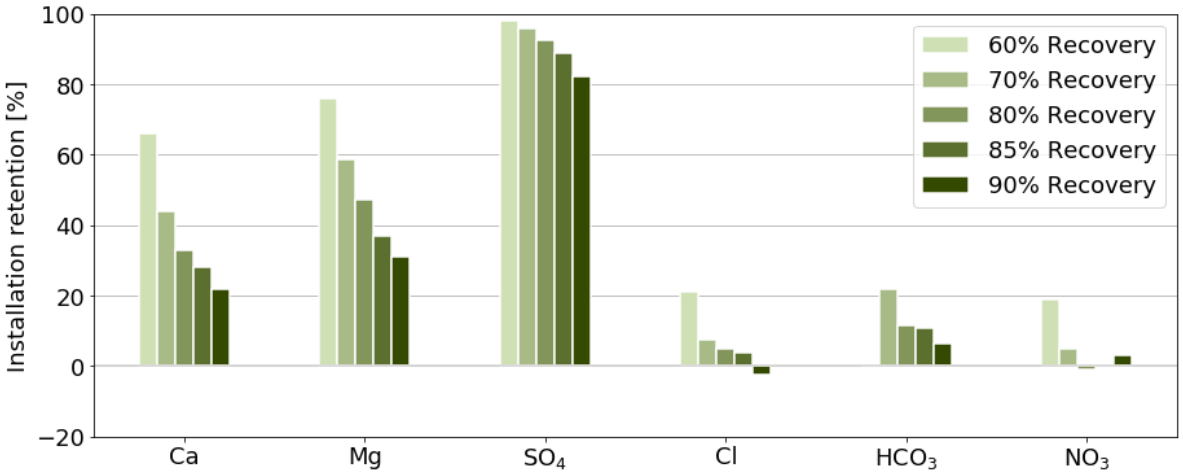

Figure C.1: Ion installation retention based on concentrations measured in feed stream and permeate stream during filtration with WPJ pre-treated water at increasing recovery velocity from 60% to 90% - 20 LMH flux - 0.2 m/s crossflow velocity.

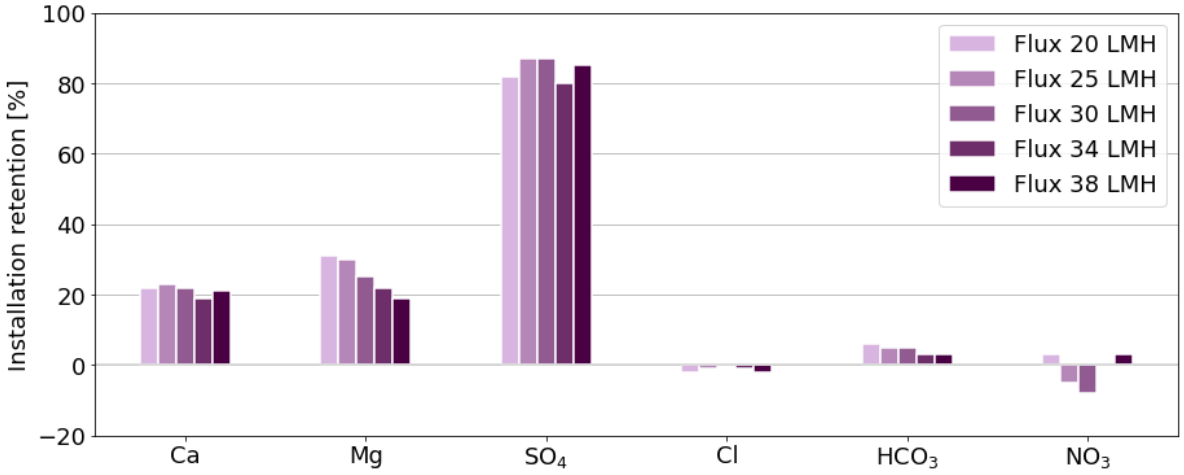

Figure C.2: Ion installation retention based on concentrations measured in feed stream and permeate stream during filtration with WPJ pre-treated water at increasing flux from 20 LMH to 38 LMH - 90 % recovery - 0.2 m/s crossflow velocity.

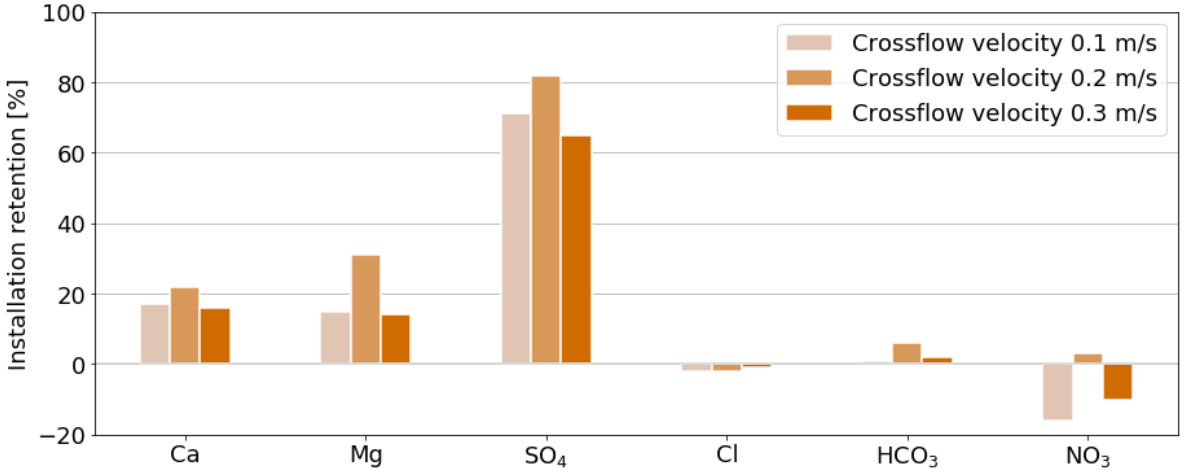

Figure C.3: Ion installation retention based on concentrations measured in feed stream and permeate stream during filtration with WPJ pre-treated water at increasing crossflow velocity from 0.1 m/s to 0.3 m/s - 90% recovery - 20 LMH flux.

D

Membrane performance parameters: pre-treated water

The previous study done at PWNT in March 2021 with the dNF40 pilot on WPJ pre-treated water also studied the influence of different operational conditions on the membrane performance parameters (MTC, TMP and NPD). Table D.1 shows the operational conditions used for the experiments on the dNF40 pilot with WPJ pre-treated water. The highlighted yellow rows have similar operational conditions as the experiments done with raw IJSsellake water.

Table D.1: Summary of operational conditions used during continuous filtration experiment when the pilot was fed with WPJ pre-treated water.

	Recovery [%]	Flux [LMH]	Crossflow velocity [m/s]
Round 1	60	20	0.2
Round 2	70	20	0.2
Round 3	80	20	0.2
Round 4	85	20	0.2
Round 5	90	20	0.2
Round 6	90	25	0.2
Round 7	90	30	0.2
Round 8	90	34	0.2
Round 9	90	38	0.2
Round 10	90	20	0.1
Round 11	90	20	0.3

The membrane performance parameters (MTC), trans membrane pressure (TMP) and normalized pressure drop (NPD) were measured during each experiment with WPJ pre-treated water to detect the fouling potential of the membrane. Figure D.1, D.2 and D.3 shows the membrane performance parameters corrected to a temperature of 20°C with increasing recovery from 60% to 90%. Figure D.4, D.5 and D.6 show the membrane performance parameters corrected to a temperature of 20°C with increasing flux from 20 LMH to 38 LMH. Figure D.7, D.8 and D.9 shows the membrane performance parameters corrected to a temperature of 20°C with increasing crossflow velocity from 0.1 m/s to 0.3 m/s. As can be seen from these graphs, limited to no fouling was observed on the membrane when the pilot was fed with WPJ pre-treated water. The changes in performance parameters were mainly correlated to a change in feed water temperature.

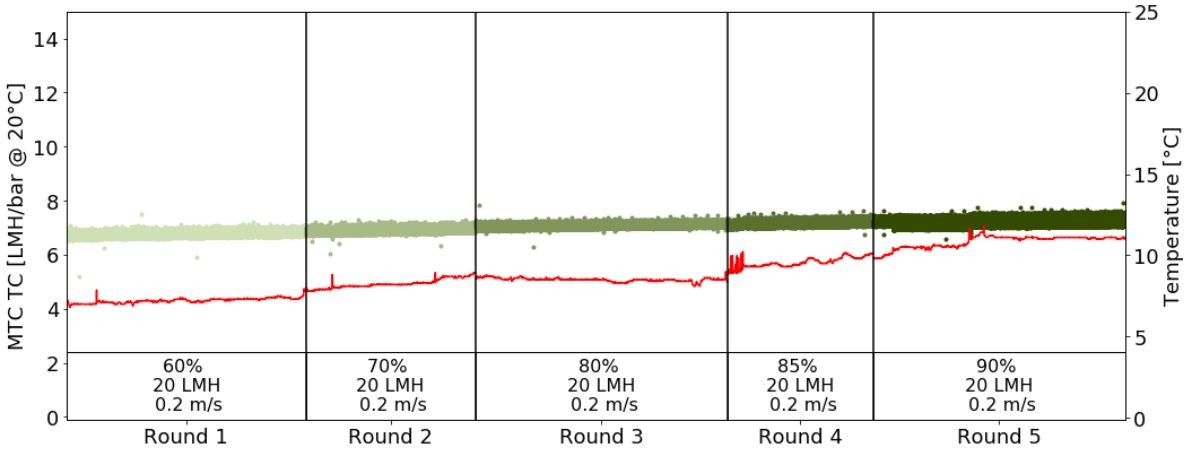

Figure D.1: Mass transfer coefficient temperature corrected during increasing recovery with WPJ pre-treated water. The red line indicates the temperature of the feed water.

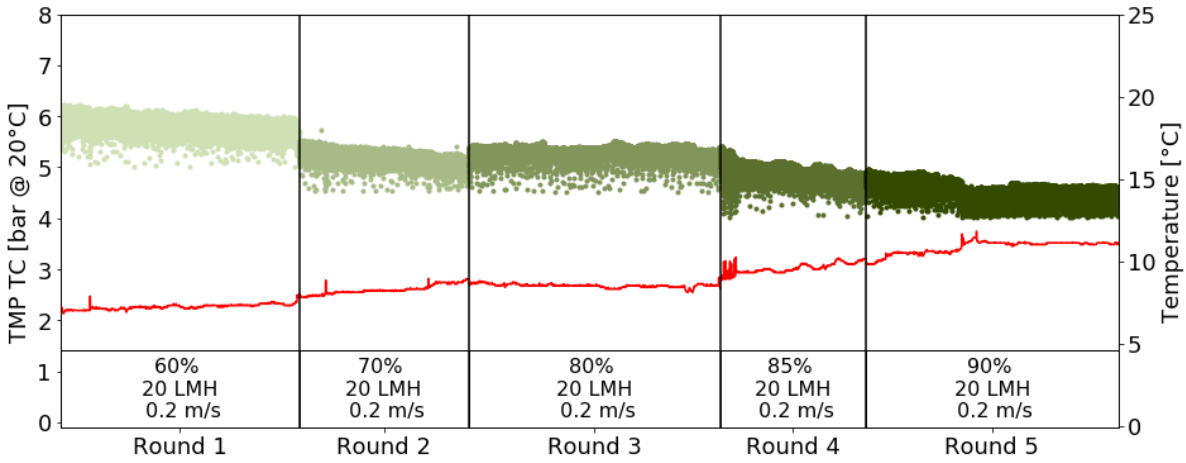

Figure D.2: Trans membrane pressure temperature corrected during increasing recovery with WPJ pre-treated water. The red line indicates the temperature of the feed water.

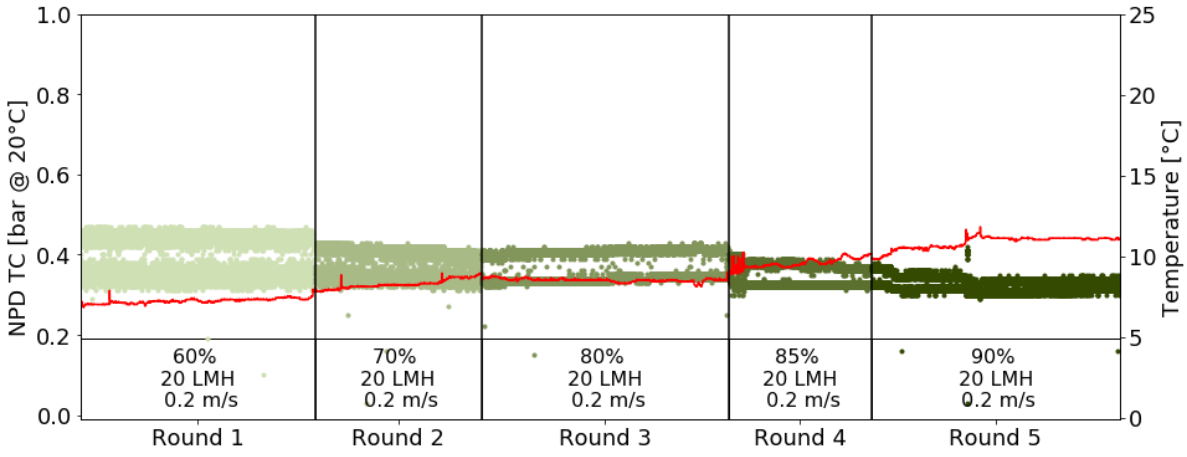

Figure D.3: Normalized pressure drop temperature corrected during increasing recovery with WPJ pre-treated water. The red line indicates the temperature of the feed water.

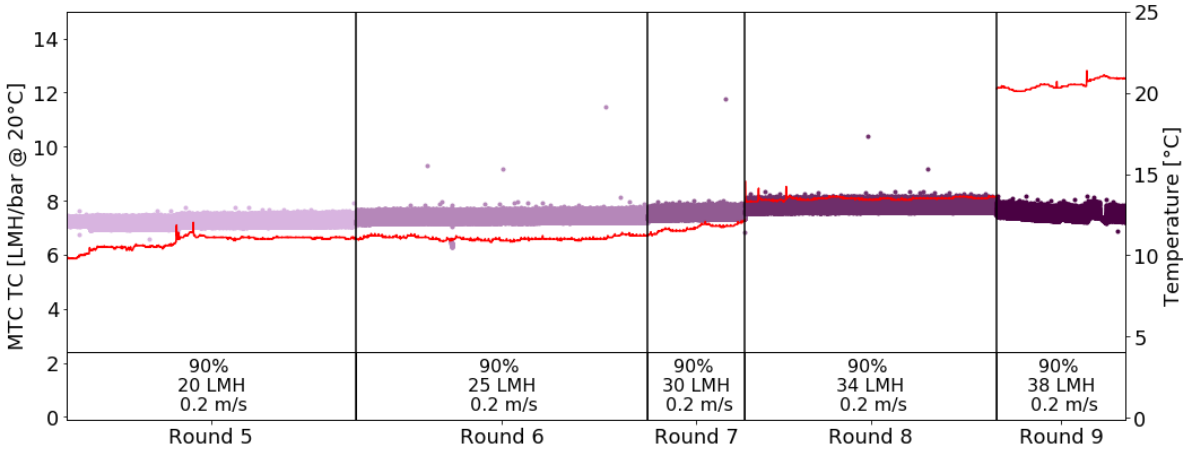

Figure D.4: Mass transfer coefficient temperature corrected during increasing flux with WPJ pre-treated water. The red line indicates the temperature of the feed water.

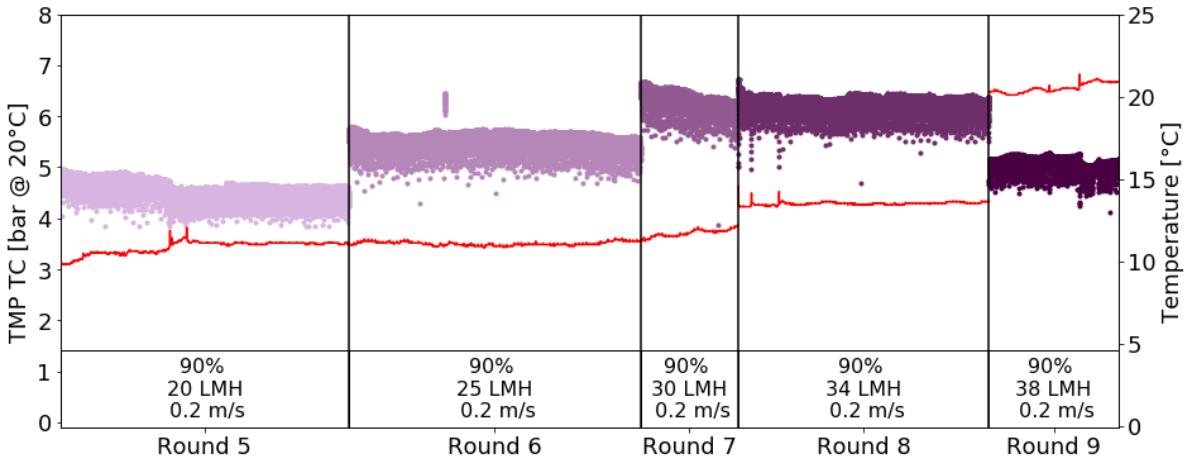

Figure D.5: Trans membrane pressure temperature corrected during increasing flux with WPJ pre-treated water. The red line indicates the temperature of the feed water.

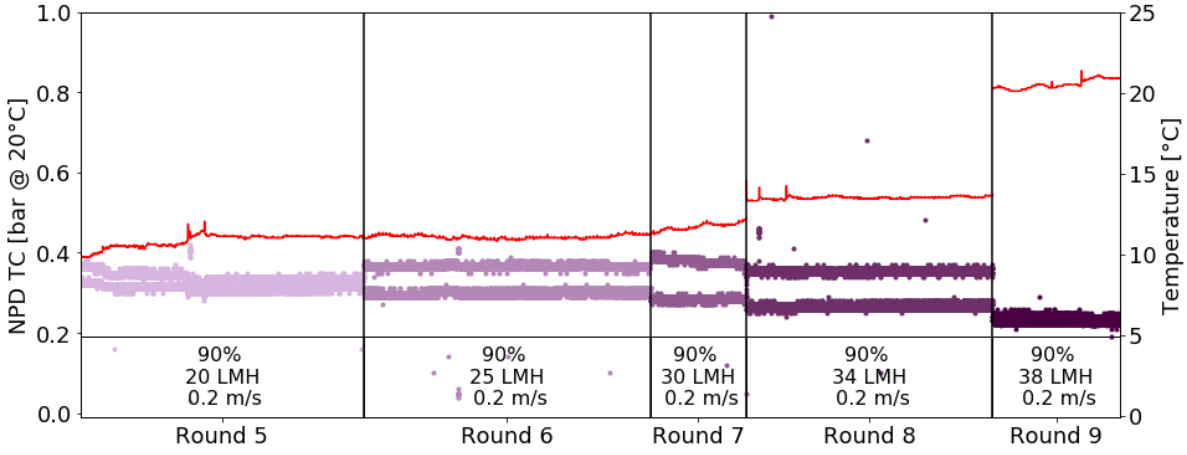

Figure D.6: Normalized pressure drop temperature corrected during increasing flux with WPJ pre-treated water. The red line indicates the temperature of the feed water.

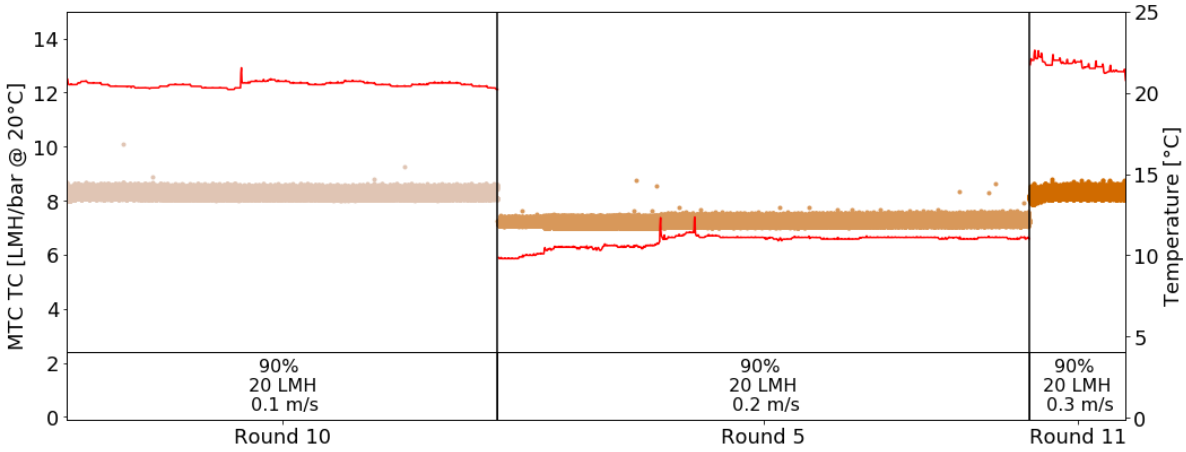

Figure D.7: Mass transfer coefficient temperature corrected during increasing crossflow velocity with WPJ pre-treated water. The red line indicates the temperature of the feed water.

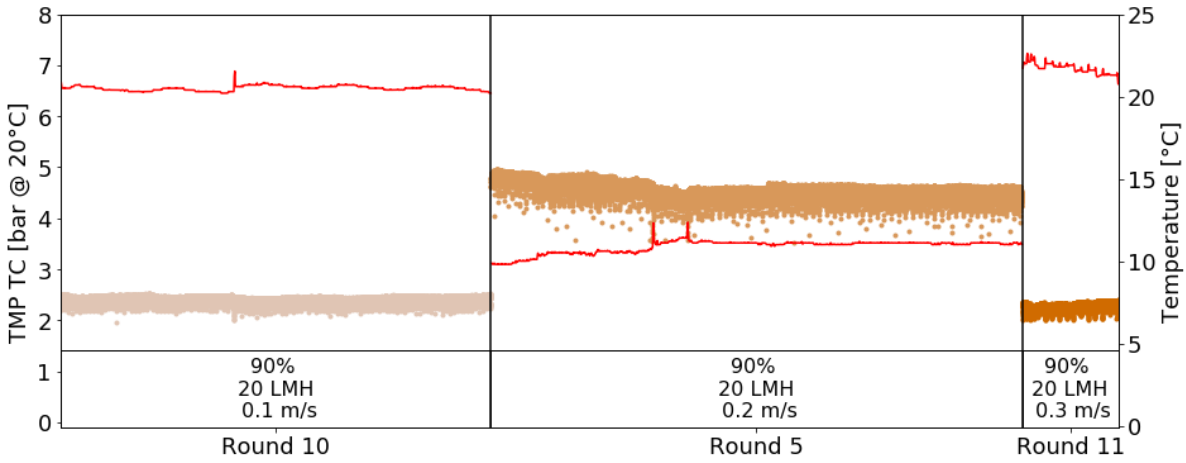

Figure D.8: Trans membrane pressure temperature corrected during increasing crossflow velocity with WPJ pre-treated water. The red line indicates the temperature of the feed water.

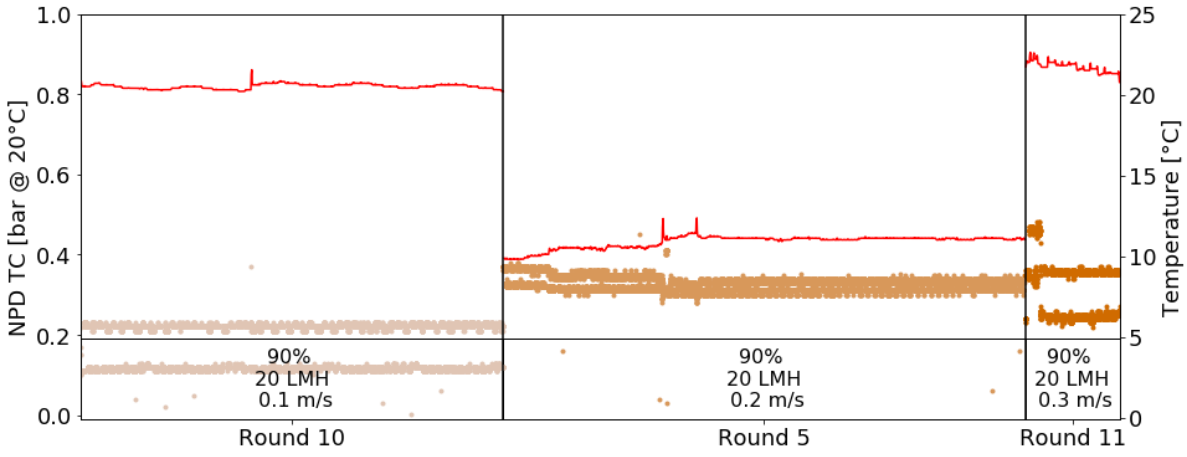

Figure D.9: Normalized pressure drop temperature corrected during increasing crossflow velocity with WPJ pre-treated water. The red line indicates the temperature of the feed water.

E

Average TMP and NPD: pre-treated water and raw surface water

Figure E.1 and E.2 show the average TMP and NPD in bar with increasing recovery of WPJ pre-treated water (green) and raw IJssellake water (blue). The flux and crossflow velocity remained constant at 20 LMH and 0.2 m/s respectively. The filtration round with WPJ pre-treated water was performed when the membrane was completely new (April 2021) and the filtration round with raw IJssellake water was performed when the membrane was one year old (April 2022).

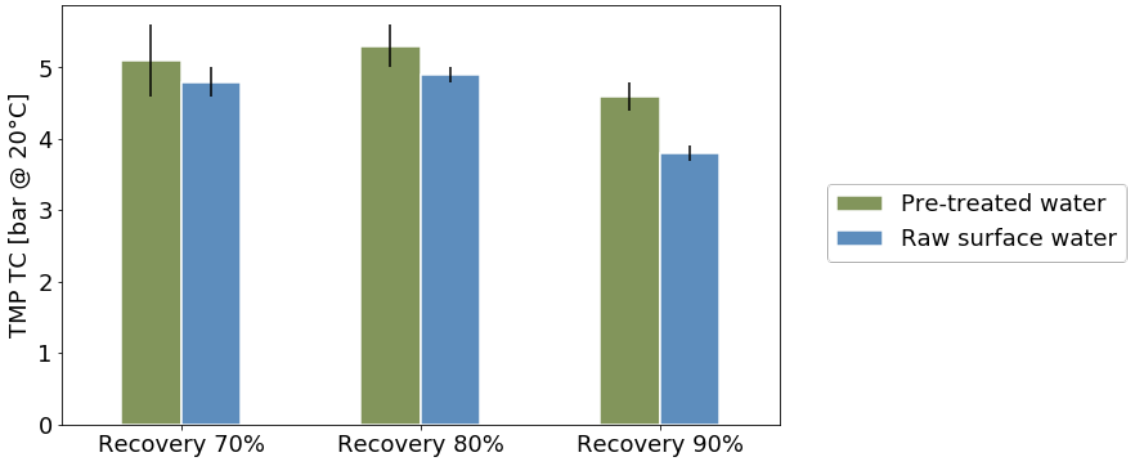

Figure E.1: Average trans membrane pressure temperature corrected of WPJ pre-treated water and raw IJssellake water with increasing recovery. Flux and crossflow velocity remained constant at 20 LMH and 0.2 m/s.

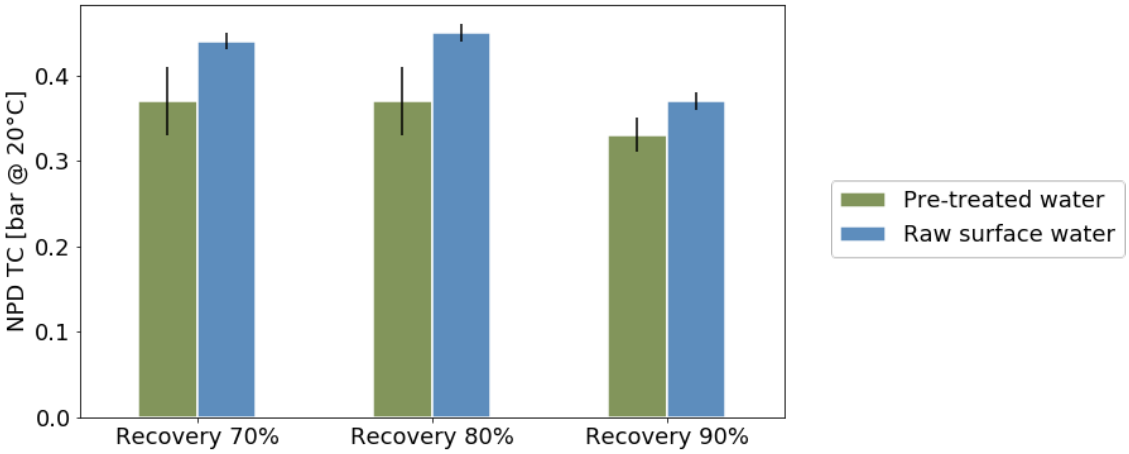

Figure E.2: Average normalized pressure drop temperature corrected of WPJ pre-treated water and raw IJssellake water with increasing recovery. Flux and crossflow velocity remained constant at 20 LMH and 0.2 m/s.

F

Feed water composition: pre-treated water and raw surface water

Figure F.1 shows the concentration in mg/L of different ions and TOC in the feed stream WPJ pre-treated water (green bars) and raw IJssellake water (blue bars) when operated at 70%, 80% and 90% recovery. The flux and crossflow velocity remained constant at 20 LMH and 0.2 m/s.

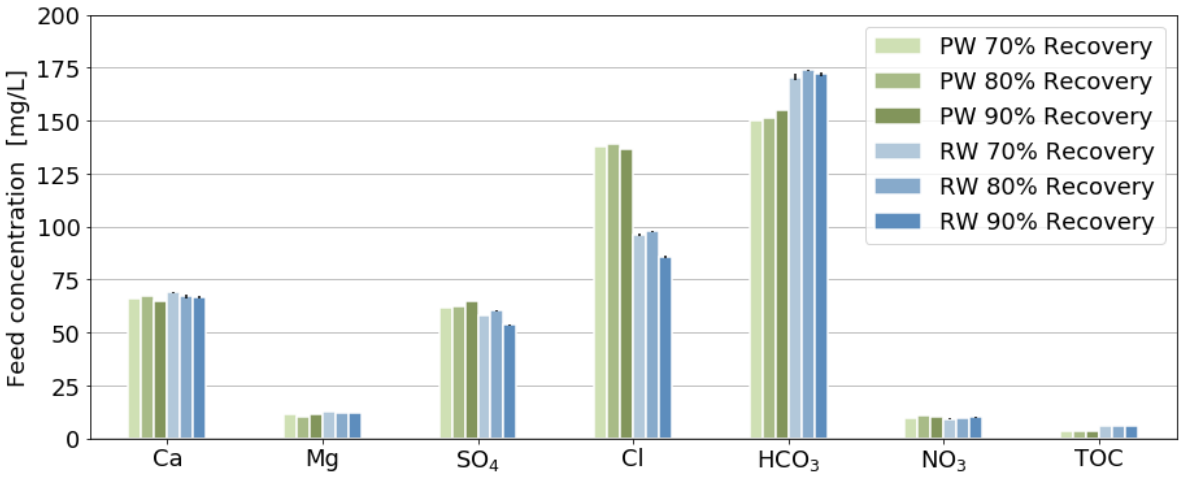

Figure F.1: Ion and TOC concentration in feed stream during filtration with WPJ pre-treated water (green bars) and raw IJssellake water (blue bars) at 70%, 80% and 90% recovery - 20 LMH flux - 0.2 m/s crossflow velocity. PW stands for pre-treated water and RW stands for raw surface water.

G

Total hardness: WPJ pre-treated water

Considering the potential application of dNF40 permeate stream when the dNF40 pilot was fed with WPJ pre-treated water to be used for water softening of PS Bergen (dune water with total hardness of 2.23 mmol/L) to achieve the total hardness value of 1.4 mmol/L (norm of PWN drinking water), the total hardness in the permeate stream was analysed. Figure G.1 shows the total hardness in mmol/L based Ca^{2+} and Mg^{2+} concentrations measured in permeate stream during filtration at 60%, 70%, 80%, 85% and 90% recovery. The flux and crossflow velocity remained constant at 20 LMH and 0.2 m/s. The red line at 1.4 mmol/L indicate the desired hardness value of PWN drinking water.

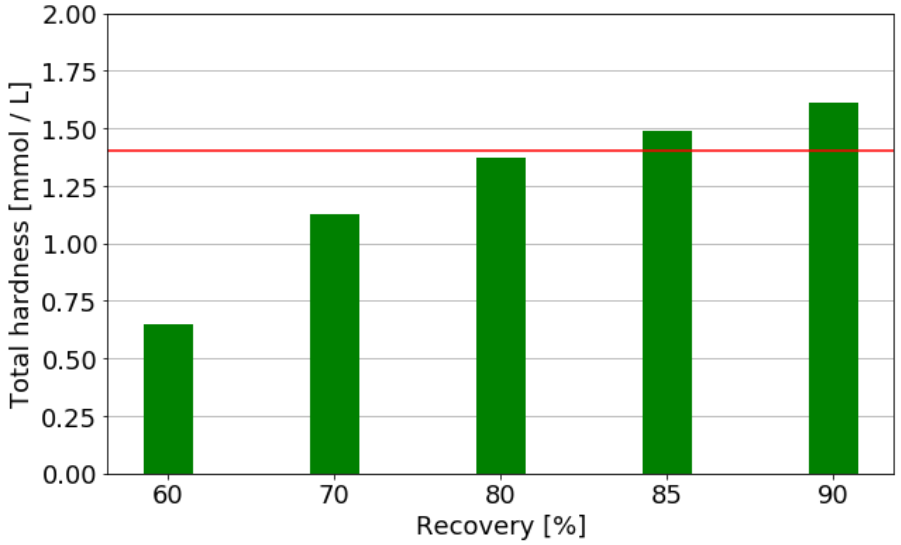

Figure G.1: Total hardness based on Ca^{2+} and Mg^{2+} concentrations in permeate stream during filtration with WPJ pre-treated water at increasing recovery - 20 LMH flux - 0.2 m/s crossflow velocity. The red line at 1.4 mmol/L represent the norm of PWN drinking water.

The total hardness in the permeate stream was around 0.65 mmol/L at 60% recovery and increased to 1.61 mmol/L at 90% recovery. This increase in the total hardness under different recovery rates causes a challenge in the suitability of NF permeate to be used for softening of Bergen dune water. Table G.1 shows that with current RO permeate quality (total hardness of 0.01 mmol/L), a 40%-60% mixing ratio of RO permeate to dune water from Bergen is required. This mixing ratio changed to around 50%-50% for dNF40 permeate at 60% recovery and to around 95%-5% for dNF40 permeate at 80% recovery.

Table G.1: Total hardness of permeate of RO (Heemskerk), dNF40 permeate at different recovery rate as well as their mixing ratio in case of application of Bergen dune water softening. Bergen dune water total hardness is 2.23 mmol/L.

Permeate type	**TH [mmol/L]**	**Mixing ratio (Permeate type - Bergen water)**
RO permeate	0.01	37%-67%
dNF40 permeate (60% recovery)	0.65	52%-48%
dNF40 permeate (80% recovery)	1.37	94%-6%

H

Membrane performance parameters: spiked experiment

Figure H.1 and H.2 show the mass transfer coefficient corrected to a temperature of 20°C at 90%, 20 LMH, 0.2 m/s and 70%, 30 LMH, 0.2 m/s respectively with spiked WPJ pre-treated water. From these graphs can be observed that no fouling was formed on the membrane.

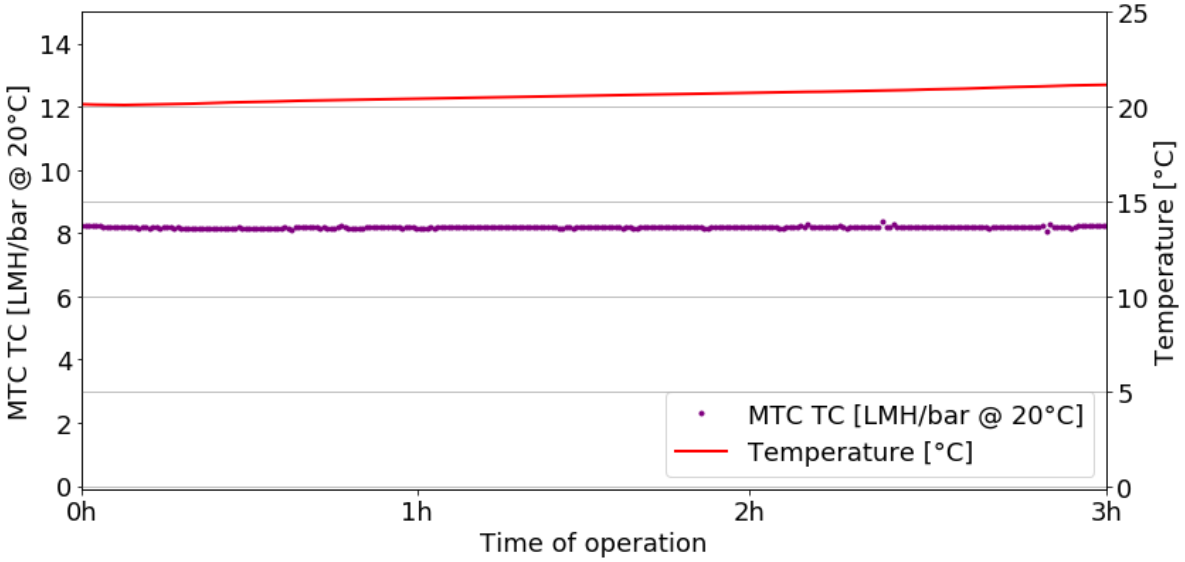

Figure H.1: Mass transfer coefficient temperature corrected at 90% recovery - 20 LMH flux - 0.2 m/s crossflow velocity with spiked WPJ pre-treated water.

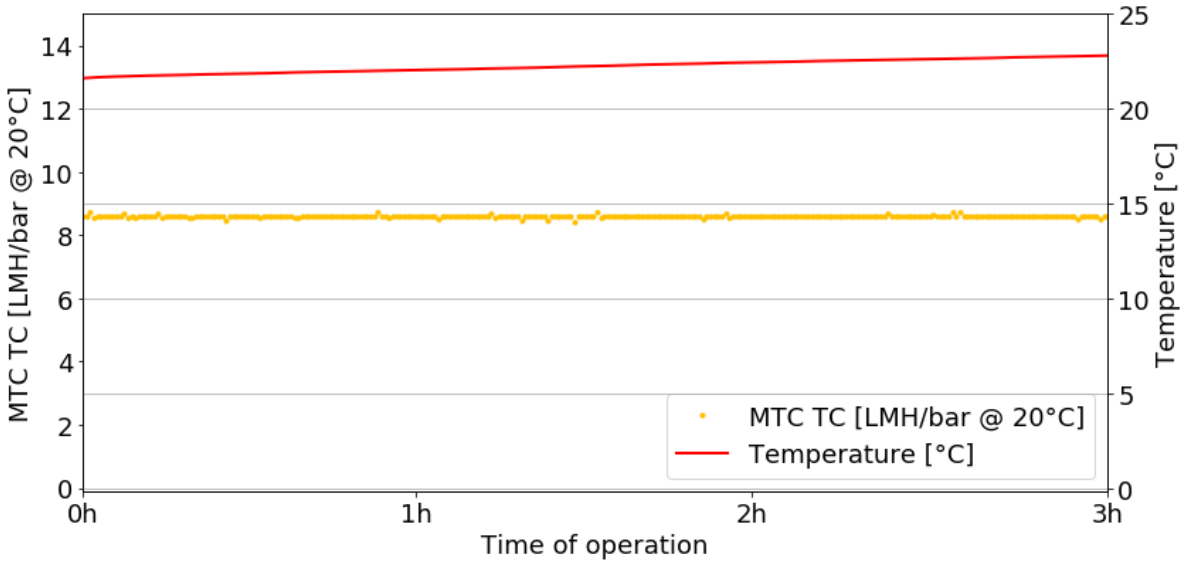

Figure H.2: Mass transfer coefficient temperature corrected at 70% recovery - 30 LMH flux - 0.2 m/s crossflow velocity with spiked WPJ pre-treated water.